BIOLOGICAL TEMPLATING METHODS OF GRAPHITIC CARBON NITRIDE

SCHOOL OF CHEMISTRY, UNIVERSITY OF BIRMINGHAM

AUTHOR: MR. ZHAO YANG

SUPERVISOR: DR. ZOE SCHNEPP

Acknowledgement

My sincere thanks are given to Dr. Zoe Schnepp, who has inspired me a lot in the field of biological templating materials as my mentor. We have worked together and published 2 paper during my master study , which gave me a great understanding about Chemistry. Dr. Zoe Schnepp's help was not only in the field of science, but also in life, she was always willing to help me when I felt confused about life in the U.K. since I'm a oversea student. It's my pleasure to work in her group and I'm looking forward to more collaborations with her group during my PhD study in Beijing.

My sincere thanks are also given to Prof. Lin Guo, who was my mentor in undergraduate and offered me a great opportunity to work in his group as a PhD student in 2016.

I also express my thanks to Dr. Zoe Schnepp's friend, Prof. Yuanjian Zhang, who did brilliant research in graphitic carbon nitride material and gave me high value comments on my review paper and my experiment last year, which inspired me a lot in my study.

My thanks are then extended to my group and my roommates, especially, thanks Mr. Asheigh Danks for his patient help on the experimental instruments and other lab issues, which allowed me finish my work and collect data on time. Thanks Dr. Tzu-Yu Chen's help to improve my oral English, my cooking skill, as well as my knowledge about University of Birmingham.

In the end, My greatest thanks to my family that supported me to finish my study in Birmingham, I love you.

Abstract

Graphitic carbon nitride (g-CN) is a semiconductor material that only consists of carbon and nitrogen, and has shown potential for applications such as photocatalytic water splitting and photoelectrochemical (PEC) conversion of solar energy into chemical fuel. As a promising candidate for sustainable materials, g-CN possesses advantages such as low cost, high physical and chemical stability and visible light sensitivity. However, the conversion efficiency of g-CN to convert sunlight into chemical energy is still low, which is ascribed to the dense materials with low surface area that are produced by standard synthesis method. To overcome this, templating method is a good choice to change the structure and morphology of g-CN and introduce porosity. The key advantages and challenges of templating methods arediscussed in Chapter 1.

In Chapter 3, different biopolymers are used as the templates to generate mesoporous g-CN, due to their unique properties. To further enhance photocatalytic activity of g-CN, a "triple-templating" approach (including biopolymer, air produced by freeze drying process and MgO formed in-situ) is firstly employed in this thesis to introduce pores on several length-scales, which has shown a good performance in degradation of Rhodamine B solution. Overall, the biotemplated g-CN proposed in this thesis not only displays improved photocatalytic properties, but isalso easy to synthesize and environmentally friendly.

Abbreviations

DCDA: Dicyandiamide

g-CN: Graphitic carbon nitride

RhB: Rhodamine B

GO: Graphene oxide

AAO: anodic alumina oxide

XRD: X-Ray Diffraction

SEM: Scanning Electron Microscopy

TEM: Transmission Electron Microscopy

FTIR: Fourier Transform Infrared Spectroscopy

TGA: Thermogravimetric Analysis

BET: Brunauer-Emmett-Teller

UV-vis: Ultraviolet-visible

PL: photoluminescence

ICCD: International Centre for Diffraction Data

Content

Introduction

1.1 Polymeric graphitic carbon nitride

As a resource with renewable and unlimited nature, the application of sunlight to drive chemical reactions is the foundation of life on Earth. The study in photochemical reaction vastly enriches the field of green chemistry,[1,2] especially with an increasing research interest toward "solar fuels" such as hydrogen from water splitting. [3] Also, the occurrence of photochemical reactions without additional reagents is an advantage, which significantly avoids the formation of byproducts. Besides sunlight, the assistance of a semiconductor photocatalyst is another key factor to perform photochemical reaction, and the photocatalyst which is investigated and discussed in this thesis is graphitic carbon nitride (g-CN).

Polymeric graphitic carbon nitride (g-CN or g-C_3N_4) is a metal-free semiconductor that consists of C and N atoms with a structure similar to graphene, it shows high thermal stability up to 600 °C in air as well as high chemical stability.[4] g-CN can be synthesized by the polyaddition and polycondensation of nitrogen-rich precursors, including cyanamide, dicyandiamide and urea, which is a simple approach, makes it one of the advantages of g-CN. Taking the synthesis of g-CN from cyanamide as an example, it can be illustrated as a 4-step process, as shown in Figure 1.1:[5]The first step is to start with condensation of the precursor towards melamine. The second step eliminates ammonia and leads to the formation of a dimer called melam, which then converts into a tri-s-triazine called melem at 390 °C. The "melem" is believed to be the structural unit of idealized graphitic carbon nitride. In the last step, g-CN is obtained via polymerization at approximately 520 °C. The aromatic structure of tri-s-triazinetecton tends to forma π-conjugated plane similar to graphite, which strongly influences the properties of g-CN.[6] The stacking of individual layers makes

full use of van der Waals forces, also makes it insoluble in most solvents.[4]Distinguished by the difference of nitrogen-linked aromatic moieties, There are two idealized model for g-CN, which consists of triazine (C_3N_3) units and tri-s-triazine (C_6N_7) units. However the reality is that ideal g-CN never forms due to the difficulty of full condensation of the precursors via releasing NH_3, which meansthe final product is probably better described as a graphite- phase polymeric carbon nitride with the formula g-$C_XN_yH_z$, rather than g-C_3N_4 or g-CN.[7] For simplicity reason, it is still named as g-CN in the thesis.

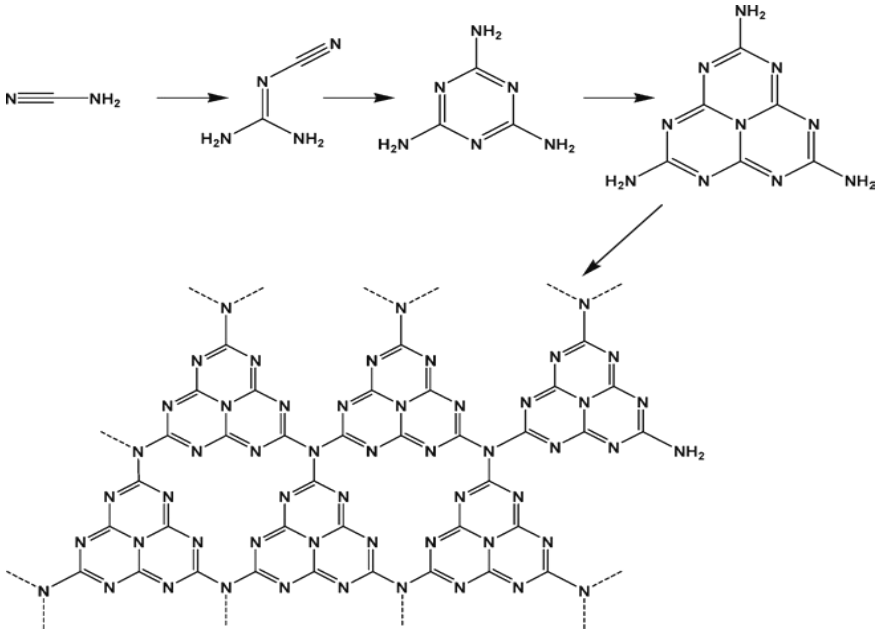

Figure 1.1 Reaction route for the formation of g-CN starting fromcyanamide

As a promising sustainable material, g-CN has been developed for many potential applications (Figure 1.2 a), including solar water splitting, photodegradation and metal-free catalysis.[8-10]The main application of g-CN that we focused on is photodegradation of organic dye in the thesis (Figure 1.2 b). With a band gap energy of approximately 2.7 eV and the positions of the valence and conduction bands well placedaround the water oxidation and reduction potentials, g-CN has a good property to absorb light in visible range. Besides, it has advantages that good

photocatalysts possess in common, including high thermal stability, non-toxicity, comprised of earth-abundant elements and relatively easy to manufacture in a controlled morphology. [11]

Despite these advantages, the low conversion efficiency of bulk g-CN in sunlight is still one of the main challenges, which is attributed to limited visible light absorption, low surface area and grain boundary effects.[12]The challenges make it clear that one major focus in terms of g-CN future research is to control grain size and surface area. By controlling the structure of the catalyst materials, more active sites can be obtained, which gives an enhancement in performance as well as possibly in size and shape selectivity. One of the common ways to achieve structural control is to introduce porosity by templating method, which is often classified as "soft" and "hard". Generally speaking, soft templating makes use of "self-assembly" characteristics of amphiphilic molecules or surfactants to directly assembly or precipitate the precursor, while hard templating uses a solid material such as silica or anodized alumina to cast the material, making it copy the structure of the template. A detail illustration of templating methods of g-CN (Figure 1.2c) is carried on in Chapter 1.2.

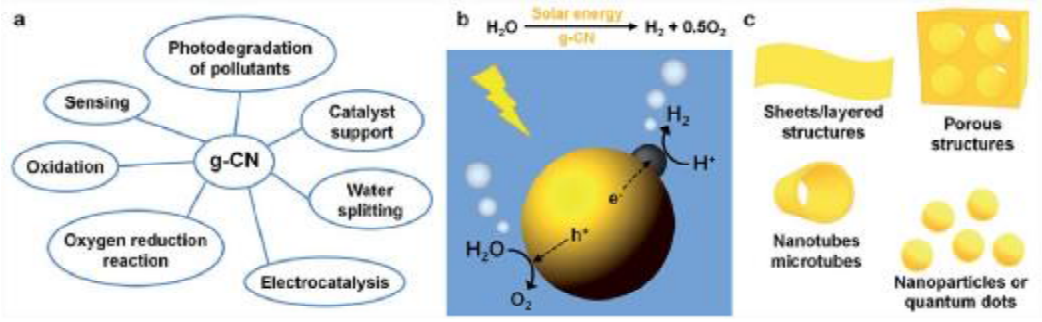

Figure 1.2 a) Different applications of g-CN. b) Schematic of photocatalytic water splitting over g-CN. c) Different structures of g-CN by templating methods.[11]

1.2 Templating methods

1.2.1 Soft templating

By directly guiding the "self-assembly" of a precursor at interfacial regions and influencing the growth of inorganic phases around them, soft templating methods have dramatically introduced porosity in the formation of g-CN porous structure. As "structure directing agents", the templates play a critical role in this series of methods, which can form micelles in solution to combine with reaction precursors and finally lead to the formation of a range of different structures. To our best knowledge, there are three common soft templates, amphiphilic surfactants and block copolymers, ionic liquids(ILs) and gas bubbles to template g-CN, which will be discussed in the following section.

Surfactants and block copolymers have been employed to template graphitic carbon nitride. As a common surfactant, Triton X-100 was used to combine with dicyandiamide (DCDA) to produce g-CN by Wang *et al*. [13] By avoiding the formation of inaccessible closed pores, the g-CN product shows a promising porous strucutre (Figure 1.3 a), with a Brunauer-Emmett-Teller(BET) surface area of 76 m^2/g, which is due to the high decomposition temperature of Triton X-100. Yan *et al*. used Pluronic 123 (P123) as a block copolymer template, and melamine, a less reactive precursor, to synthesize mesoporous g-CN.[14] Figure 1.3 b showed a typical TEM image of a mesoporous g-CN in which the mass ratio of melamine: P123 is 5:1. Also the product showed a low concentration of carbon residue, high BET surface area, and good light absorption performance, up to 800 nm towards the peak intensity of solar spectrum. Surfactants and block copolymers have witnessed great success in manufacturing a range of g-CN porous structures. However, the mechanisms have not been well

explained, which is just attributed to inherent self-assembly characteristic, and as the shortages that most soft templates have in common, the hydrolysis of surfactants during a high temperature reaction may cause some redox reactions in the precursors and weaken its interaction with the precursors. Thermal breakdown of the surfactant may also occur during the calcination, leaving carbon residue, which affects the performance of g-CN product.[15]

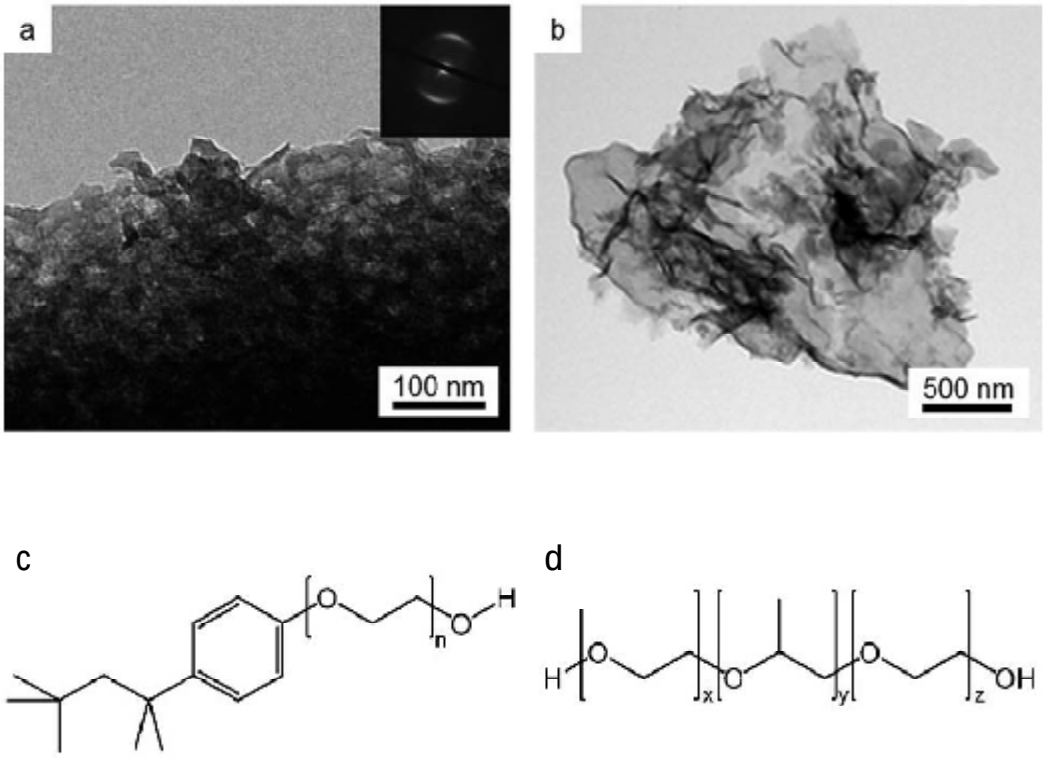

Figure 1.3 TEM images of g-CN synthesized from a) DCDA and Triton X-100(with SAED inset) and b) melamine and Pluronic P123;[13,14]the structures of c) Triton X-100 and d) Pluronic P123 are also shown.

Another choice in soft templating is ionic liquids (ILs). Ionic liquids are liquid state salts that contain an organic, nitrogen-containing cation and an inorganic anion. They exist at relatively low temperature (less than 100 °C), and can be heated without evaporation since they have no measurable vapor pressure.[16]As one of the most

common ionic liquids, 1-butyl-3-methylimidazolium hexafluorophosphate (BMIM-PF_6) was used to template the precursor dicyandiamide (DCDA) by Zhang *et al.*, PF_6^- reacted with amine group to give P-doped carbon nitride solid during calcination, which maintained the structural feature of C-N framework, but significantly increased its electric conductivity by 4 orders of magnitude, as shown in Figure 1.4.[17]The liquid state is one of the advantages of ionic liquids, since they can be well incorporated with the precursors. Also, the presence of heteroatoms (like phosphorous) in organic nitrogen-containing cation can introduce dopants during the templating process. The third advantage of ionic liquid templates is their high thermal stability and negligible vapor pressure, which makes it possible to combine sol-gel chemistry and molten salt synthesis, which further influences the crystallization process of graphitic carbon nitride.[18]However, drawbacks like high cost compared to other solvents and insolubility of some ionic liquids in water still limit theirapplication.

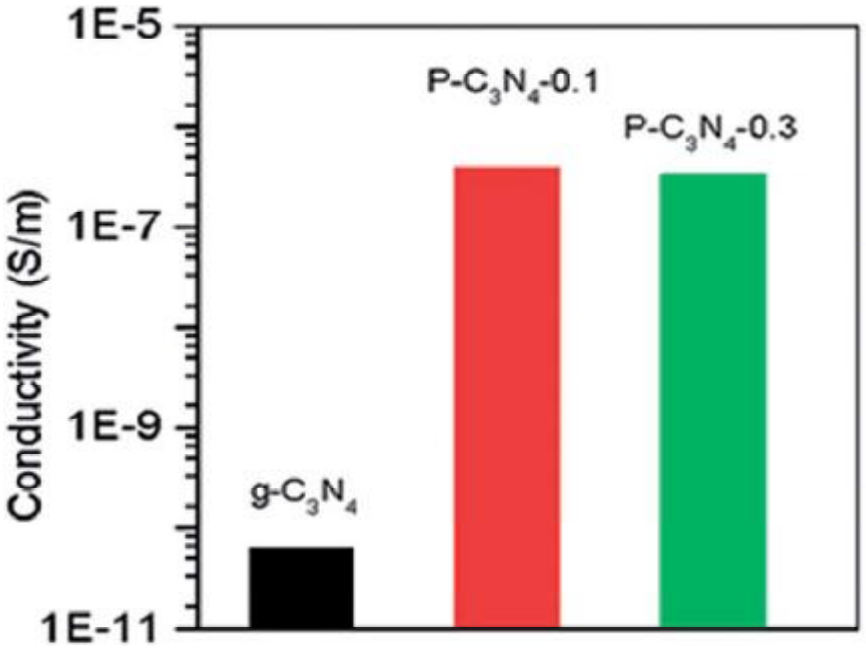

Figure 1.4 Electrical conductivity of P-doped and pure g-CN,[17]where 10 wt% and 30 wt% of BMIM-PF_6 to DCDA were used in P-C_3N_4-0.1 and P-C_3N_4-0.3 respectively.

The gas bubbles that are producedfromheating the precursor can also be an option in templating g-CN. For instance, Zhang *et al.* used urea to produce g-CN directly.Ammonia released during the decomposition of urea and bubbles from water vapor are considered to be the template in this system.[19]The bubble template can effectively avoid introducing impurities and post treatment, whichis the main advantage. More investigation should be carried on in this field to study how bubble template can enhance the performance of g-CN.

In summary, soft templating methods provide a flexible and straightforward approach to give g-CN porosity. However, soft methods still have drawbacks, like the organic templates would yield a high levels of residual carbon, which may hinder the performance of g-CN. Besides, the self-assembly characteristic and the dynamic nature of some soft templating systems make it hard to synthesize a predictable product. Also, many organic templates would decompose at relatively low temperature, no longer exist at the temperature where the condensation of the nitrogen-rich precursors start, this may hinder the templates to guide the self-assembly of g-CN crystals. To avoid the drawbacks of soft templating, the study on hard templating is carried out.

1.2.2 Hard templating

Hard templating is also known as "nanocasting". In a typical nanocasting process, the precursor is filled or coated insidea rigid template, and the template will finally be removed after the treatment of the precursor to create a desirable replica. The essential difference between the soft and hard templating is that soft methods do notreplicate a surfactant structure. Instead they rely on the self-assembly of

surfactant molecules or interaction of surfactant molecules with a precursor to influence growth of the desired phase, which would be known as "structure directing" rather than "templating" in zeolite chemistry. The product of hard templating shows a more fixed structure than soft methods, since their morphologies are easier to control.[20]Our study shows silica, alumina oxide and carbon are most common templates in hard methods, and a detail illustration of these templates is involved in this section.

Silica is a common material to template g-CN, due to its high stability during reaction, easily controlled morphologies with ideal pore size distribution. Vinu *et al.* used SBA-15, an ordered mesoporous silica as the template and a mixture of ethylenediamine and carbon tetrachloride as the g-CN precursors, firstly obtained an ordered carbon nitride matrix with uniform mesoporedistribution,a high BET surface area up to 500 m^2/g, also high mesopore volume.[21]High resolution transmission electron microscopy (HRTEM) and energy filtered transmission electron microscopy (EF-TEM) images of the sample are shown in Figure 1.5.Using silica as hard template gives the final g-CN product an ordered mesoporous framework with large surface area and uniform pore size, which can be attributed to strong interactions between the precursor and the silica surface. However, one limitation in Vinu's method is the high ratio of carbon to nitrogen (C/N), making the material a nitrogen doped carbon, rather than carbon nitride.

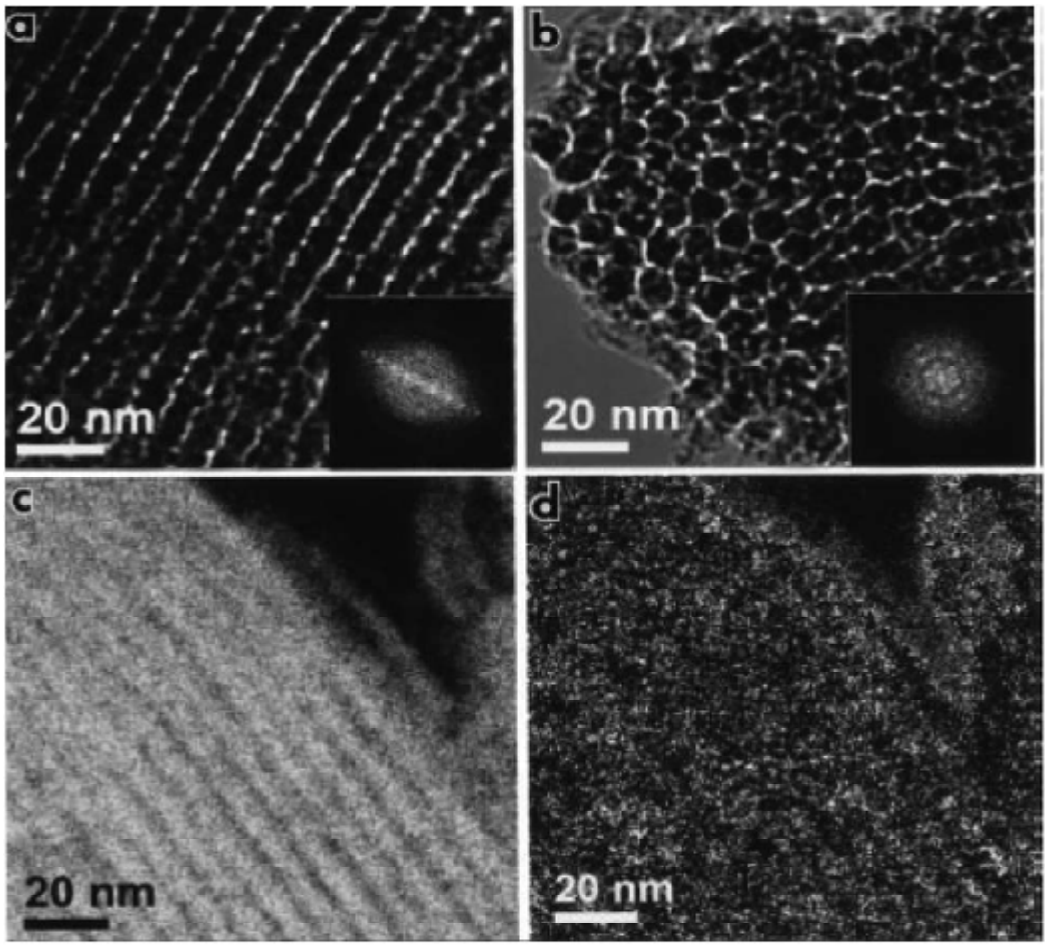

Figure 1.5 a, b) HRTEM and c, d) EF-TEM images of mesoporous g-CN: a) along the mesopores, b) across the mesopores. Elemental maps of C (c) and N (d) correlate well.[21]

Another choice to template g-CN is porous anodic aluminiumoxide (AAO), which is formed by potentiostatic anodization of aluminium. Li *et al*. synthesized rod-like g-CN by using AAO as the template and cyanamide as precursor. After the removal of AAO template, rod like g-CN product was obtained with improved orientation and crystallinity, which was attributed to the confinement effect of AAO channels. The confinement effect was confirmed by transmission electron microscopy (TEM), where g-CN formed a close-packed layer on pore wall. These layers then act as a nucleation center, leading to the condensed secondary crystals adsorbed on the pore

wall. The blue shift of UV/vis spectrum indicated AAO templating g-CN has a lower Highest Occupied Molecular Orbital (HOMO), which can improve photocatalytic performance of g-CN.[22]By improving the condensation and orientation of g-CN, AAO membranes can dramatically increase the crystallinity and lower the HOMO position, leading to high performance in photocatalysis.

Besides metal oxide, graphene, a single layer sheet of sp^2 carbon atoms with a honeycomb structure can also template g-CN, which is due to the outstanding thermal and electrical properties of graphene. For instance, it has a high thermal conductivity up to 5000 $Wm^{-1}K^{-1}$, a high specific surface area of 2600 m^2g^{-1}. Graphene can be synthesized via a simple 2-step approach, where the first step is oxidation of natural graphite into graphene oxide (GO), and the second step gives graphene by the reduction of GO.[23,24] All advantages above make graphene a promising alternative to synthesize graphene based g-CN. Xiang *et al.* firstly reported a graphene/g-CN composite on the generation of hydrogen under irradiation of visible light.The composite was obtained by means of polymerization of melamine in the presence of GO and hydrazine hydrate, calcined to 550 °C under nitrogen atmosphere. The introduction of graphene can enhance the photocatalytic activity of g-CN by acting as conductive channels and as good electron acceptor materials, separating the photogenerated electrons and holes, and hinder charge recombination via the 2D π-conjugated structure.[25]The influence of the graphene weight percentage in the composite was also investigated by photoluminescence (PL) emission and transient photocurrent, as shown in Figure 1.6. A lower value of PL emission and a higher value of photocurrent occurred with 1.0 % graphene in the sample, suggesting a significant separation of photogenerated electron-hole pairs at the interface between g-CN and graphene.The graphene/g-CN composite indicates that graphene has potential application in enhancing photocatalytic activity of g-CN and obtaining high photocatalysts. [26]

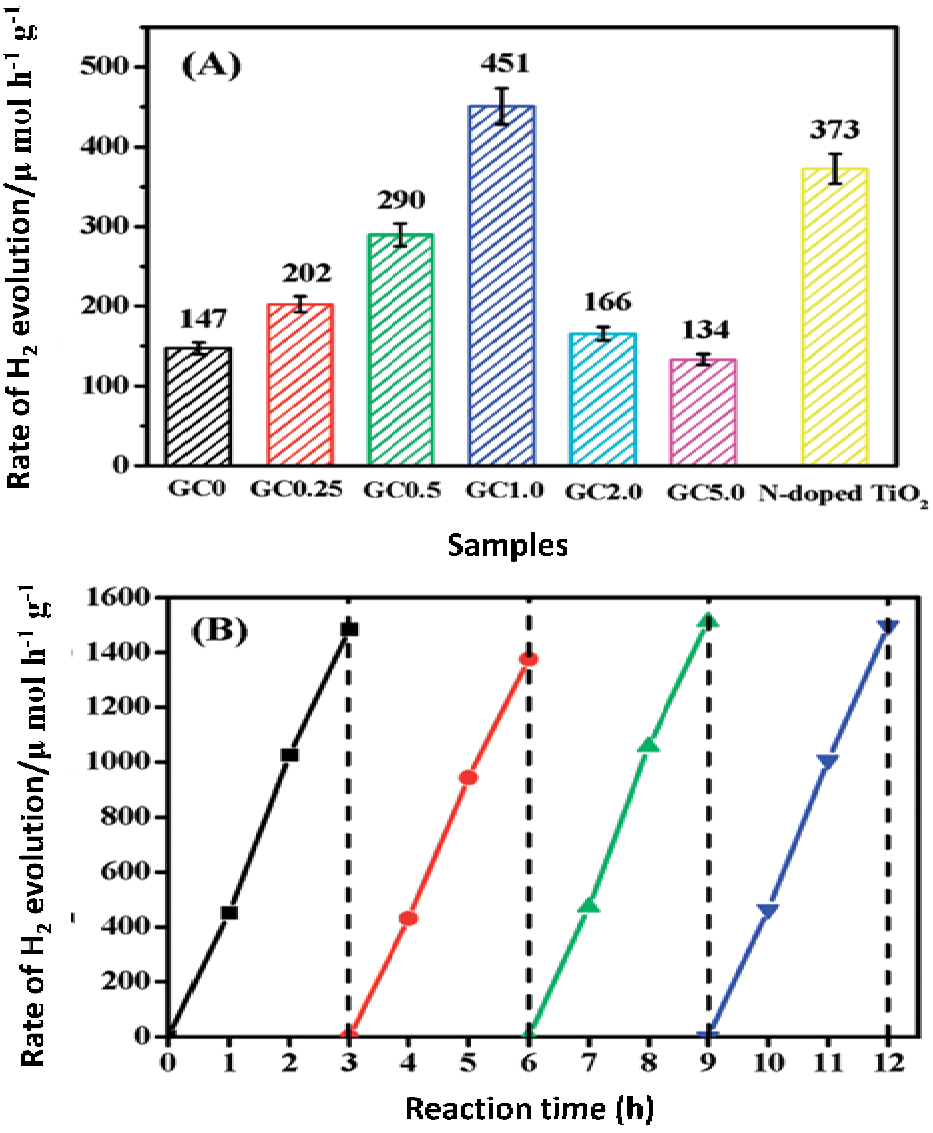

Figure 1.6 A) Comparison of the photocatalytic activity between GCx and N-doped TiO_2 for the hydrogen generation from methanol aqueous solution (x is the weight percentage of graphene in graphene/g-CN composite, x=0, 0.25, 0.5, 1.0, 2.0, 5.0) B) Cyclic H_2 evolution curve for GC1.0 sample.Figure modified from ref.25.

In summary, hard templating methods have witnessed great success in preparing highly-ordered and porous g-CN. However, there is still drawback in this method. For instance, hazardous acids such as aqueous ammonium bifluoride (NH_4HF_2) or

hydrogen fluoride (HF) are needed to remove silica template, which can cause safety concerns and may damage the target material. Moreover, increasing the loading ability of the templates with high concentration precursor to avoid collapse of the porous structure after removal of the templates is another challenge.[27]

1.2.3 Biotemplating g-CN

From the disadvantages of soft and hard templating methods that we discussed above, it seems difficult to achieve 'high order', 'sustainable' and 'convenient' in one method. As there is increasing interest in sustainability and green chemistry, it is necessary to develop a new route to high performance g-CN, and the inspiration to achieve it may come from nature, just as the stripes of a zebra can inspire camouflage patterns, biopolymers can be a choice to template g-CN. The term biopolymer we focus on refers to those macromolecules that areproduced directly by living organisms. The reason for discussing biotemplating methods in a new section is that they are not easy to classify as 'soft' or 'hard' methods, it indeed depends on what characteristic that the biopolymer is being used. Some biopolymers show 'self-assembly' characteristic to form hierarchical aqueous gels of double or triple helices, which can be classified as 'soft' methods. Meanwhile, they can also be used to cast fibers or sponge-like structure as 'hard' methods. More interestingly, even whole biological structures, like bacteria, viruses and butterfly wings can be used in 'hard' methods of biotemplating.[28]

Alginate and gelatin were added into aqueous dicyandiamide (DCDA) as the templates to form sponge-like structure by Zhang *et al*. The sponge structure g-CN (Figure 1.7) can enhance mass transfer and visible light adsorption during photocatalysis by reducing the diffusion path, which can be proven by the positive

result of photocurrent of sponge g-CN during PEC measurements.[12] Besides, diatoms, a very different biological material with unique frustule architectures can also template g-CN.[29]The g-CN product with a diatom frustule structure was obtained by heating the mixture of cyanamide and diatom. The SEM and confocal fluorescence both confirmed that g-CN wrapped on the frustule well. Although the surface area of diatom g-CN is much lower than that of silica templating g-CN, the test of regeneration of NADPH from nicotinamide adenine dinucleotide phosphate (NADP) showed a different result, with diatom templating g-CN gave the best regeneration yield. This good photocatalytic ability can be ascribed to the diatom structure, which can enhance light trapping and scattering abilities.

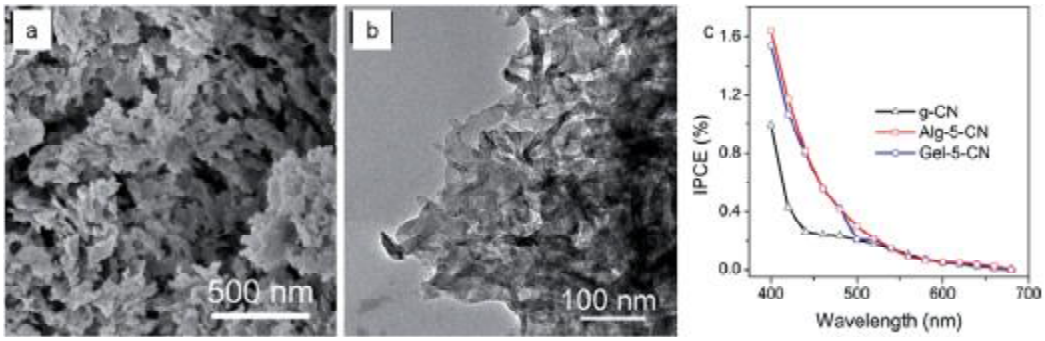

Figure 1.7 a) SEM and b) TEM images of alginate-templated g-CN showing porous structure of g-CN and c) photo action spectra of control g-CN, alginate templating g-CN and gelatin templating g-CN biased at -0.2V vs. Ag/AgCl (sat. KCl).[12]

In summary, biopolymers provide a new route to template g-CN, due to their unique structure and good properties to form gel and bind precursors to 'self-assembly' g-CN crystals that synthetic templates may not have. Besides, biopolymers meet the request for 'green chemistry' when working as hard templates, since usually no need for hazardous acid to remove templates. The advantages mentioned above give biotemplated g-CN a promising future. However, the challenge for biotemplating is that many biological templates can only control the porosity on one length-scale, which limits further application of this method.

1.3 The mechanism of photocatalysis

One of the most important potential applications of graphitic carbon nitride is photocatalysis, which was firstly reported by Wang et al.[30]We believe it is a good time to discuss about the mechanism of photochemical reactions, to better guide us find a route to high performance g-CN product.

As a semiconductor photocatalyst, it is characterized by a highest occupied energy band, called the valence band (VB), and a lowest occupied energy band, called the conduction band (CB).Between the two bands is the band gap. The mechanism of a semiconductor photocatalysis is described as follows. When the semiconductor absorbs energy from light irradiation higher or equal to that of band gap energy, an electron is promoted from the VB to the CB, leaving a positively charged hole (h+) in the VB. The photo-excited electron and the positively charged hole would distribute on different position of the catalyst to react with those donor (D) or acceptor (A) species that are adsorbed on or near the surface. By providing high chemo- and regioselectivity, the photoactive center significantly reduces the height of activation barrier and increases the reaction rate. The use of water as a solvent and photons as an energy source also makes photocatalytic reactions environmentally friendly, which has a grown potential and interest in the scientific and engineering application.[31-34]

The investigation of semiconductor photocatalysts for solar energy conversion and pollutant remediationhas started since Fujishima and Honda discovered the photocatalytic splitting of water with TiO_2 in 1972.[35] However, the high recombination rate of electron-hole pairs at or near its surface would still result in the relatively low value of overall quantum efficiency.[34] The methods, such as doping metal ions or heteroatoms or controlling crystallinity, particle size and porosity,[36,37] can improve photocatalytic activity by increasing the rate of transfer

of electron-hole pairs, also enhancing the transport of reagents to the catalyst surface. For instance, there are lots of studies on the control of structure and morphology in ceramic semiconductors such as TiO_2 or ZnO have been carried out and well understood.[38,39] Compared with traditional semiconductors, many properties of graphitic carbon nitride give it advantages over its ceramic counterparts. Most importantly, as a metal-free semiconductor, g-CN is composed only of carbon and nitrogen, which are highly abundant in nature. Besides, this yellow solid also possesses a favorable band gap that placed in the visible light region, with a better position of the valence and conduction bands embedded near the water oxidation and reduction potentials, compared to TiO_2, as shown in Figure 1.8.

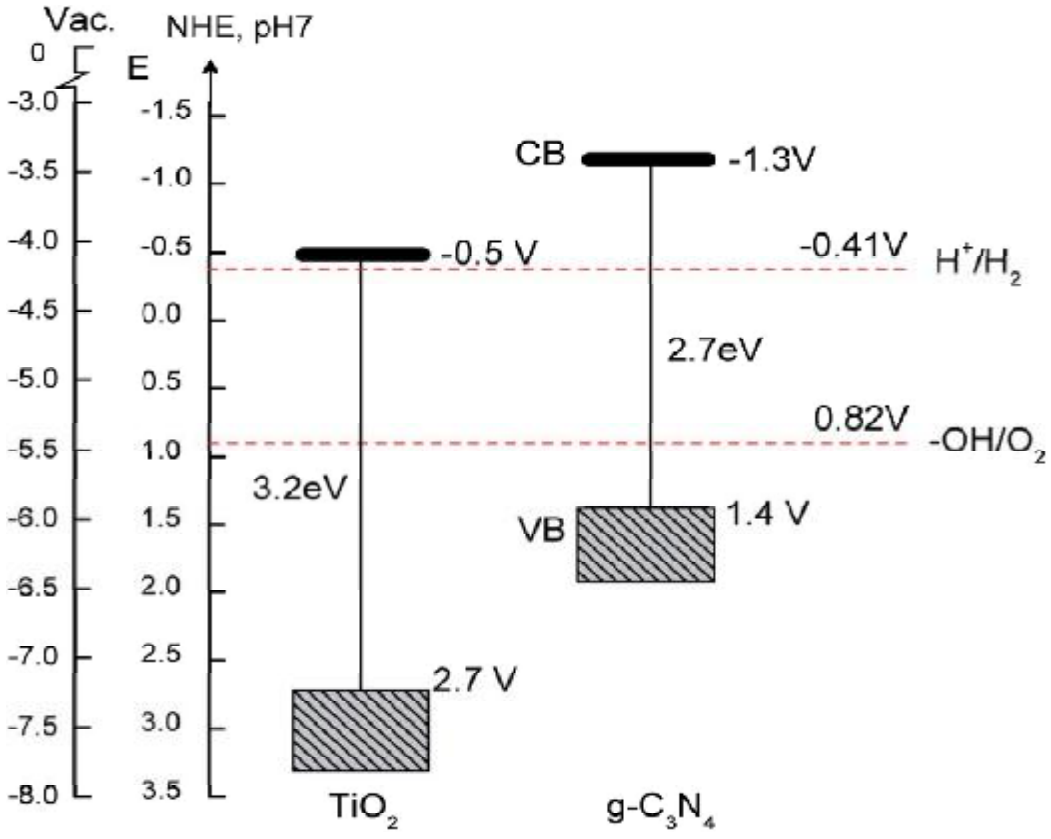

Figure 1.8 Electronic band structure of g-CN, compared with TiO_2.[32]

1.4 Aim of research

Generally speaking, there are several requests to achieve a highperformance photocatalyst. The first is an appropriate band gap to absorb visible range light, which is necessary to ensure energy can drive the reaction. The second is stability, requiring the catalyst can be recycled without being poisoned during photocatalysis. The third is low or zero toxicity, not only of the catalyst itself, but also the route to synthesize it. Also, the approach to the photocatalyst should be simple, which allows the final product tobe obtained in a controlled shape easily. The last is, the elements that comprise the catalyst should be low-cost and earth-abundant.

Given the requests listed above, g-CN is an attractive choice to be the photocatalyst. Besides, lots of efforts have been done to control the morphology of g-CN by templating method, resulting in an improvement in photocatalytic activity. However, traditional templating methods still can't overcome their limitation. For soft methods, it's the unpredictability of self-assembly of g-CN, and carbon residue that may hinder the photocatalytic activity. The use of hazardous acid to remove templates is the challenge of hard methods. The research of biological templates seems to be a breakthrough in templating methods and draws lots of interests, but the limitation in this sort of methods is that most biological templates can only control the porosity in one length-scale, which challenges the further application of biotemplating. The question is,are there any methods that can combine the advantages of both soft and hard templating, and achieve morphology control on multiple length scales? That's our research mainly focused on.

The investigation would start from using different biopolymers to template g-CN, which is aiming at taking advantages of unique properties of biopolymers, and widening the research in this field as well. After then, the most promising biopolymer in our research range would be selected to do further enhancements, which is

expected to achieve our final aim, thus minimizing the shortcomings of templating methods. Those enhancements include the introduction of freeze-drying to the synthesis of g-CN, and an addition of aqueous $Mg(NO_3)_2$ to the precursor. The use of a freeze dryer can remove water from precursor through sublimation, which is presumed to give macroscale porosity. Meanwhile, MgO would be formed in-situ during the calcination of precursor, which can be removed then and leave microscale porosity. By introducing porosity in different dimensions, the shortage of biotemplating shall be overcome, and a hierarchical structure product can be obtained. Besides, the approach we proposed to improve templating method of g-CN also make use of self-assembly characteristic of biopolymers, and nanocasting of MgO particles. Compared with traditional hard methods, MgO template can avoid the use of hazardous acid, such as HF.

We hope the combination approach of both soft and hard methods can overcome each limitations and achieve a g-CN product with high photocatalytic activity, in a "greener" way. The influence of templates on g-CN crystallization would be recorded by electron microscopy, and the way to evaluate final product is the photodegradation of Rhodamine B under visible light, by observing which sample takes the least time to make RhB solution become clear.

Chapter references

1. H. D. Roth,*Angew. Chem., Int. Ed.*, 1989, 28, 1193.

2. N. Hoffmann, *Chem. Rev.,* 2008, 108, 1052.

3. K. Maeda, K. Teramura, D. Lu, T. Takata, N. Saito, Y. Inoue and K. Domen, *Nature*, 2006, 440, 295.

4. Z. Zhou, J. Wang, J. Yu, Y. Shen, Y. Li, A. Liu, S. Liu and Y. Zhang, *J. Am. Chem. Soc.*, 2015, 137, 2179.

5. A. Thomas, A. Fischer, F.Goettmann, M. Antonietti, J. Muller, R. Schlogl and J. M. Carlsson,*J. Mater. Chem.*, 2008, 18, 4893.

6. M. Groenewolt and M. Antonietti, *Adv. Mater.*, 2005, 17, 1789

7. Algara-Siller G, Severin N, Chong S Y,.*Angew Chem*, 2014, 126: 7580.

8. N. Cheng, J. Tian, Q. Liu, C. Ge, A. H. Qusti, A. M. Asiri, A. O. Al-Youbi and X. Sun, *ACS Appl. Mater. Interfaces.,*2013, 5, 6815

9. X. Wang, K. Maeda, X. Chen, K. Takanabe, K. Domen, Y. Hou, X. Fu and M. Antonietti, *J. Am. Chem. Soc.,*2009, 131, 1680

10. K. Maeda, X. Wang, Y. Nishihara, D. Lu, M. Antonietti, K. Domen, *J. Phys. Chem. C.*, 2009, 113, 4940

11. Z. Yang, Y. Zhang, Z. Schnepp. *J. Mater. Chem. A.*, 2015,3, 14081.

12. Y. Zhang, Z. Schnepp, J. Cao, S. Ouyang, Y. Li, J. Ye and S. Liu, *Sci. Rep*., 2013, 3, 2163.

13. Y. Wang, X. Wang, M. Antonietti and Y. Zhang, *ChemSusChem*, 2010, 3, 435

14. H. Yan, Chem. Commun., 2012, 48, 3430

15. Y. Zheng, J. Liu, J. Liang, M. Jaroniec and S. Z. Qiao, *Energy Environ. Sci.*, 2012, 5, 6717.

16. P. Wasserscheid and W. Keim, *Angew. Chem*., 2000, 39, 3772.

17. Y. Zhang, T. Mori, J. Ye and M. Antonietti, *J. Am. Chem. Soc.*,2010, 132,6294.

18. D. C. Green, S. Glatzel, A. M. Collins, A. J. Patil and S. R. Hall, Adv. Mater., 2012, 24, 5767.

19. Y. Zhang, J. Liu, G. Wu and W. Chen,*Nanoscale*, 2012, 4, 5300.

20. A. H. Lu and F. Schuth,*Adv. Mater*., 2006, 18, 1793.

21. A. Vinu, K. Ariga, T. Mori, T. Nakanishi, S. Hishita, D. Golberg and Y. Bando, *Adv. Mater.*, 2005, 17, 1648.

22. X.-H. Li, J. Zhang, X. Chen, A. Fischer, A. Thomas, M. Antonietti and X. Wang, *Chem. Mater.*, 2011, 23, 4344.

23. M. J. Allen, V. C. Tung and R. B. Kaner, *Chem. Rev.*, 2010, 110, 132.

24. D. R. Dreyer, S. Park, C. W. Bielawski and R. S. Ruoff, *Chem. Soc. Rev.*, 2010, 39, 228.

25. Q. Xiang, J. Yu and M. Jaroniec,*J. Phys. Chem. C*, 2011, 115, 7355.

26. A. Du, S. Sanvito, Z. Li, D. Wang, Y. Jiao, T. Liao, Q. Sun, Y. H. Ng, Z. Zhu, R. Amal and S. C. Smith,*J. Am. Chem.Soc.,* 2012, 134, 4393.

27. J. Xu, Y. Wang and Y. Zhu, *Langmuir*, 2013, 29, 10566.

28. Z. Schnepp,*Angew. Chem., Int. Ed*., 2013, 52, 1096.

29. J. Liu and M. Antonietti, *Energy Environ. Sci*., 2013, 6, 1486.

30. X. Wang, K. Maeda, A. Thomas, K. Takanabe, Gang Xin, J. M. Carlsson, K. Domen, M. Antonietti. *Nat. Mater*.,2009, 8, 76.

31. P. Wessig,*Angew. Chem., Int. Ed.*, 2006, 45, 2168.

32. X. Wang, S. Blechert and M. Antonietti, *ACS Catal.,* 2012, 2,1596.

33. M. R. Hoffmann, S. T. Martin, W. Choi and D. W. Bahnemann,*Chem. Rev.*, 1995, 95, 69.

34. J. Liqiang, Q. Yichun, W. Baiqi, L. Shudan, J. Baojiang, Y. Libin, F. Wei, F. Honggang and S. Jiazhong, *Sol. Energy Mater. Sol. Cells,* 2006, 90, 1773.

35. A. Fujishima and K. Honda,*Nature*, 1972, 238, 37.

36. A. Kudo, R. Niishiro, A. Iwase and H. Kato, *Chem. Phys.*, 2007, 339, 104.

37. J. Tian, Z. Zhao, A. Kumar, R. I. Boughton and H. Lou, *Chem. Soc. Rev.,* 2014, 43, 6920.

38. J. H. Jung, H. Kobayashi, K. J. C. van Bommel, S. Shinkai and T. Shimizu, *Chem. Mater.,* 2002, 14, 1445.

39. Y. Sun, G. M. Fuge, N. A. Fox, D. J. Riley and M. N. R. Ashfold,*Adv. Mater.,* 2005, 17, 2477.

Experimental techniques

2.1 Analytical methods

To characterize the properties of g-CN materials, different analytical methods were carried on, including X-ray diffraction (XRD), electron microscopy, elemental analysis, FTIR and UV-vis spectroscopy, thermogravimetric analysis and BET method.

2.1.1 X-ray diffraction (XRD)

When X-rays hit a solid crystalline sample, they will scatter in predictable patterns based upon the internal structure of the solid and produce distinct scattering patterns similar to fingerprints, which are then identified and cataloged for further investigation on crystal structure.[1]Bragg's law is one of the most important aspects of XRD, illustrating the X-ray scattering process, which is

$$2d\sin\vartheta = n\lambda,$$

where d: lattice plane distance, ϑ:angle of incidence, n: order of interference and λ: X-ray wavelength.

When the parallel X-ray waves are directed with an angle θ onto a system with a lattice-plane distance d, the reflecting waves from different lattice plane will have different optical pathway, in which the difference is calculated as '2dsinθ', between two reflecting waves, and the value of this difference is equal to the integer multiples

of the wavelength. (As shown in Figure 2.1) Bragg's diffraction only occurs in solids which have a periodic arrangement of atoms, and it explains that the diffraction position and the relative intensity of diffraction peaks correspond to certain type and arrangement of atoms in the crystal.

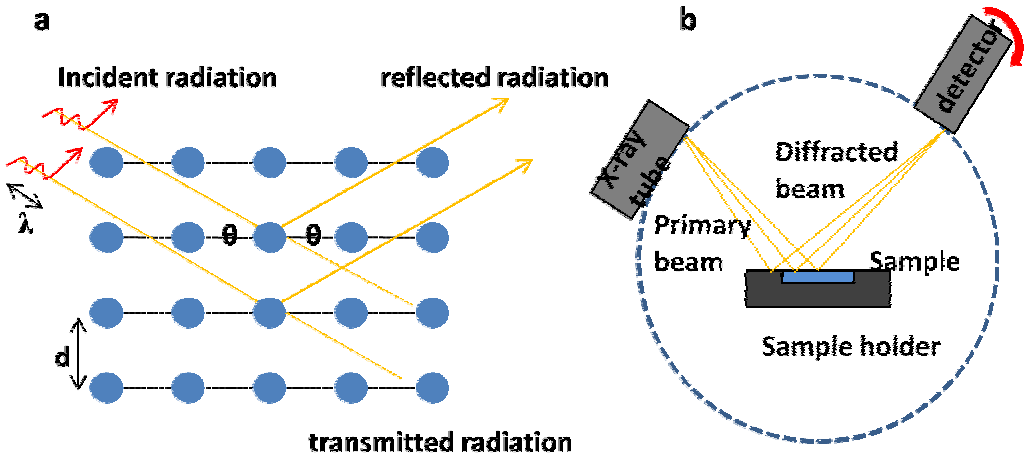

Figure 2.1 a) Schematic diagram of an X-ray scattering. b) Schematic diagram of Bragg-Brentano geometry, which is used to record X-ray powder diffraction pattern.

To identify a crystalline substance, the observer takes a look at the resulting graph of the XRD pattern, then selects the most prominent spikes from its angles that produce the most diffraction to compare with the ICDD(International Centre for Diffraction Data) card in the database, the phase composition and structure of the studied materials can be obtained. [2]

2.1.2 Scanning Electron Microscopy (SEM)

Two main parts of the SEM instrument are the electronic console and the electron column. The electron column is where the electron beam is generated under vacuum, while electronicconsoleprovides instrument adjustments such as filament current,

accelerating voltage, focus, magnification, brightness and contrast.[3]

When the electron beam hits the sample, different types of signals are produced, including secondary electrons (SE), back-scattered electrons (BSE), characteristic X-ray, light and transmitted electrons. (Figure 2.2 a) Back scattered electrons are electrons (Figure 2.2 c) which have been emitted from the primary beam and have reacted elastically with the sample's atoms, thus having very little energy loss. Meanwhile emitted lower-energy electrons resulting from inelastic scattering are called secondary electrons, (Figure 2.2b) which transfer part of their energy to the sample. Imaging with secondary electrons provides information about morphology of the sample surface, since more secondary electron can leave the sample at edges leading to increased brightness there, called edge effects. And as there is a proportional relationship between the intensity of back scattered electrons and atomic number of the atoms, imaging with back scattered electrons provides information about the composition of the sample. To create an SEM image, the incident electron beam is directed onto the surface of a sample. The emitted electrons in the scanned region are received by an electron detector. The morphology of the sample is displayed by synchronizing the position of emitted electrons and that of incident electron beam.

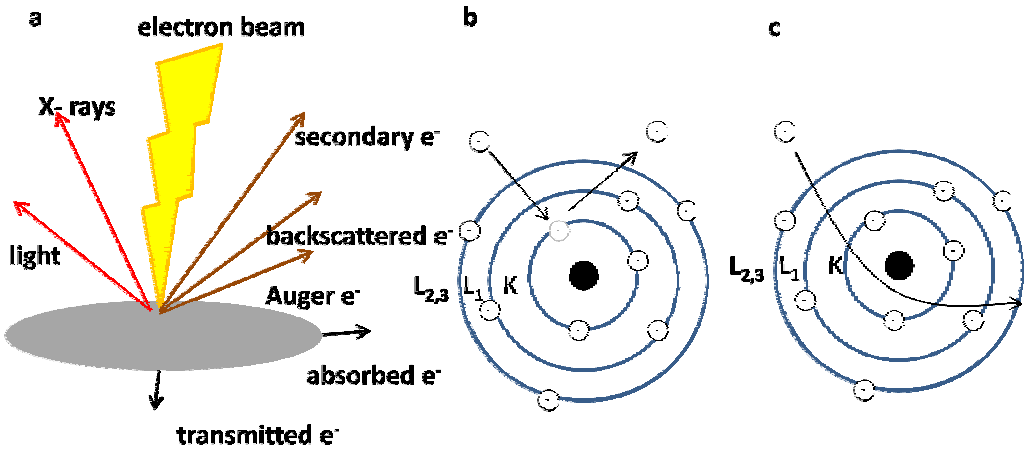

Figure 2.2 a)The interactions between electron beam and samples. b) Secondary electron (SE). c) Back scattered electron (BSE)

2.1.3 Transmission electron microscopy (TEM)

Transmission electron microscopy is a microscopy in which a high energy electron beam is transmitted through ultra thin specimens, and interacts with the specimens as it passes through it. The TEM image is created by collecting electrons that are transmitted through the sample. A magnified image is firstly formed by the objective lens, which can focus the transmitted electrons, and the image is further magnified by the projective lenses to create the final image that are presented on a fluorescent screen or a CCD camera. Compared with SEM, which creates images by collecting electrons emitted from or near the surface of the sample, TEM provides a much higher resolution than SEM, that allows it to facilitate the analysis of the sample features at atomic scale.

2.1.4 BET method

Brunauer-Emmett-Teller (BET) theory was developed to determine surface area from

nitrogen adsorption isotherms and to explain multilayer gas adsorption onto flat surfaces, which was firstly published in 1938.[4]The determination is usually carried out at the boiling point of liquid nitrogen (77 K), and the amount of gas adsorbed can be measured by continuous flow procedure. The adsorption isotherm is the plot of the amount of gas adsorbed as a function of the relative pressure P/P_0, which is described as:

$$\frac{1}{[Va(\frac{P_0}{P}-1)]} = \frac{C-1}{V_m C} \times \frac{P}{P_0} + \frac{1}{V_m C}$$

where P is the partial vapour pressure of adsorbate gas in equilibrium with the surface at 77K, P_0 is the saturated pressure of adsorbate gas, Va is volume of gas adsorbed at standard temperature and pressure, V_m is the volume of gas adsorbed at standard temperature and pressure to produce an apparent monolayer on the sample surface, C is dimensionless constant that is related to the enthalpy of adsorption of the adsorbate gas on the sample.

The surface area can be calculated with the formula

$$\mathrm{S} = \frac{V_m \mathrm{N_a}}{m \times 22400},$$

where N_a is Avogadro constant, m is the mass of test powder, and 22400 is the volume occupied at STP allowing for minor departures from the ideal in milliliters

2.1.5 Elemental analysis

Elemental analysis is an experiment that determines the amount of an element in a

compound, usually in a weight percent. The most common type of elemental analysis is for carbon, hydrogen and nitrogen, which is accomplished by combustion analysis. In this analysis technique, a sample is burned in an excess oxygen and various traps, the combustion products carbon dioxide, water and nitric oxide are then collected.

2.1.6 FTIR and UV-Vis spectroscopy

Fourier transform infrared (FTIR) spectroscopy is used to obtain an infrared spectrum of absorption of a solid, liquid or gas in a wide range normally from 400-4000cm^{-1}. During the measurement, IR radiation is passed through a sample, part of the radiation is absorbed by the sample while part of it is transmitted. The molecular absorption and transmission create a spectrum of the sample, much like a fingerprint, since no two unique molecule structures produce the same infrared spectrum.

Ultraviolet-visible (UV-Vis) spectroscopy is to investigate the ability of a compound to absorb light in the visible, near-UV and near-infrared ranges of the electromagnetic spectrum in a range from 800-200 nm. Beer's Law states that the absorbance of a solution is directly proportional to the concentration of the absorbing species in the solution and the path length. For a fixed path length, UV-Vis spectroscopy can be used to determine the concentration of absorbing species in the solution.

2.1.7 Thermogravimetric Analysis

Thermogravimetric Analysis (TGA) measures weight changes in a material as a function of temperature or time under a controlled atmosphere, which is used to

evaluate the thermal stability of a material. If the sample is thermally stable, there will be no observed mass change. Three ways can result in mass change of the material are chemical reactions, the release of adsorbed species and decomposition, when further increasing the heating temperature. During a TGA measurement, the material is heated or cooled in a sample pan, which is resided in a furnace and supported by a precision balance to monitor the mass of sample. And the atmosphere, either inert or reactive, is controlled by a sample purge gas, which would flow over the sample and exit through an exhaust.

2.2 Experimental methods

There are three key techniques to achieve high photocatalytic activity g-CN product from DCDA in our experiment, thus sol-gel process, templating method and freeze drying. This chapter would focus on sol-gel and freeze drying process, since templating methods have been already carefully discussed in the introduction.

2.2.1 Sol-gel process

The sol-gel process is a method that used to produce solid materials from small molecules. A "sol" is a stable suspension of colloidal particles surrounded by a liquid, in which the particles are rather small, to overcome gravity and allow their dispersion in liquid. And a "gel" is an porous three-dimension interconnected solid network that expands in a stable model throughout a liquid medium, which is only limited by the container.[5] The first step of this chemical procedure is the formation of either colloidal particles or polymeric gels, depending on the chemical properties of

precursors. In order to get the desired ceramic, the obtained colloidal particles would then be treated via one of the conventional processing techniques, including cold pressing, hot pressing and sintering, or dispersed into a stable sol before being transformed into a gel. Also, sols and gels can be spun into fibers or transformed into a coating material if required. The second step is a drying process, in which the remaining solvent is removed, typically accompanied by shrinkage and densification. The rate of the removal of solvent is determined by the distribution of porosity in the gel. During the drying process, monosized droplets are formed, which can reach several hundred micrometers in diameter. Afterwards, a thermal treatment is needed to obtain the final products and enhance mechanical properties and structural stability via the polycondensation of precursor.

As a low-temperature method to produce ceramics and glasses with high purity and homogeneity, by using inorganic precursors, sol-gel process has witnessed great successes in manufacturing a wide range of products, especially the oxides of silicon and titanium. [6,7] In metal oxides synthesis, metal alkoxides are most popular precursor because they react readily with water. Tetramethoxysilane (TMOS) and tetraethoxysilane (TEOS) are most widely used metal alkoxide precursors, in which the alkoxide group (OR) would then be replaced by hydroxyl groups (OH) through a hydrolysis reaction, with the addition of water. Subsequent condensation reactions involve the silanol groups (Si-OH) produce siloxane bonds (Si-O-Si) and the by-products of water or alcohol. As the number of siloxane bonds increases, the individual molecules would then be bridged and aggregate into the sol or inter-knit into a network to form gel. Afterwards, the by-products of water or alcohol are removed, and the network shrinks and further condensation occurs upon drying process. Final calcination of gels would yield mesoporous products, which can be applied as promising sensing materials, since they possess photocatalytic activity and good optical charateristic.[8]

More interestingly, there are lots of examples of sol-gel process to synthesize g-CN.

For instance, Kailasam*et al.* employed afacilesol-gel route to mesoporous carbon nitride or alternatively mesoporous silica, by evaporating the mixture of cyanamide and TEOS to form gel, which was then heated to form silica/g-CN composite, following by the removal of one of the phases to obtain final product.[9]By simply adjusting the ratio of cyanamide to TEOS in starting precursor, the porous characteristics of materials can be tuned, including surface area, pore volumes and pore sizes. This simple sol-gel process can also increase the photocatalytic activity of g-CN materials, which is much higher than that of bulk g-CN and pre-formed silica templating g-CN.

Moreover, Zhang *et al.* illustrated that the chemical protonation of g-CN solid with concentrated HNO_3 can form a stable colloidal suspension via a sol process, since the powerful oxidizing strength of NO_3^- can easily break the structural hydrogen bonding of g-CN units, and facilitate the depolymerization. As a soft matter, this g-CN colloidal suspension with high flexibility and compatibility widens the preparation of g-CN based nanocomposites, including hybrid of g-CN/carbon nanotube, and the thin-film electrode, which are fabricated by coating the suspension on FTO glass and further heat treatment.[10]Compared with g-CN thin film that obtained by physical methods under non-equilibrium conditions, such as plasma jet chemical vapor or pulsed-laser deposition, the sol-gel process gives a better crystallinity and richer nitrogen content in matrix, which would improve their photoinduction performance. Also, it is easy to address the problem of the abundant boundary defects and the poor contact between particles and substrates in manufacturing thin-film electrodes via sol-gel process.

In summary, the advantages of sol-gel process are: 1. Compatible with many organic or inorganic reagents. 2. High chemical and thermal stability. 3. Easy to manufacture monoliths or thin film with uniform pore size distribution and controllable surface area. 4. The densification can be achieved at lower temperature compared to traditional process. And all those advantages would result in porous

photocatalystswith high performance.

2.2.2 Freeze drying

Freeze-drying, also known as lyophilisation, is a typical dehydration process to sublime frozen water in the material by reducing the surrounding pressure, which was first developed as a commercial technique in World War 2to ensure chemically stability and viability of serum during transport, without having to be refrigerated. After then, the applications of this technique have been widened to many fields, including the processing of food, pharmaceuticals and biotechnology. To be specific, the use of freeze-drying on ginger leaves can significantly preserve their antioxidant properties (AOP), compared with other drying methods, making this method can be applied to produce high-value speciality tea or spice ginger leaves powder.[11]And in biotechnology, the freeze-drying method allows the long-term storage of intact RNA and helps elucidate the pathogenesis of CaP (carcinoma of the prostate), which was illustrated in the study by Tsuka et al.[12]As a treatment on target materials, freeze-drying process gives the following desirable characteristics, the first is the preservation of the primary physical and chemical characteristics of the materials, the second is an acceptable relative humidity, and the last is long-term stability.[13]

A typical freeze-drying process consists of three steps, thus freezing step, primary drying step and secondary drying. The first step of freezing forms ice crystals of pure water, increases concentration of the liquid suspension and its viscosity, which would induce inhibition of further crystallization, resulting in an amorphous or combined amorphous crystalline phase.[13] After then, the primary drying step would remove ice from the product via sublimation, leaving pores in the sample, which was once occupied by ice crystal.[14] At last, the adsorbed water, which did not separate out

as ice during freezing step and did not sublime off would be removed in secondary drying step. By freezing the precursor and subliming water inside, the collapse of its structure can be avoided, which is expected to result in high photocatalytic activity, in our study.

2.3 Experimental details

Synthesis method. All reagents were purchased from Sigma Aldrich. Aqueous dicyandiamide (DCDA, 99 %, 5 g) was heated in deionized water (50 mL) with different amounts of biopolymers and 10 % $Mg(NO_3)_2.6H_2O$ aqueous solution to form a homogeneous solution. The solutions were then frozen with liquid nitrogen followed by freeze drying to obtain white sponge-like structure solid with negligible shrinkage compared to original gel that formed at room temperature. The white solids were heated to 550 °C in air for 4 hours with a 2.3 °C/min ramp rate. The obtained g-CN solids were ground into fine powders and soaked in diluted nitric acid (50 mL, 1M) for 24 hours followed by washing several times with water then drying in an oven. The air bubbles that produced during the contact of the solid with the acid indicated the removal of MgO. The sample was named after its preparation method. For instance, D5-agar-x-F-Mg-y, where D5 is 5g DCDA solid, agar-x denotes the mass of agar powder, F means freeze drying and Mg-y indicates the mass (g) of 10% (by weight) of $Mg(NO_3)_2$ solution.

Different series of samples were prepared, including those without biopolymers, without $Mg(NO_3)_2$, and just directly heating DCDA as the control experiment. To identify the effect of freeze drying, some solutions were dried in an oven at 80℃ rather than freeze drying. Also, to give a wider investigation of precursors, melamine was dissolved in water, followed by adding alginate, the solution was then added to

10 % (by mass) H_2SO_4 in dropwise fashion to form beads. The beads were collected and carefully washed with water before furnace calcination. (Table 2.1)

Group name	Samples
Control	D5, D5-F
Oven dried	D5-agar-x, D5-gelatin-x, D5-dextran-x
Freeze dried	D5-agar-x-F
Triple templates	D5-agar-x-F-Mg-y
Others	10g melamine+ 2g alginate sodium in 10% H_2SO_4 (Not success)

Table 2.1 samples of different groups that synthesized in our research

Photocatalysis experiment. The evaluation of photocatalytic activity was carried outusing the degradation of rhodamine B (RhB), under visible light (λ>420 nm). A 300 W xenon lamp with a 420 nm cutoff filter and a cooling water jacket outside was used as the light source. In a typical RhB degradation experiment, 0.02g sample powder was dispersed in 200ml of RhB aqueous solution (5mg/L) in a tube. To ensure an adsorption-desorption equilibrium between the RhB and the sample, the solution was firstly stirred in dark for 1 hour. Samples were collected with a syringe every 5 minutes, then filtered and transferred into cuvettes before running on UV-Vis.Characterization. X-ray diffraction (XRD) patterns were collected by a Panalytical Empyrean X-ray diffractometer (Cu Ka_1 irradiation= 1.5406 Å). A Philips XL-30 FEG Environmental SEM with Oxford INCA was used to obtain scanning electron microscopy images. Transmission electron microscopy was carried out on a JEOL 2100 200 KV LaB_6 TEM with Oxford INCA EDS. UV-Vis diffuse reflectance spectra were collected by a Varian Cary 5000 Scan UV-Vis spectrophotometer fitted with a Praying Mantis, and barium sulfate ($BaSO_4$) was used as the background sample. Also the spectrophotometer was used to evaluate RhB solution from

photocatalysisexperiments. Fourier transformed infrared (FTIR) were recorded by a Nicolet Magna 670 FTIR spectrometer. N_2 adsorption-desorption isotherms were collected at 77K by a Nova-e porosimeter (Quantachrome, USA) to calculate Brunauer-Emmett-Teller (BET) surface area.

Chapter reference

1.W. Friedrich, P. Knipping, von M. Laue, Sitzungsberichte der MathematischPhysikalischenClasse der Königlich-BayerischenAkademie der WissenschaftenzuMünchen 1912.

2. Y. Li, PhD thesis, LMU München, Munich, 2012, p. 31.

3. H Wang, PhD thesis, LMU München, Munich, 2013, p.23.

4. S. Brunauer, P. H. Emmett, E. Teller. *J. Am. Chem. Soc,* 1938, 60, 309

5. A. C. Pierre. *Introduction to sol-gel processing*.Springer Science& Business Media, 2013.

6. Peng F, Cai L, Huang L, Yu H, Wang H.*J. Phys. Chem. Solids*, 2008, 69,1657

7. M. Aziz, S. S. Abbas, W. R. W. Baharom, W. Z. W. Mahmud. Mater. Letters, 2012, 74; 62-64

8. Klein, L. C. (Ed). *Sol-gel optics.Processing and applications.*Kluwer Academic Publishers, Norwell, MA, 1994.

9. K. Kailasam, J. D. Epping, A. Thomas, S. Losse and H. Junge.*Energy. Environ. Sci*, 2011,4,4668.

10. J. Zhang, M. Zhang, L. Lin, X. Wang.*Angew.Chem,* 2015, 127, 6395.

11. E. W. C. Chan, L. L. Lim, S. K. Wong, K. K. Lim, S. P. Tan, F. S. Lianto, M. Y. Yong. *Food. Chem,* 2009, 113, 166-172.

12. H. Tsuka, H. Mori, K. Okada, S. Matsukawa. Analy.Biochem. 1997, 247, 458-461.

13. W. Abdelwahed, G. Degobert, S. Stainmesse, H. Fessi. *Adv. Drug. Delivery.Rev.* 2006, 8,1688.

14. N. A. Williams, G. P. Polli. J. Parenter.*Sci. Technol.* 1984, 38, 48.

Result and discussion

3.1 Biopolymers as templates

As a promising candidate to template g-CN, biopolymers have advantages such as well-defined chain lengths, monomer sequences with specific functional, stereochemistry, and bind to the precursor DCDA tightly. Also they are natural abundant and can be produced industrially on a large scale. [1] In the first series of our experiment, different biopolymers, including agar, gelatin and dextrans were added to DCDA solution as the templates, to study and compare their influences on the crystallization of g-CN solid.

The XRD patterns (Figure 3.1) firstly confirmed that the presence of biopolymers does not hinder the formation of graphitic carbon nitride. The characteristic peak at ~27.4 is an inter-layer stacking peak of the g-CN layers, was indexed as (002), reflecting an interlayer distance of 0.336 nm for g-CN. The other peak at 13.1 is related to an in-plane structural packing motif, indexing as (100). The similar XRD patterns of biotemplating g-CN prove that graphitic structure of the samples almost stay the same with respect to that of a control sample, which was prepared by directly heating DCDA in furnace.

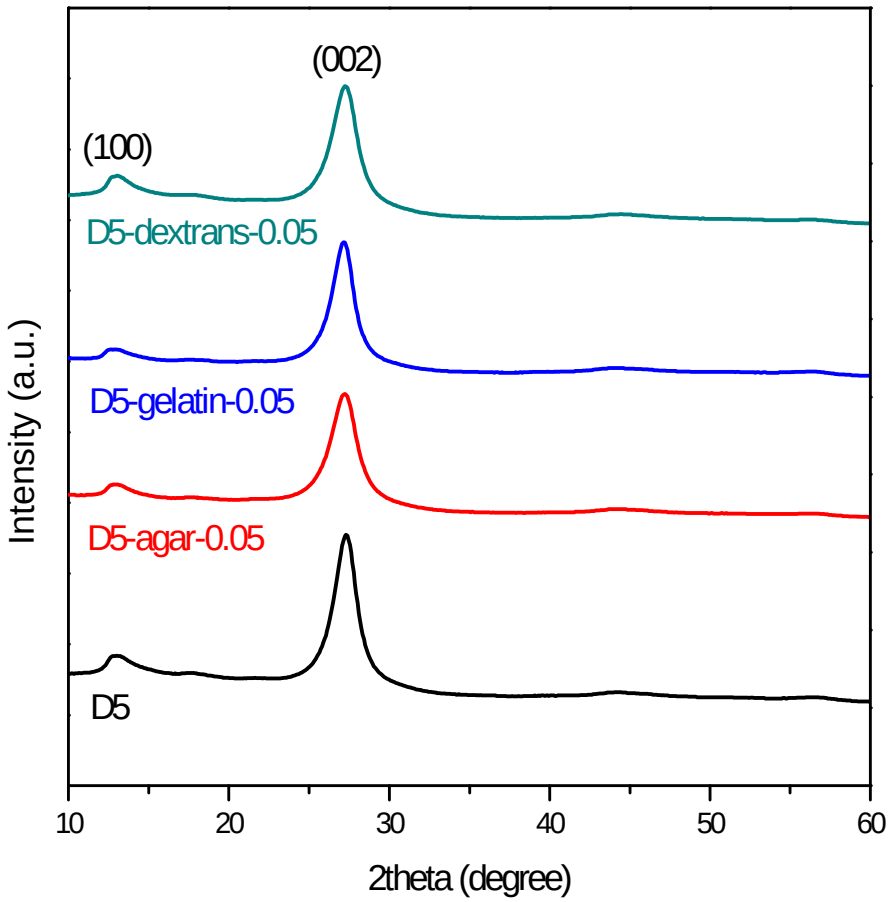

Figure 3.1 XRD patterns for biopolymer-templated g-CN vs control experiment

The second proof of the unchanged structure of the biotemplating g-CN is Fourier transform infrared (FTIR) spectra for samples vs a g-CN control, (Figure 3.2) which indicated g-CN sample was successfully prepared by showing typical stretches of extended C-N network ranging from 800 to 1700 cm^{-1}. It can be detected from biotemplating samples the typical breathing mode of the tri-s-triazine units at 809cm^{-1} and the aromatic C-N heterocycle stretches at 1200-1700 cm^{-1}, which proves that the -C=N- conjugated network of g-CN almost stayed unchanged after biotemplating.

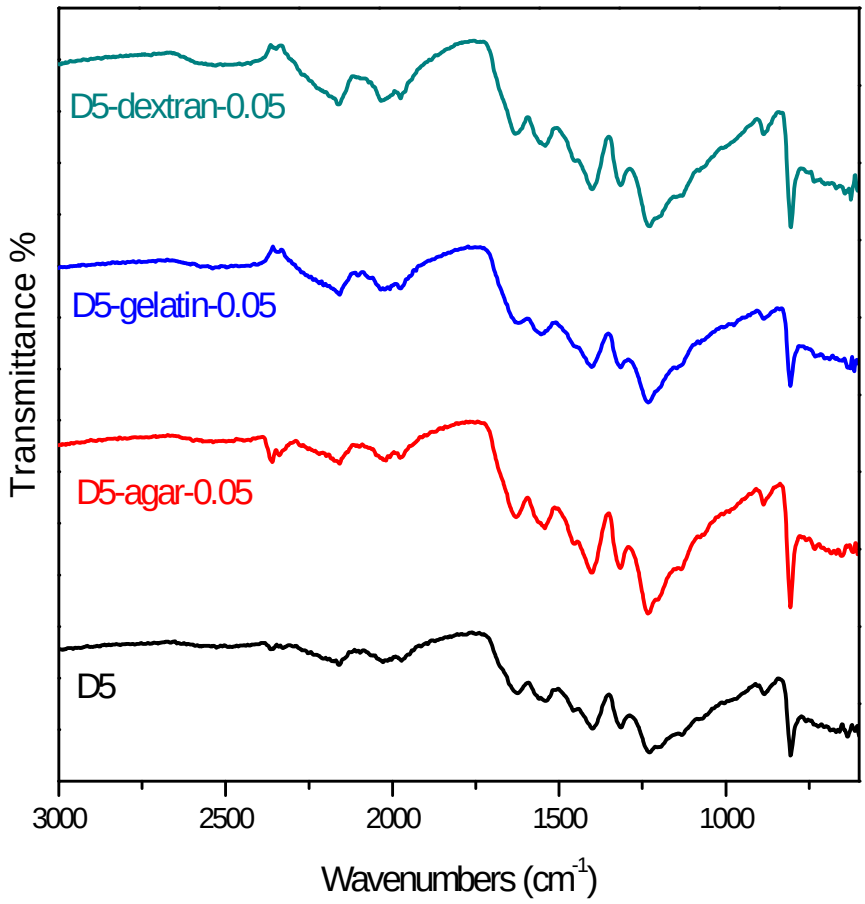

Figure 3.2 FTIR spectra for biopolymer-templated g-CN vs control samples.

To give an investigation on how biopolymers influence self-assembly of DCDA to g-CN, it is necessary to study the morphologies by running the samples on Scanning Electron Microscopy (SEM). (Figure 3.3) Indeed, the SEM image of control g-CN sample (D5) showed a bulky, irregularlyshaped solids whereas agar and gelatin templating g-CN (D5-agar-0.1 and D5-gelatin-0.1) gave the materials a rough surface with features <100 nm in dimensions, suggesting that these two biopolymers have played a role in structuring g-CN solid. However, the bulky solids with wide size distribution after dextrans templating g-CN indicated that dextrans is not a promising choice to be the template.

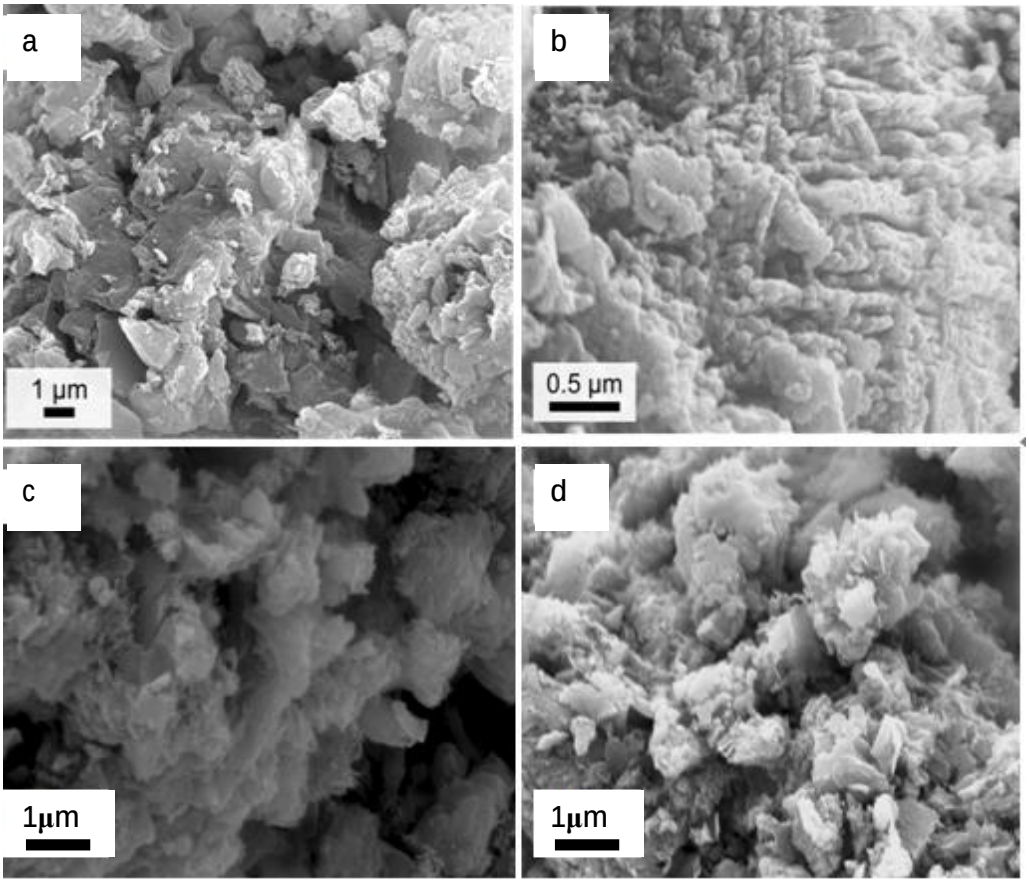

Figure 3.3 SEM images of a) D5; b) D5-agar-0.1; c) D5-gelatin-0.1; d) D5-dextrans-0.1

To stabilize the properties of biotemplating g-CN, the priority is to ensure the homogeneity of the precursor and templates, which means both of them can dissolve in water well. We once tried to dissolve the same mass (5 g) melamine and alginate sodium in water, then transferred to diluted H_2SO_4 (10 % by weight) to form melamine sulfate beads, as the precursors, which was calcined to g-CN afterwards. However, the poor solubility of melamine in water makes it hard to ensure the homogeneity of the precursor and templates. Also, when we tried agar gel (10g agar powder dissolved in 90 g water then cooled to room temperature) instead of agar powder as the template, the gel didn't well dissolved in DCDA water solution, making it unsuitable to template DCDA.

All experimental phenomenon make it clear that both agar and gelatin powder are promising choice to template DCDA, as they can form strong gel in DCDA solution and influence the crystallization of g-CN solid, resulting in rough surface with potentially more active catalytic sites. Besides, the morphologies of agar and gelatin templating g-CN didn't show too much difference, it is a time to select one between them to do further study. As a candidate for templating g-CN, agar does not contain any nitrogen or sulfur so there is no risk of contaminating the sample,andthere was no report focused on agar templating g-CN before, to our best knowledge,making agar chosen as the template in the following investigation.Toenhance the effect of agar and introduce porosity to enhance g-CN performance, freeze drying and $Mg(NO_3)_2$ were also involved in synthesis methods, which was never reported by people before.

3.2 Agar templating g-CN and freeze drying

Agar can form strong gels in cold water to bind precursor and produce porous and homogeneous foams after freeze drying process, making it possible enhance the performance of g-CN product. The effect of freeze drying and the optimum concentration of agar in DCDA solution were investigated in this chapter, and the data in Chapter 3 was selected from our previous study. (Attached document B)

After heating freeze dried agar/DCDA mixture to 550 °C, agar-templated g-CN products were finally obtained with different colors, from pale yellow to orange, brown and black, (Figure 3.4 a-e) reflecting amorphous carbon residue from the decomposed agar, which was consistent with increasing in agar content, moving from pale yellow (the control sample) to black (0.5 g agar, highest concentration).

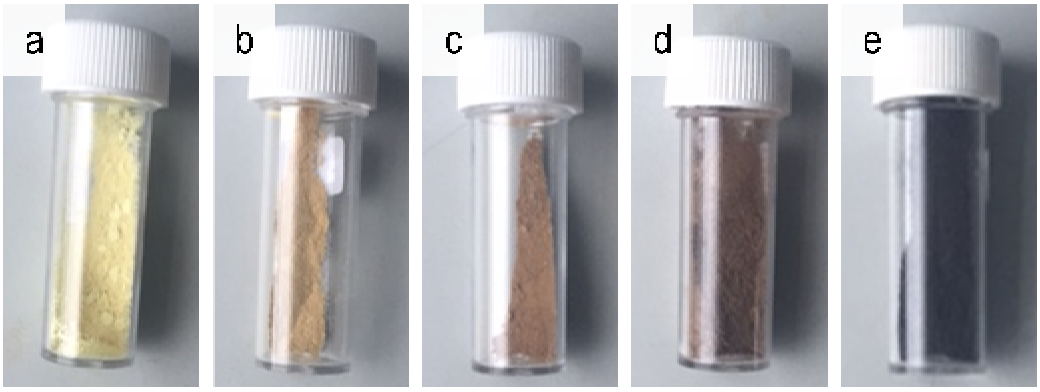

Figure 3.4 Photos of samples a) D5-F; b)D5-agar-0.01-F; c) D5-agar-0.05-F; d) D5-agar-0.1-F; e) D5-agar-0.5-F. SEM images of f) D5-F; g) D5-agar-0.01-F.

The effect of freeze drying and the concentration of agar in DCDA solution was evaluated by using the samples as catalysts in photodegradation of Rhodamine B (RhB), an organic dye, under visible light, which is a common method to evaluate the photocatalytic activities of g-CN [2,3] and metal containing carbon nitride [4,5]. The peak intensity at the maximum of 554 nm in the UV-Vis absorbance spectrum against time for oven dried and freeze dried samples with different concentration agar were plotted to study their decoloration performance (Figure 3.5 a). Although the SEM image shows agar influenced the crystallization of g-CN solid, the result from photodegradation of Rhodamine B suggests that no obvious change was observed in photocatalytic activity with only agar to template g-CN, compared to the control sample (D5). (Figure 3.5 b) This may be due to shrinkage of the precursors during the oven drying process, which was caused by the capillary forces in the agar gel, leading to collapse of the network and resulting in materials possess very low porosity and poor photocatalytic activity. To avoid the capillary forces in the agar gel collapsing the network of product during the oven drying process, freeze drying was introduced to the preparation of agar templating g-CN. Interestingly, even freeze drying a solution of DCDA (D5-F) can resulted in a small increase in activity compared to that of oven drying control sample (D5), (Figure 3.5 b) since the freeze drying process removes

water through sublimation rather than evaporation in a oven drying step, which effectively avoids the shrinkage of the precursors and eliminates the effect of capillary forces.

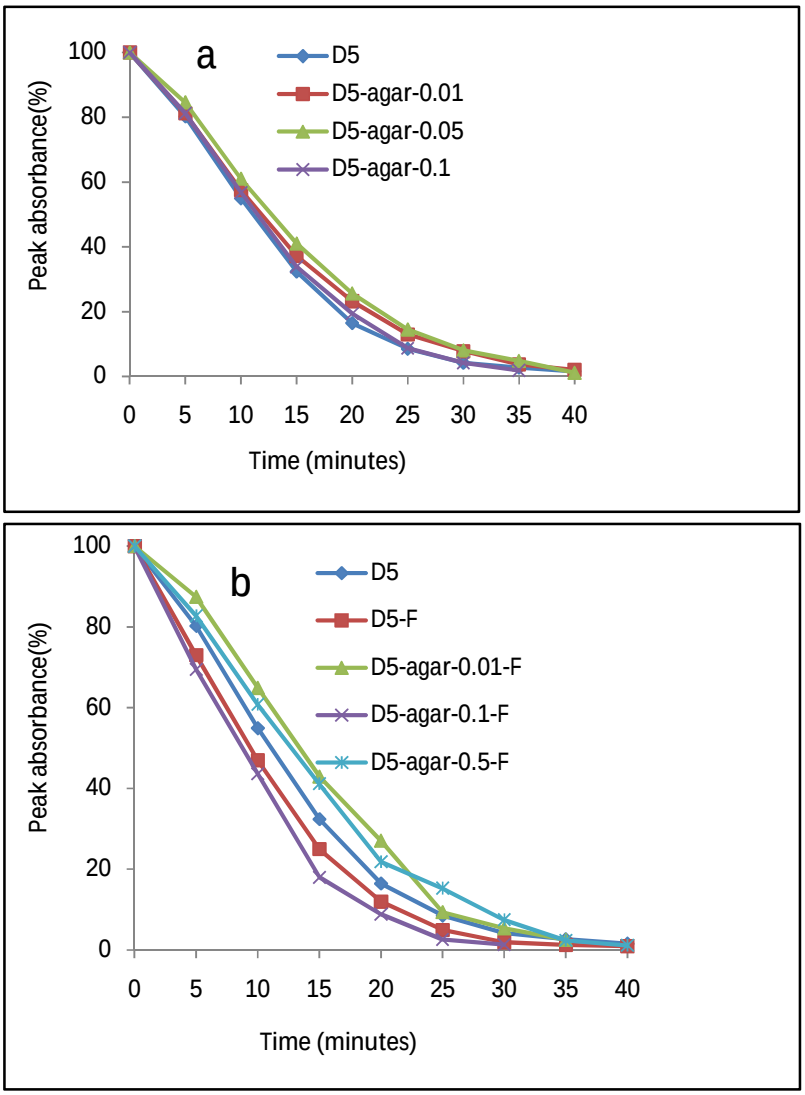

Figure 3.5 Photodegradation of Rhodamine B over time plotted from the intensity of UV-Vis peak absorbance at 554 nm for a) oven dried and b) freeze dried samples

The concentration of agar in DCDA solution to influence photocatalytic activity during freeze drying process was studied by adding different amounts of agar, from very small amount (0.01 g) to large amount (0.5 g). When the concentration of agar is too low, it is hard to influence crystallization of DCDA precursor and so may have little or no influence on templating the sample. When 0.5 g agar was added to DCDA solution, the low activity of the sample is probably due to the high carbon residue from agar. (Figure 3.5 b) In this case, a certain amount but not too much (0.1g) can enhance absorption of visible light and improve photocatalytic activity. However, if excess agar is added, it produces too much carbon residue, resulting in the material to be a nitrogen-doped carbon rather than a graphitic carbon nitride, which would dramatically decrease photocatalytic properties.[6] And in fact, the combination of freeze drying and agar slightly improves the performance of g-CN materials, but it doesn't offer a significant improvement. On one hand, it indeed points out a possible route to template bulky g-CN with low-efficiency. However, to further improve its photocatalytic activity is still a challenge.

To give a further investigation on the excess carbon from agar, elemental analysis was carried out. Once increase the amount of agar, the molar ratio of C/N changes from 0.67 to 0.74, (Table 3.1) which is consistent with the increasing in carbon content, also can be observed by color change of samples, from pale yellow to black. The slight increase in carbon content is also consistent with the ratio of g-CN to carbon after calcination, since the theoretical yield of DCDA to g-CN is 3.7 g and the maximum yield of carbon from 0.5 g agar is 0.2 g (by only releasing H_2O). All samples showed a small (~5 %) excess of nitrogen when compared to the theoretical value of C/N ratio (0.75). This is consistent with what we have mentioned in the Introduction part, the idealized g-CN structure never exists due to the difficulty of fully condensation of the precursors via release of NH_3. The amine condensation is not complete in the samples, leaving excess nitrogen content.

Composition (weight %)	C	N	H
D5	34.4	59.8	1.91
D5-agar-0.01-F	34.3	59.7	1.90
D5-agar-0.1-F	34.1	58.3	1.91
D5-agar-0.5-F	35.3	55.2	2.00

Table 3.1 Elemental analysis of samples prepared with increasing agar content.

Thermogravimetric analysis was also used to study the thermal stability and decomposition of agar. (Figure 3.6) The 20% mass remaining at near 600°C indicated the carbon residue, which can also be observed from black powder in crucible after calcination. The dramatic mass loss in the temperature zone between 300 to 380°C suggested the decomposition of agar occurred, which makes agar a promising optionto template g-CN, since it high thermal stability allows it still exist at high temperature, where the condensation from DCDA to "melem" (the structural unit of idealized g-CN) starts, meaning agar can better guide nucleation and growth of g-CN crystals when compared to some polymers that decompose at relatively lower temperature. Besides, the carbonized agar can combine with g-CN network, enhance its ability to absorb visible light and also act as porogens in the formation of g-CN macrostructure.

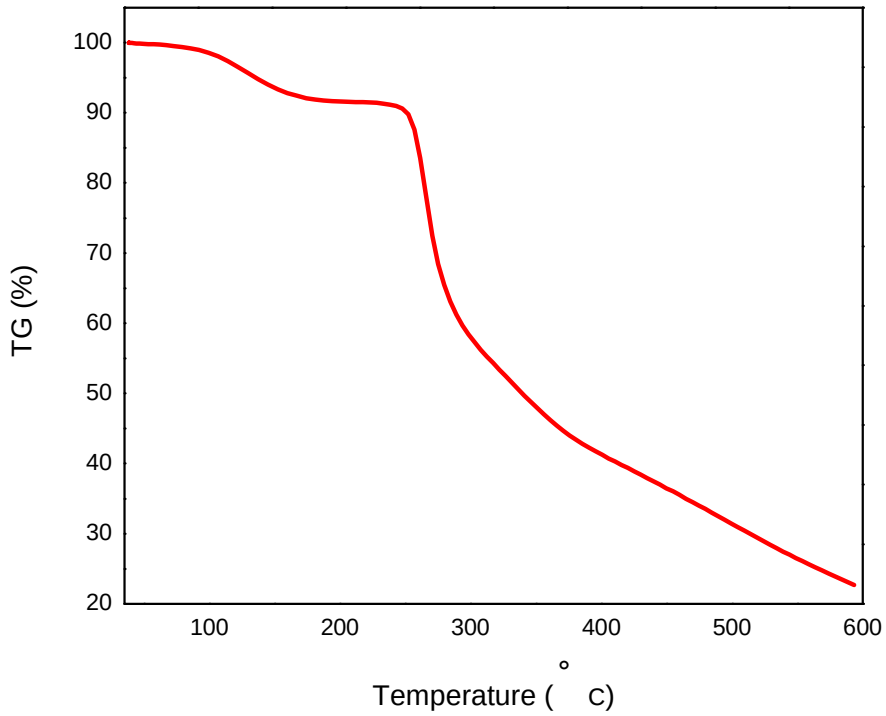

Figure 3.6 TGA curve of agar in air (10 °C/min in air, flow rate 100 mL/min). [22]

The enhancement in photocatalytic activity from the combination of freeze drying and agar can be explained by electron microscopy. Compared to oven-dried samples, the SEM images of freeze-dried ones have a more 'fluffy' appearance, with open and 'sponge-like' structure. (Figure 3.7) Also, bubbles with diameters from 100 to 500 nm can be observed throughout freeze-dried samples, indicating the freeze-drying process maintained the open network structure of agar gel and avoided the capillary force to collapse its network. The oven-dried samples have a rough surface, but they still appeared to be relatively dense, due to the shrinkage of the precursors.

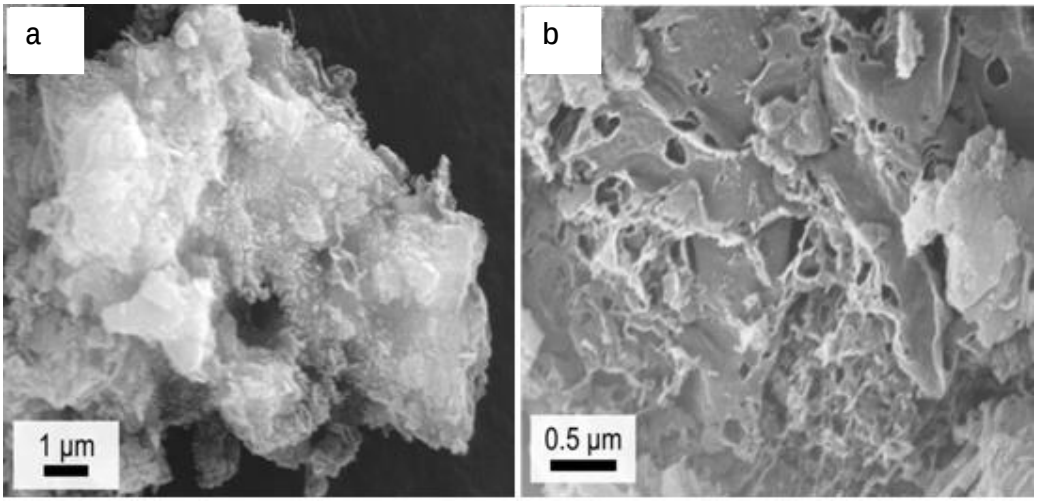

Figure 3.7 SEM images of a) D5-F; b) D5-agar-0.01-F.[22]

To obtain a better view of the open structure of the freeze-dried agar samples, TEM was carried out. Figure 3.8shows TEM images of both freeze and oven dried, compared to oven dried one, open 'bubbles' structure from agar gel can clearly be seen from TEM image of freeze dried sample. Also, nitrogen porosimetry was used to investigate porosity of the open 'bubble' structure. The adsorption/desorption isotherms of both control (D5 and D5-F) and agar templating (D5-agar-0.1 and D5-agar-0.1-F) samples (Figure 3.9) showed the features of type IV isotherms with type H3 hysteresis loops, indicating mesoporosity (pores with diameters of 2-50nm) in the samples. No plateau appeared at high P/P_0 region suggests the existence of macropores (>50nm) in these samples, which can also be seen from electron microscopy images. The isotherms make it clear that freeze drying can significantly increase adsorbed volume with or without agar. However, the meso and macroporosity in freeze dried agar samples didn't significantly affect the BET (Brunauer-Emmett-Teller) surface areas which are 12 m^2/g, 17 m^2/g, 11 m^2/g and 19 m^2/g for D5, D5-F, D5-agar-0.1 and D5-agar-0.1-F respectively. The small increase in BET surface area in freeze dried agar samples may be a factor in the improvement of photocatalytic activity, since more active sites are provided.

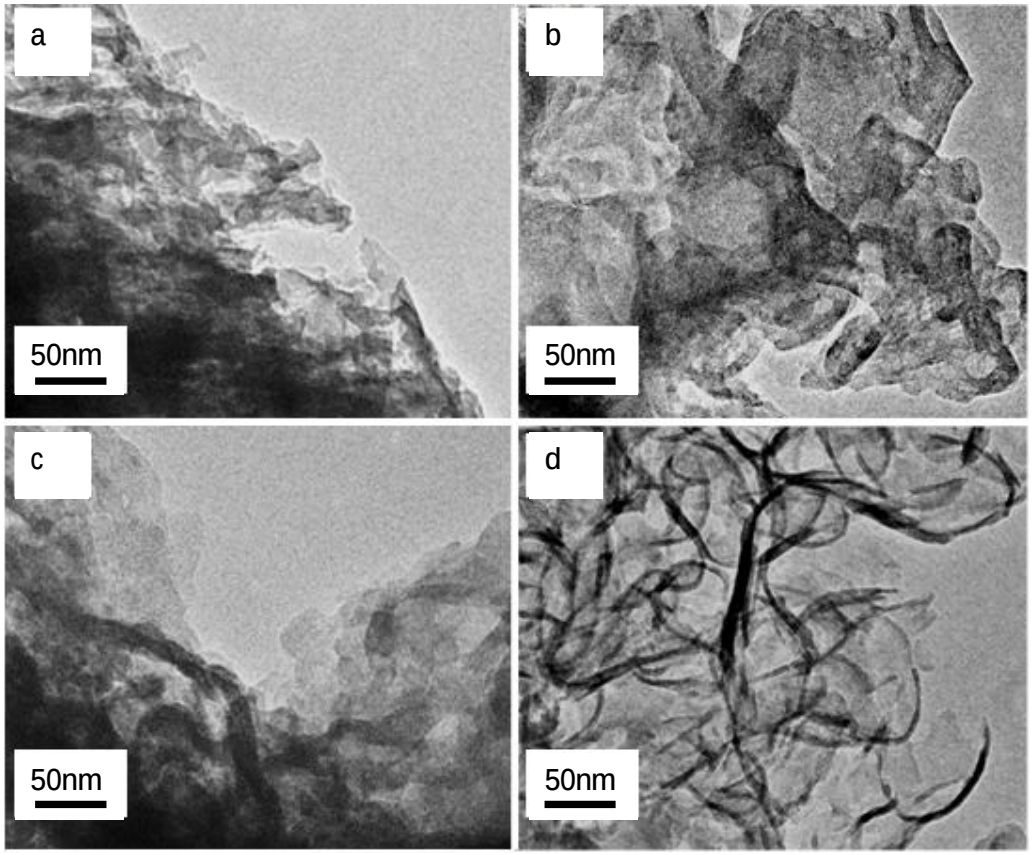

Figure 3.8 TEM images of a) D5; b) D5-F; c) D5-agar-0.01 and d) D5-agar-0.01-F. [22]

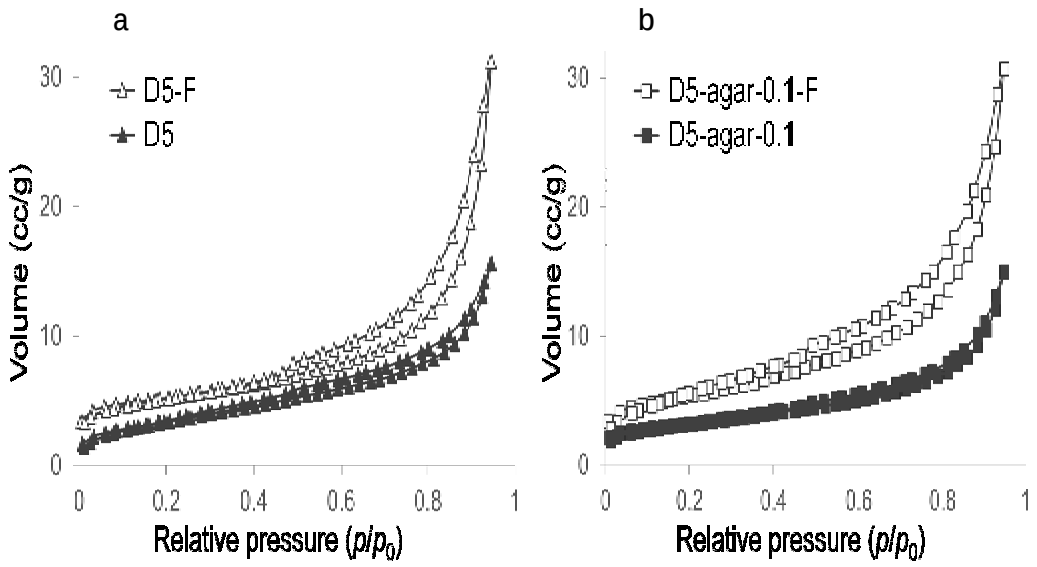

Figure 3.9 Nitrogen absorption/desorption isotherms of a) the control samples; b) agar templating samples. [22]

The biopolymer introduces mesoporosity during the self-assembly of g-CN crystals while the carbon residue and freeze drying process give macroporosity. The combination of air/biopolymer affects the morphologies of the samples and slightly increases photocatalytic activity. To further introduce porosity and enhance photocatalytic properties, a third template, MgO is needed.

3.3 Triple-templating of g-CN

To further improve g-CN performance in degradation of g-CN, we firstly proposed a triple-templating method to create a hierarchical structure of g-CN. Open and porous structure with macroscale pores was obtained by freeze drying, whereas agar control the morphology of g-CN on a meso-scale level. Aqueous $Mg(NO_3)_2$ was added to

initial agar/DCDA gel and then decomposed to produce very small MgO particles, which was finally removed by diluted acid to leave micro pores in g-CN structure, thus working as the third template. (Figure 3.10)

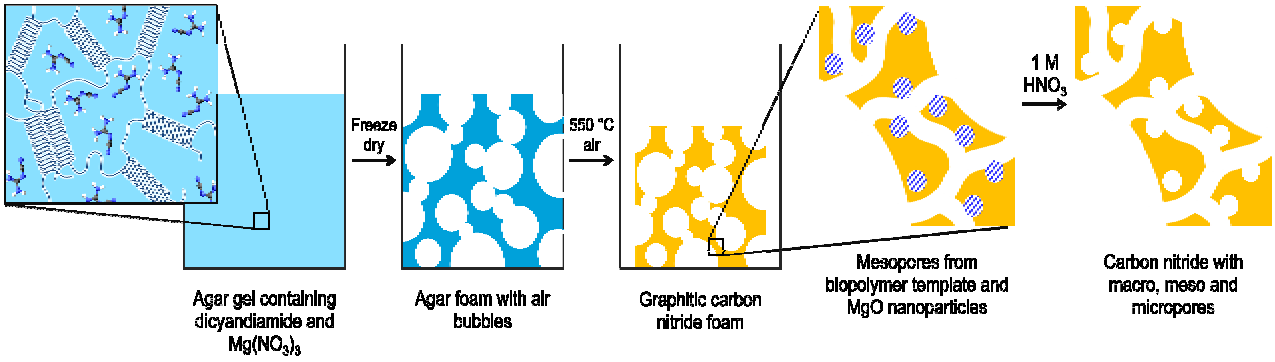

Figure 3.10 Schematic diagram shows the process of triple-templating (air, agar and MgO) method for making porous g-CN.[22]

By adding different amounts of magnesium nitrate (1, 5 and 10 g of 10% solution by weight) in gel with the optimized mass ratio of DCDA: agar of 5: 0.1, the use of MgO in structuring g-CN was studied in this section. (Table 3.2) The observation of slight fizzing when the samples were soaked in 1 M HNO_3 after calcination, indicated a reaction of the acid with the basic magnesium oxide salt. After acid treatment, the final products were characterized by XRD, which has confirmed the formation of g-CN, but the slight shift of (002) peak to a lower angle when increasing the amount of $Mg(NO_3)_2$, indicating a larger interlayer distance. Also, broadening of the (002) peak was observed, indicating a smaller grain size of the samples. The result of XRD patterns showed that the Mg has interacted with the condensation of dicyandiamide and inserted in the g-CN matrix as MgO particles.

Sample codes	Dicyandiamide (g)	Agar (g)	10% $Mg(NO_3)_2$ (g)
D5-agar-0.1-F-Mg-1	5	0.1	1
D5-agar-0.1-F-Mg-5	5	0.1	5
D5-agar-0.1-F-Mg-10	5	0.1	10

Table 3.2.The formula of different tripe-templating g-CN samples.

Indeed, there was a significant improvement in photodegradation of Rhodamine B with those triple-templating g-CN samples. Figure 3.12 a shows the change in absorbance of UV peak over time for control g-CN sample to those with different amount of Mg. The enhancement in photocatalytic properties as increasing the amount of 10% $Mg(NO_3)_2$ solution was shown in UV-Vis, and D5-agar-0.1-F-Mg-10 gave the best result over all the samples by halving the time of degradation compared to bulk g-CN. This is considered to be due to the removal of MgO template with diluted HNO_3 creating pores in g-CN matrix, and providing more active sites for the reaction. To prove it is the porous structure, rather than the addition of MgO to influence the photodegradation, the result of D5-agar-0.1-F-Mg-10 before and after acid wash is also shown in Figure 3.12 b, where clearly suggested MgO must be removed to produce high-performance g-CN product, as it took more than 40 min to decolorize RhB solution with the sample that has not been acid-washed. The photodegradation rate constants (k) was then calculated for various samples, giving a value of 0.18 min^{-1} for D5-agar-0.1-F-Mg-10 compared to a value of 0.11 min^{-1} for the control sample.

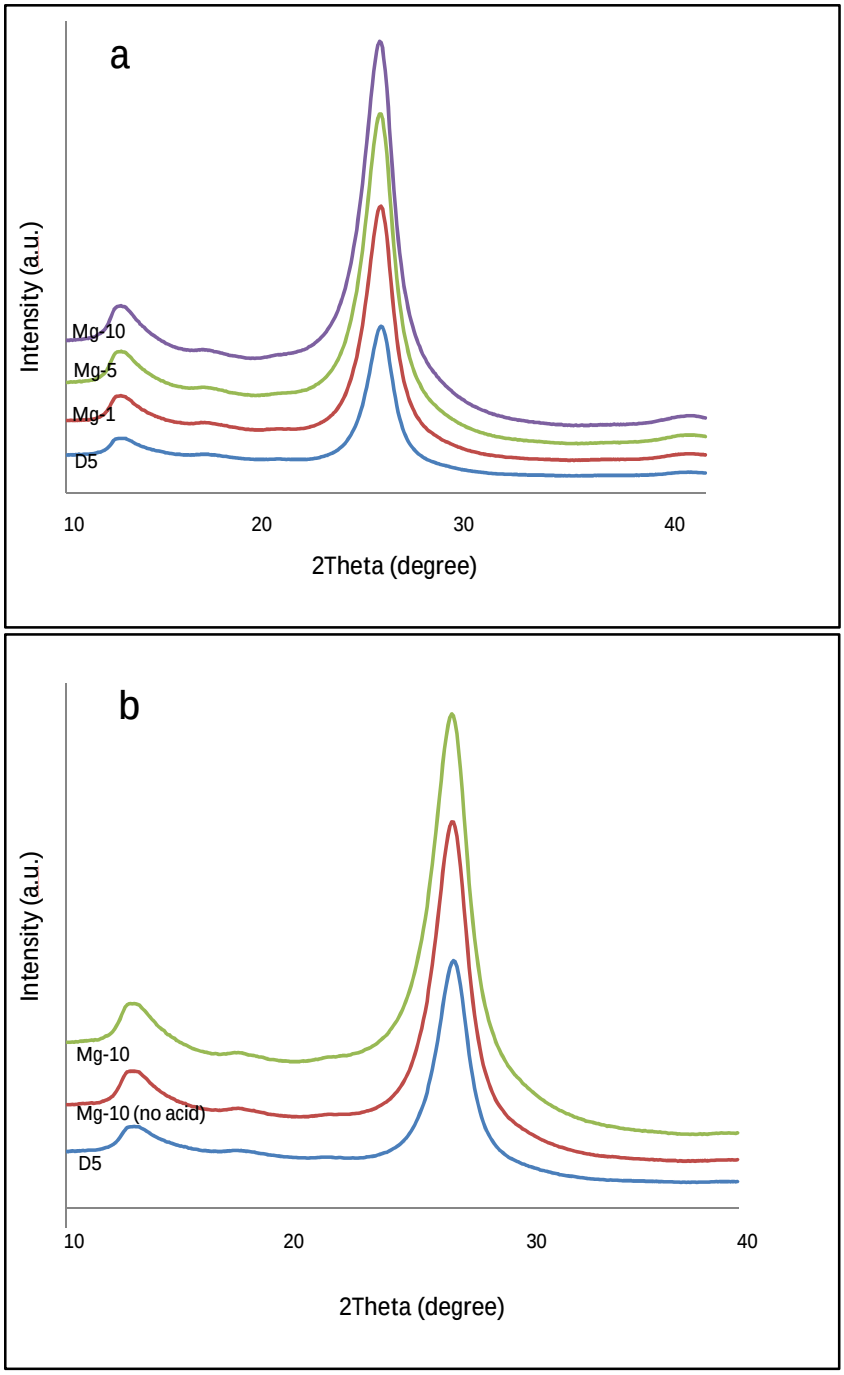

Figure 3.11 a) XRD patterns for a control (D5) sample compared to triple-templating (air, agar and MgO) samples after acid wash. b) XRD patterns indicating the similarity between D5-agar-0.1-F-Mg10 before and after acid wash.

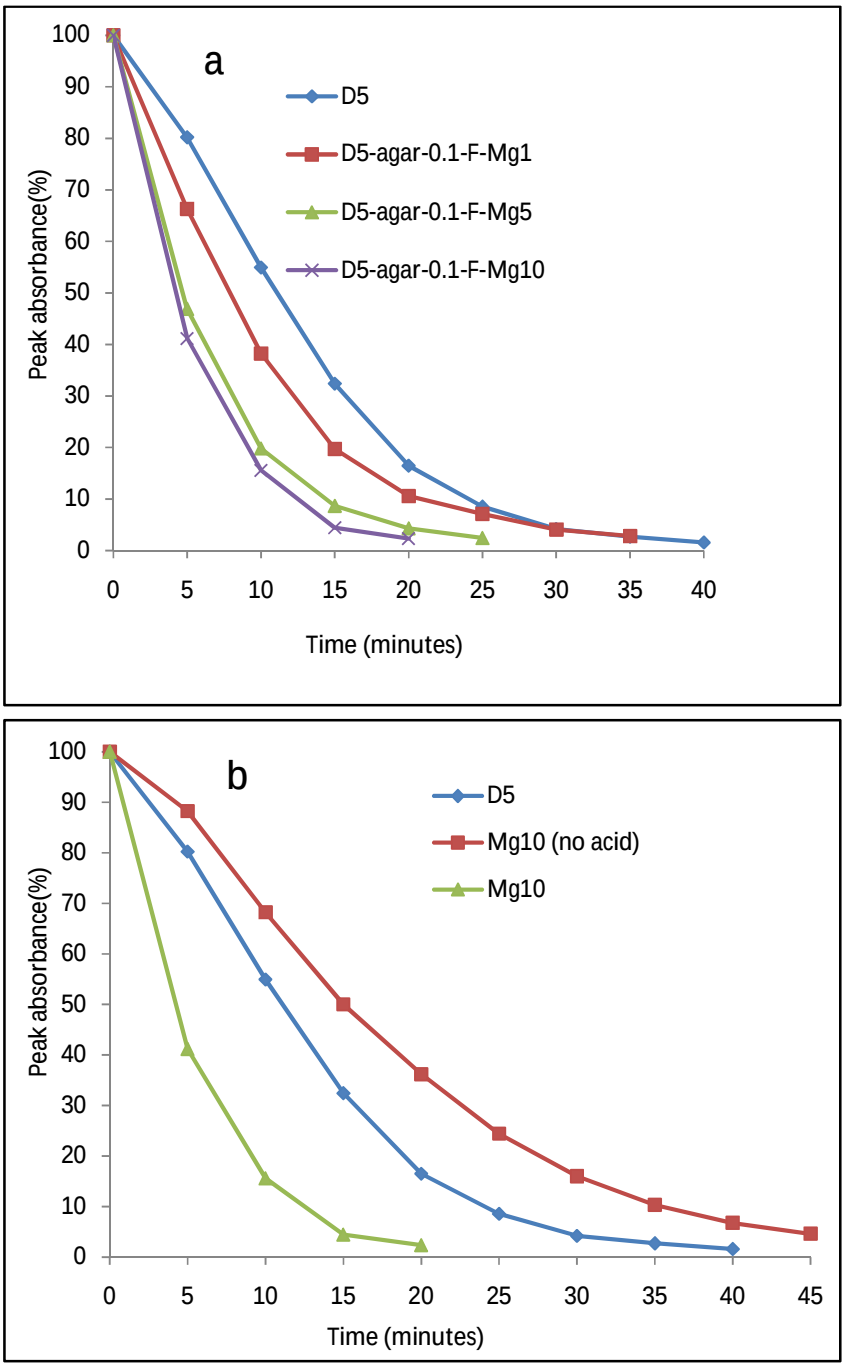

Figure 3.12a) Photodegradation data for a control sample vs triple-templating samples after acid wash. b) Photodegradation data for D5-agar-0.1-F-Mg10 before and after acid wash.

Microscopy techniques were also used to investigate those triple-templating samples. Since the theoretical yield of 5 g DCDA to g-CN is 3.7 g, and that value for MgO is 0.16g when added 10 g $Mg(NO_3)_2$ solution, it was unsurprisingly difficult to identify such low levels of MgO in those samples by using microscopy. Interestingly, the morphologies of triple-templating samples show significant differences compared to sample prepared only with agar and freeze drying. The 'honeycomb' structure with interconnected pores through the material was shown in SEM image, (Figure 3.13 a-c) a grainy appearance can be observed at high resolution. The structure even has no change after acid washing, which was identified by TEM imaging, also indicating MgO particles can't be observed in such small amount. (Figure 3.13 d) The 'honeycomb' structure of triple-templating g-CN is typical of sol-gel combustion of metal oxides, where igniting a mixture of metal nitrate and a fuel (e.g. glycine or citrate) in the furnace.[7]Gases are generated when reaction between the nitrate and the organic content occurs, leaving pores in the materials. Also the similar phenomenon can be observed from the synthesis of carbon foam by mixing metal nitrates with biopolymers such as gelatin.[8]When moving back to our 'honeycomb' structure g-CN, it is possible that nitrate from $Mg(NO_3)_2$ is reacting with the organic content of agar to produce gases and increase porosity in the system. However, the theory of enhancing photocatalytic properties by the additional introduction of porosity was finally precluded by the low activity of the sample (D5-agar-0.1-F-Mg-10)without acid wash. And even N_2 may not be the best gas for characterizing the porosity in our hierarchical structure g-CN, it is still surprising to see the result from nitrogen porosimetry showed a low surface area of 5 m^2/g after acid wash for D5-agar-0.1-F-Mg-10, given the high catalytic activity. So it is necessary to develop a new theory to explain the enhancement in photocatalytic activity, if 'the increasing in surface area' is not suitable.

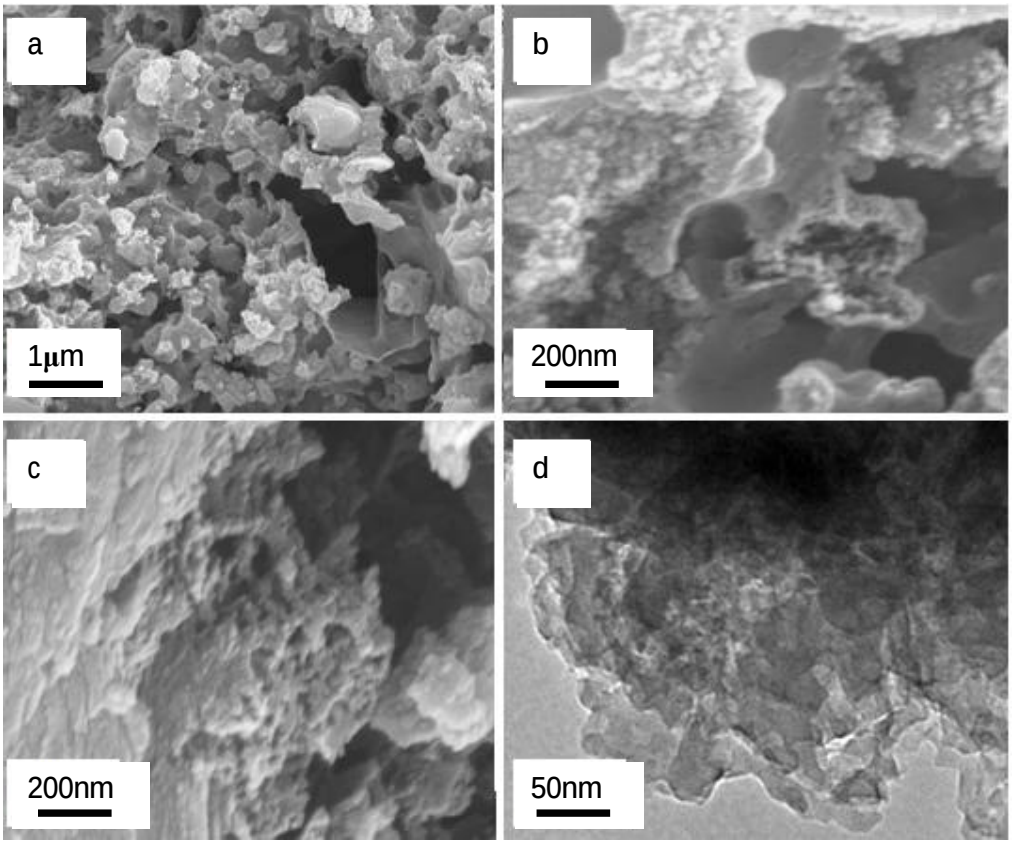

Figure 3.13 SEM images of sample D5-agar-0.1-F-Mg10 a), b) before acid wash and c) after acid wash. d) TEM image of D5-agar-0.1-F-Mg10.[22]

In fact, we can ascribe most positive result to 'quantity' term, and 'quality' term. When discussing about 'quantity', it usually means enough amounts of positive factor are provided during the process, like high surface area can provide more active sites in this case. If the 'quantity' term no longer gives explanation, it is a time to move to 'quality' term, which means focusing on the positive factor itself, rather than the amount of it. To be specific, we can ascribe the high activity of triple-templating g-CN to the enhancement of light scattering and light trapping ability, just like high activity of diatom templating g-CN with a relative low surface area ($5m^2/g$), where the introduction of diatom can improve its coherent light trapping and scattering, [9,10] since the diatom frustule was simplified as a two dimensional quasi-periodic

or disordered media, which can enhance broadband absorption for photovoltatic and photocatalytic applications.[11,12]When comes to our biotemplating g-CN research, obviously, the introduction of these three templates can result in higher internal irregularities of g-CN solid and enhance light scattering in the grain boundaries. Also, the gases produced by the reaction of nitrate from $Mg(NO_3)_2$ and organic content of agar can 'bubble up' g-CN material during its polycondensation, leaving textured sheets and honeycomb structure on the final product, which would give a longer optical path length than the material thickness and allow the light bounce back and forth within the material many times, by changing the angle of light travels on an angled surface, thus improving the light trapping ability. This explanation makes sense, since both light trapping and light scattering ability can enhance the 'quality' to use light during reaction. (Figure 3.14)

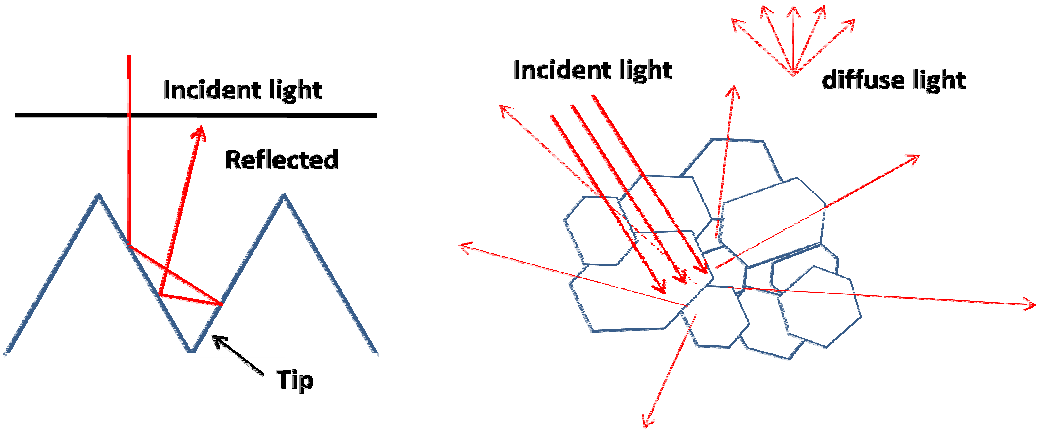

Figure 3.14 Schematic showing left: light trapping, right: light scattering of the sample.

Another question before we carry on our study is: is it the triple templates, rather than individual MgO that significantly improve the photocatalytic activity? We don't deny MgO can influence photocatalytic activity individually, just like Zhang *et al.* used $CaCO_3$ nanoparticles to template g-CN. However, such tiny amount of MgO (~0.16 g in D5-agar-0.1-F-Mg-10) is not enough to influence g-CN matrix from 5g DCDA. If

more MgO is added, side reaction happens, leaving impurities in the final product even after acid washing. The method to avoid such side reaction is to calcine the mixture of DCDA and MgO to a lower temperature (400 °C) first, then remove the template with diluted HNO_3 before heating it at higher temperature (550 °C) to obtain final g-CN product. Compared to our relative simple one-pot approach with triple templates, the complicated 2-step calcination of g-CN with MgO is certainly one of its drawbacks.

Having established the photocatalysis experiment to evaluate the effectiveness of the g-CN materials, it is necessary to discuss the mechanism of activity of the triple-templating g-CN material. Wang *et al*. firstly reported the application of g-CN as a photocatalyst.[21] Under visible light irradiation, the photoelectron is excited from valence band to conduction band, causing a charge separation between the two bands. In our g-CN sample, it has been calculated that nitrogen atoms act as the oxidation sites while the carbon atoms provide the reduction sites. Two possible mechanism were proposed by Shalom *et al.* for the photodegradation of rhodamine B. [13] The first is cleavage of the aromatic conjugated structure and the second is N-deethylation. The main difference between the two mechanisms is that cleavage of the conjugated structure would keep the main absorption peak at 554 nm while the N-deethylation route would blue-shift the main absorption peak up to 498 nm. The dramatic decrease at 554 nm for the main absorption peak, with the blue shift of the absorption band, as shown in Figure 3.15 indicating that deethylation process was the mechanism of RhB degradation by g-CN materials.[14]

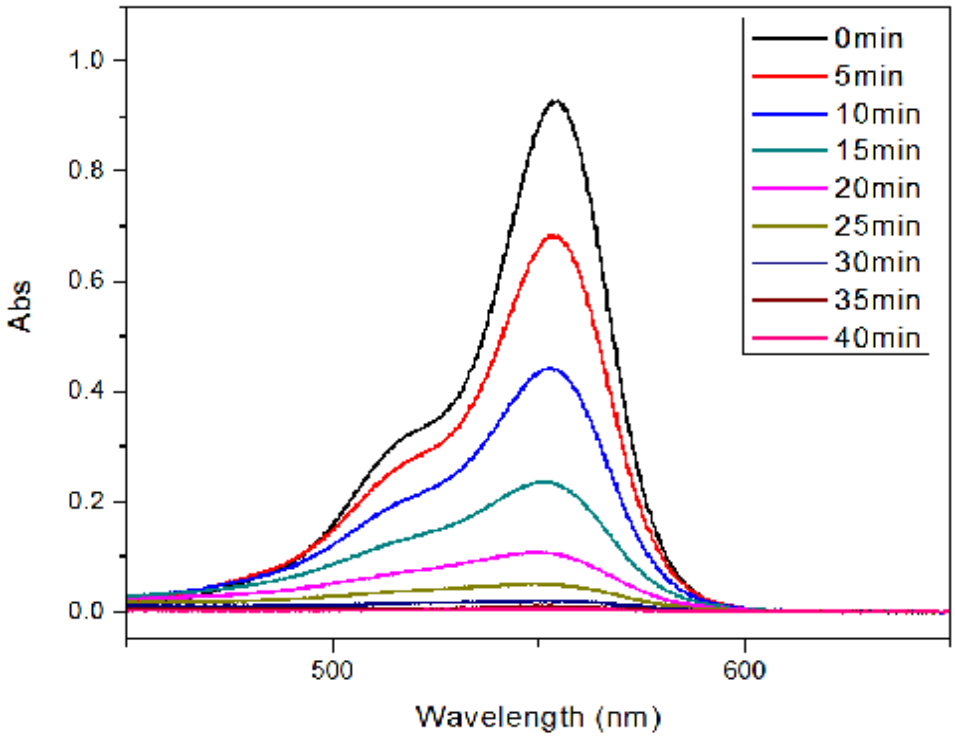

Figure 3.15The temporal absorption spectrum changes of RhB solution in the presence of g-CN sample (D5-F) under visible light.[22]

3.4 "Bubble up"

To identify the use of triple templating method, it is necessary to confirm the formation of MgO first. Given that the aqueous $Mg(NO_3)_2$ precursor can highly dissolve in agar/DCDA solution, the size of MgO particles after calcination are presumed to be small, and with the addition of tiny amount of Mg in D5-agar-0.1-F-Mg-10, XRD peaks of MgO would be broadened and even more likely to be lost in the background noise. So a much higher level of aqueous $Mg(NO_3)_2$ was added to agar/DCDA solution (e.g. D5-agar-0.1-F-Mg-40 and D5-agar-0.1-F-Mg-60) to identify peaks for MgO in the product. The XRD peak of MgO was observed from

D5-agar-0.1-F-Mg-60 before acid washing, which then disappeared to leave the characteristic g-CN peak after HNO_3 treatment. (Figure 3.16) The success of our triple templating method also avoided the side reaction from MgO with a higher amount of $Mg(NO_3)_2$ in the precursor, which is obviously one of the advantages and may be ascribed to that g-CN matrix and MgO particles formed simultaneously.

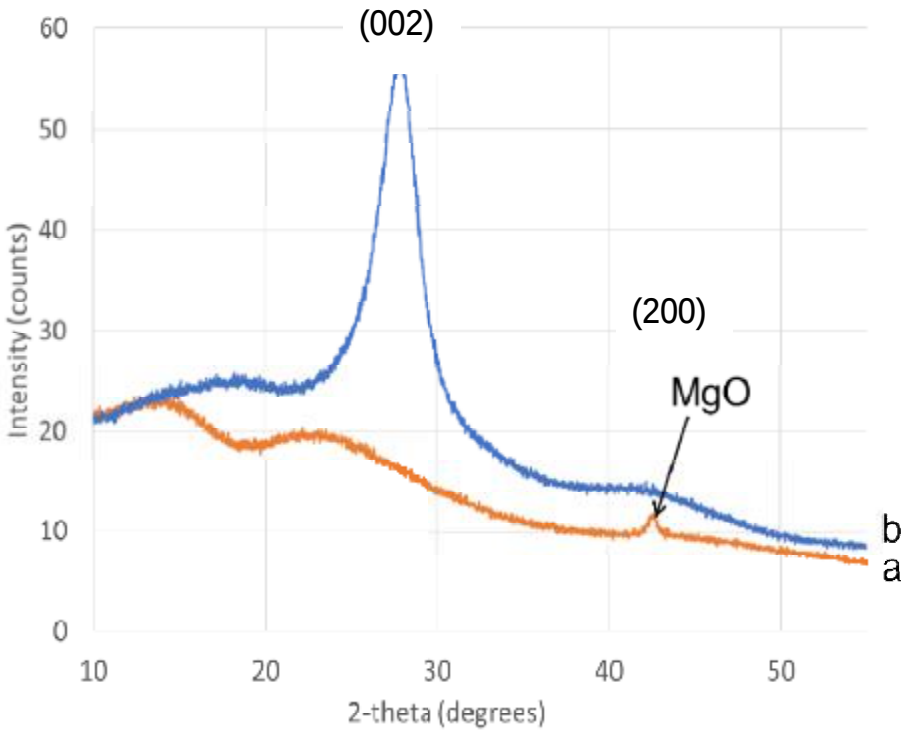

Figure 3.16XRD patterns for a sample of D5-agar-0.01-F-Mg60 before (a) and after (b) acid washing, showing the peak for MgO.[22]

More interestingly, the obtained solid of D5-agar-0.1-F-Mg-60 from the furnace showed an open sponge structure, like a "desert rose", or "cornflake", (Figure 3.17) which was then ground into powder and washed by HNO_3. Also, the result of photodegradation of RhB was observed by eyes, which happened in 20min for D5-agar-0.1-F-Mg-60, indicating its high photocatalytic activity compared to that of bulk g-CN. This is not difficult to understand, since more nitrate is added to the precursor to react with agar to produce gases and 'bubble up' g-CN matrix to form sponge-like solid. Besides, the use of agar not only influences self-assembly of g-CN

solid, but also the crystallization of MgO from $Mg(NO_3)_2$. This is due to the remarkable properties of biopolymers and especially their ability to bind metal cations either through adsorption onto raw biomass [15] or embedded in crosslinked gels.[16] Obviously, the interaction between Mg^{2+} and agar can be classified into the second occasion. The highly dispersed MgO in g-CN was finally removed, but the trace of agar-templating was retained in the final product, influencing the behavior of g-CN in RhB degradation.

Figure 3.17 Image of D5-agar-0.1-F-Mg60 before acid wash, showing a "cornflake" structure.

Considering the foam structure of g-CN material would not be obtained via the polycondensation of DCDA, this templating method is of great value in our experiment and may even have potential to template other materials, especially when we get an insight into dye sensitised solar cells (DSSCs), which is a promising

technology for high solar energy conversion efficiencies at relatively low cost, compared to their counterpart, industrially dominant silicon p-n junction photovoltaics.[17]DSSCs use a photosensitive dye (sensitiser) to bound to a mesoporous metal oxide semiconductor (e.g. titania nanoparticles), and the semiconductor layers act as a transport medium for the photoexcited electrons from the dye, and carry the electron to the working electrode. [18]The use of metal oxide semiconductor makes it an important factor to influence the performance of DSSCs, which is worth to be enhanced by our templating method, for the following reasons: First, the reaction of agar and nitrate from $Mg(NO_3)_2$ can generate lots of gases to 'bubble up' the metal oxide and form textured structure, which would then enhance its light trapping and scattering ability. Second, the carbonization of agar can not only introduce porosity to the material, but also work as a carbon dopant to increase the conductivity to move photogenerated electrons. Also, diluted HNO_3 that used to remove MgO would not damage the target materials, like titania, the most common semiconductor in DSSCs, and more porosity would be provided to allow dense dye attachment and help light scattering after MgO is finally removed. Obviously, the potential application in DSSCs that we proposed above makes our triple templating method, or "bubble technique" in other word, be of equal importance to that of g-CN material, for the consideration of this method that may not just be limited in templating graphitic carbon nitride, it can also provide an option as template for other materials, which is worth further investigation by people. In this sense, what we did to "bubble up" g-CN is beyond traditional chemistry, perhaps "crystal engineering" can better describe our work.

Another thing that we can't ignore is the advantages of the freeze drying in synthesis method, which was firstly reported in g-CN preparation. Avoiding shrinkage of the soft, gel-like precursor to give open and porous structure is certainly its advantage over oven drying. And as a general method, freeze drying technique can also have a wider application, for it provides a way to ensure homogeneity during drying process and efficiently avoid phase separation or 'settling out' of a hard template, giving a

better interaction between precursor and template. Directly freezing the hot solution of precursor by liquid nitrogen is most funny part during the whole synthesis process, it is necessary to do this in a metal bowl, rather than a glass flask, to avoid the damage from expansion of solution to solid. Stirring when pouring the hot aqueous precursor in the liquid nitrogen can form smaller solid, which makes it easier to get through the narrow neck of flask and remove off water. By illustrating the experimental detail here, we hope the readers can have more chances to repeat our experiment successfully.

3.5 Overview

Generally speaking, there are three factors for the improvement of photocatalytic activity of g-CN. Firstly, a high surface area can provide more active sites to adsorb target pollutant for photocatalytic reaction.[19] Secondly, a small grain size is needed to shorten the migration distance for photoexcited electron from excitation site to active site and improves light scattering ability.[20]Finally, intrinsic electronic properties,[14] including the bandgap, the band-edge potential and charge-carrier mobility can enhance the ability to absorb visible light more effectively. In our study, the combination of triple templates showed the best performance of degradation of RhB solution, which is ascribed to its porous and textured structure, as well as the grain size of g-CN. Certainly, the broader g-CN characteristic peak displayed as increasing the amount of $Mg(NO_3)_2$ in the precursor suggested that g-CN crystallization is constrained in the presence of Mg content, since g-CN and MgO formed simultaneously, or it may be due to the open structure that generated from the reaction of nitrate and agar. In any case, there is no doubt that the introduction of multiple levels of templating for graphitic carbon nitride can produce optimized materials. The result of nitrogen porosimetry showed a relatively low value of surface

area, indicating that surface area is not the determinant to influence photocatalytic activity of the samples in our study. The textured structure of triple-templating product, which can be confirmed by electron microscopy, is obviously another key factor for the enhancement of photodegradation, since a longer optical path was given within this structure to improve light trapping ability.

The method to evaluate the performance of g-CN product is the photodegradation of Rhodamine B under visible light, by observing which sample takes the least time to decolour the solution. In the photocatalysis experiment, an appropriate amount of catalyst (0.02 g in our study) is needed to ensure that it is the photoreaction, rather than adsorption to degrade the dye. If too much g-CN (like 0.04 g) is added in, it would be difficult to observe the improvement of photocatalytic activity from templating g-CN product. (Figure 3.18) However, there is still one limitation in our method: that is the strong intensity of light source, which is much stronger than the sunlight, and even can decolour the RhB solution in 75 min. It would be better to lower the output current of light source to get closer to the intensity of the sunlight in the future study(from 1500 W/m^2 to 1000 W/m^2). But considering the aim of our study is to develop a simple and relatively green method to enhance the photocatalytic activity of g-CN, and photodegradation of RhB is just a process to examine the effect of templating methods, the limitation of strong light intensity is acceptable.

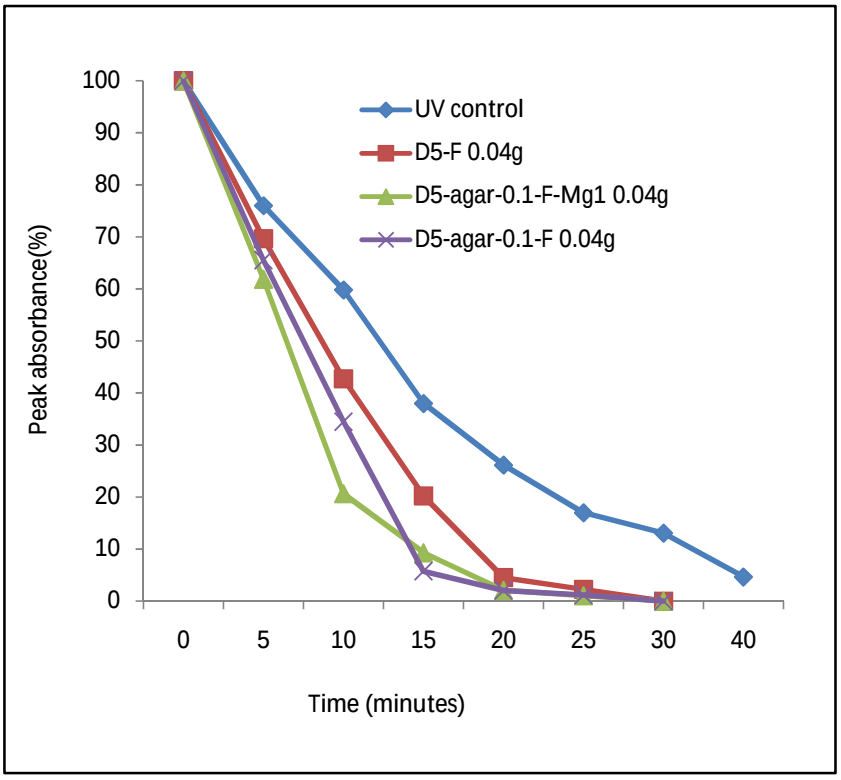

Figure 3.18Photodegradation data for UV-control (without any catalyst) vs RhB solution in the presence of 0.04 g freeze dried samples.

As a metal-free semiconductor and a potential candidate for photocatalyst, graphitic carbon nitride is advantageous for its favorable band gap, stable chemical property and low cost. And the triple templating method was proved to be a successful way to improve the photocatalytic activity of g-CN, which can halve the reaction time of photodegradation of RhB compared to that of bulk g-CN, and obtained in a green one-pot route. As a biopolymer, agar is a good option to combine with $Mg(NO_3)_2$ to template g-CN, which has already been confirmed in our study. Gelatin and $Ca(NO_3)_2$ may also be the compositions of triple templates, and even the combination of agar and $Ca(NO_3)_2$, but those combinations were not included in our investigation. However, there is still necessity to carry on the study of above combinations in the future to widen the study of triple templating methods, and seek for g-CN product with the best photodegradation performance in this field.

Chapter references

1. S. Weiner, I. Sagi, L. Addadi, *Science*,2005, 309, 1027.

2. Y.Cui, Z.Ding, P.Liu, M.Antonietti, X. Fu and X. Wang, *Phys. Chem. Chem. Phys.*2012, 14, 1455.

3. G. Dong and L. Zhang, *J. Mater. Chem.*,2012, 22, 1160.

4. S. Ye, L. G. Qiu, Y. P. Yuan, Y. J. Zhu, J. Xia and J. F. Zhu, J. Mater. Chem.A, 2013, 1, 3008.

5. X. Wang, X. Chen, A. Thomas, X. Fu and M. Antonietti, *Adv. Mater.,*2009,21,1609

6. W. Li and D. Zhao, *Chem. Commun.*,2013, 49, 943

7. Y.Li, L. Xue, L. Fan and Y. Yan, *J. Alloy. Compd.*2009, 478, 493.

8. Z. Schnepp, Y. Zhang, M. J. Hollamby, B.R. Pauw, M. Tanaka, Y. Matsushita and Y. Sakka. *J. Mater. Chem. A.*2013, 1, 13576.

9. C. Jeffryes, J. Campbell, H. Li, J. Jiao and G. Rorrer, *Energy Environ. Sci.,* 2011, 4, 3930.

10. J. Toster, K. S. Iyer, W. Xiang, F. Rosei, L. Spiccia and C. L. Raston, Nanoscale, 2013, 5, 873.

11. K. Vynck, M. Burresi, F. Riboli and D. S. Wiersma,*Nat. Mater.,* 2012, 11, 1017.

12. J. Liu, G. Liu, M. Li, W. Shen, Z. Liu, J. Wang, J. Zhao, L. Jiang and Y. Song,*Energy Environ. Sci.,* 2010, 3, 1503.

13. M. Shalom, S. Inal, C. Fettkenhauer, D. Neher and M. Antonietti, *J. Am. Chem. Soc.*2013, 135, 7118

14. L. W. Zhang, H. B. Fu and Y. F. Zhu, *Adv. Funct. Mater.,*2008,18, 2180

15. J. Huang and T. Kunitake,*J. Am. Chem. Soc.*, 2003, 125, 11834.

16. S. R. Hall,*Adv. Mater,* 2006, 18, 487.

17. M. Gratzel, J. *Photochem. Photobiol.,A*, 2004, 164, 3.

18. O. K. Varghese, M. Paulose and C. A. Grimes, *Nat. Nanotechnol.,* 2009, 4, 592.

19. W. Wei, C. Yu, Q. Zhao, G. Li and Y.Wan, *Chem. Eur. J.*2013, 19,565.

20. Y. F. Li, D. Xu, J. Oh, W. Shen, X. Li and Y. Yu, *ACS Catal*,2012, 2, 391

21. X. Wang, K. Maeda, A. Thomas, K. Takanabe, G. Xin, J. M. Carlsson, K. Domen and

M. Antonietti, *Nat. Mater*., 2009, 8, 76

22. Z. Yang, A. E. Danks, J. Wang, Y. Zhang and Z. Schnepp.*APL.Mater.*,2016, 4, 1

Overviews, conclusions and outlook

4.1 Overviews and conclusions

The research of templating graphitic carbon nitride has been discussed in detail, including soft, hard and biological methods. Self-assembly characteristics of soft methods provide a flexible route to form different morphologies of g-CN. However, poor thermal stability of the templates may produce too much carbon residue, which would decrease the nitrogen content, hinders light absorption, and gives poor catalytic activity. The rigidity of the hard templates makes it easy to control the morphology of g-CN and result in uniform structural materials. But the hazardous acid, such as HF, which is used to remove the templates, can bring safety and sustainability concerns. And the difficulty to synthesize hard templates makes it hard to cast materials in large scale. Another problem in hard methods is the loading ability of the template to carry the precursor, which would influence the stability of the structure after the removal of the templates. Biological templates is also applied to g-CN materials. The unique properties of biopolymers, such as rich functional groups and strong gels to trap water, can give many advantages, and may also offer improving sustainability if an abundant biomaterial is employed. However, biopolymers still may not overcome the limitations of traditional soft and hard methods, thus produce residue carbon, or the problem of removal of the templates, which would challenge the potential of application in this field.

As a general method to improve the performance of g-CN material, there are three important factors to influence templating methods. The first is the importance of the nitrogen content in the material. The theoretical value of C/N ratio in bulk g-CN is 0.75. If the carbon content is much higher than the theoretical value, there is likely to

leave residual carbon, which may decrease g-CN content and further hinder its photocatalytic properties. [1] And the material may be better classed as a nitrogen-doped carbon rather than a graphitic carbon nitride. The second is that there is no proportional relation between the surface area and the performance of g-CN material, the low surface area doesn't mean low photocatalytic activity, which can be seen from diatom frustules templating g-CN.[2]There are multiple chemical and physical factors to determine the photocatalytic activity of g-CN, including pore size, pore accessibility and also metal, carbon dopants, or heteroatoms, not only surface area. The last and the most important observation from our review of literature is the lack of study on the interaction between the precursor and template surfaces. In most cases, the synthesis methods were simply described as 'mix' or 'impregnate' templates with precursors, not considering whether the interaction between them are ideal. And this lack of study is obvious when compared to investigation of the mechanisms of soft templating, where discussed a lot in the interaction between the precursor and template. The precursor-template interaction may impact the loading ability of a template, structural collapse may occur after chemical or physical removal of the template,[3]if this interaction is too weak. Another question is, some template may be left in the g-CN matrix even after acid washing, making the material no longer g-CN, but a template-g-CN composite, this may not be a problem if it is applied in electrocatalysis. However, it is possible to impact photocatalytic activity. So far, there have been efforts to improve the interaction between precursor and template in the study of metal oxide materials, for example hydrolyzing the surface of biomass,[4] or hydrolyzing the precursor layer-by-layer. Certainly, those efforts in the templating of metal oxide materials worth to be tried in g-CN synthesis, and perhaps in the future, more attention should be paid to the interaction between the hard templates and precursors in g-CN synthesis.

Also, a simple and green route to hierarchical structure g-CN was proposed by our study, which is aiming at improving its photocatalytic activity, by combining three

templates (air, biopolymer and MgO), and heating the gel precursor to obtain final product. The enhancement in photocatalytic activity was confirmed by degradation of Rhodamine B solution, with the value of photodegradation rate constants (k) for triple-templating is 0.19 min^{-1} compared to 0.11 min^{-1} for the control sample. Freeze drying was firstly introduced to structure g-CN and efficiently avoid the capillary force that brings from traditional oven-drying process, giving an fluffy and porous precursor. As a combination of soft and hard templating method, our one-pot approach took the advantages of both soft and hard methods, g-CN product was obtained through self-assembly of agar and the nanocasting process by MgO particles from $Mg(NO_3)_2$ in the precursor. MgO showed its advantage over traditional hard templates such as SiO_2 or anodic aluminium oxide (AAO), since it can be removed by diluted HNO_3, which is less hazardous than HF. Besides, the use of aqueous $Mg(NO_3)_2$ makes Mg template highly dispersed in the precursor and significantly avoids the side reaction of MgO during the polycondensation of DCDA, since the formation of g-CN matrix and MgO particles occur simultaneously. Furthermore, the reaction of nitrite from $Mg(NO_3)_2$ and organic content of agar can 'bubble up' the product to give textured structure, which would possess better light trapping and scattering ability, also have potential to apply in other materials. The last is the investigation of the use of agar in g-CN synthesis, as a biopolymer template with multiple functional groups to form gel, it can be obtained from nature on a large scale, which is obvious advantage over synthetic surface. Although the agar didn't significantly influence the performance of g-CN material as an individual template, it finally worked when coordinating with $Mg(NO_3)_2$ and freeze-drying technique, which gives agar potential application in templating g-CN.

4.2 Outlook

Indeed, to structure the morphology of bulk g-CN and introduce porosity by templating method is an efficiency way to improve the performance of g-CN when working as a photocatalyst, since templating method can control the grain size and provide more active sites for reaction. Another strategy to enhance photocatalytic activity is to combine g-CN with other semiconductors to form semiconductor/g-CN composite, such as WO_3/g-CN [5], CdS/g-CN[6]and ZnO/g-CN[7], in which the photocatalytic activity is enhanced by forming heterostructure with improved charge separation. The incorporation of the graphitic carbon nitride into metal oxide crystal would produce an intermediate energy level, reduce the band gap for metal oxide and the energy for exciting photoelectrons. Also, CeO_2/g-CN is proved to be a possible combination from some research. [8](Figure 4.1) As one of the reactive rare earth oxide, CeO_2 has potential to work as a photoactive material in solar cells and a photocatalyst in the degradation of dye pollutants and hydrogen evolution.[9,10] Huang *et al.* obtained CeO_2/g-CN composite by calcining the mixture of CeO_2 and g-CN to 400°C. The relative low combustion temperature is due to the introducing of CeO_2, which can oxidize the g-CN matrix at lower temperature. The characteristic diffraction peaks of both CeO_2 and g-CN were observed from XRD pattern. TEM image confirmed dispersion state and heterojunction structure of the composite. The result of photodegradation of methylene blue (MB) for the composite exhibited higher photocatalytic activity than both CeO_2 and g-CN, but further increased the weight content of CeO_2 to 22.4 % led to a decrease in phtocatalytic activity, which is attributed to the agglomerating of CeO_2 in the composites that destructs the heterojunction structure, resulting in the reduce of the efficiency of charge separation.[8]The enlarged surface area of CeO_2/g-CN composite was regarded as one of the crucial factors that govern its photocatalytic activity, which can absorb more dye molecules on the surface. Another factor is the π-π stacking between g-CN and MB, suggesting as a good supplement for the improved property of

photocatalysis.[11]Besides, the excited electrons at the conduction band of g-CN crystallites would transfer to the conduction band of CeO_2, and the photogenerated hole would transfer from CeO_2 crystallites to g-CN through the heterojunction structure of the composite, since the conduction band (-1.13 eV) and the valence band (1.57 eV) of g-CN are lower than that value of CeO_2 (-0.39 eV for conduction band, 2.50 eV for valence band). This would easily suppress the charge recombination, resulting in more charge carriers in the material compared to that of pure g-CN catalyst

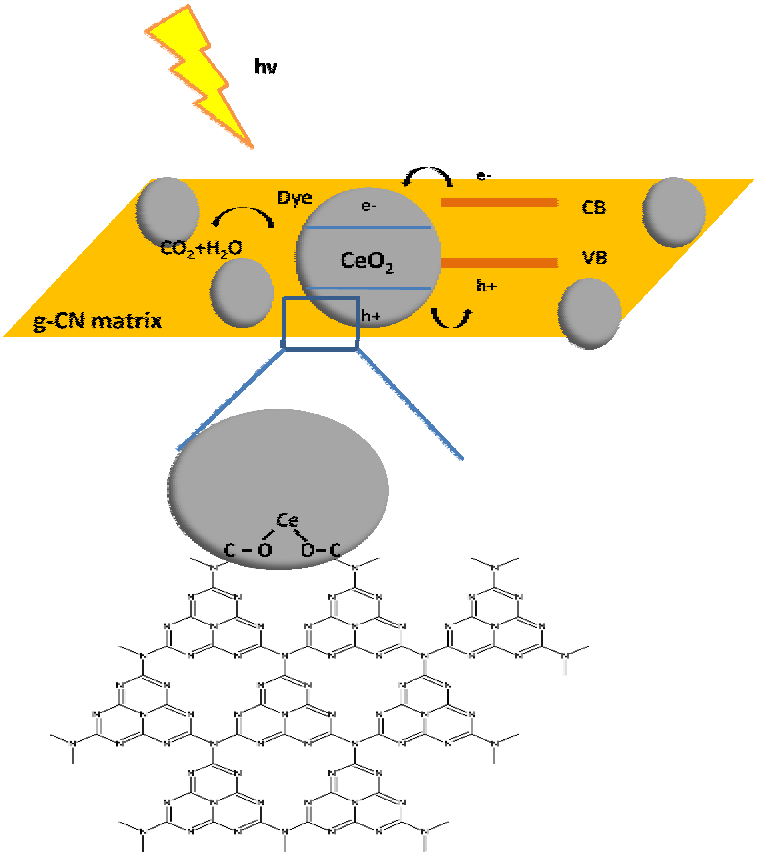

Figure 4.1 Schematic showing the CeO_2/g-CN composite can improve the separation efficiency of photoinduced electron-hole pairs.

The synergistic effect between the interface of CeO_2 and g-CN enhanced adsorption

ability and provided suitable band position for the composite, making the combination of CeO_2 and g-CN have great potential in photocatalyst application. However, the approach to the CeO_2/g-CN composite still has its limitations. For instance, the final product was obtained by heating the mixture of CeO_2 and g-CN, which was not convenient, since it took three steps before the formation of the composite. Also, CeO_2 and g-CN were synthesized via a relatively rough approach, making it difficult to fully take advantage of each component in the composite. To further enhance the performance of this composite in photodegradaion and simplify the reaction route to the final product, we believe it is a time to introduce our triple templating method in CeO_2/g-CN composite synthesis. Aqueous cerium nitrate and dicyandiamide (DCDA) would be used as the precursor to give highly uniform dispersion, form the composite simultaneously and avoid the side reaction from oxidative CeO_2, which is also a relatively simple one-step approach to the final product. Agar would be added to guide the self-assembly, and react with the nitrite from $Ce(NO_3)_3$ to produce gases to give textured structure, which would then enhance the light trapping and scattering ability. Freeze-drying would also be carried out to give fluffy and porous precursor, instead of oven-drying process. Moreover, it is also necessary to add different amount of aqueous $Mg(NO_3)_2$ in the precursor to introduce microporosity in the composite after removed by diluted nitric acid. In summary, by using the aqueous mixture of DCDA and $Ce(NO_3)_3$ as precursor, the composite would be obtained via a relatively easier route compared to the calcination of solids mixture. Also, the introduction of triple templates is presumed to be a efficient way to modify the nanostructure of this composite.

Chapter references

1. W. Li and D. Zhao, *Chem. Commun.,* 2013, 49, 943.

2. J. Liu and M. Antonietti, *Energy Environ. Sci.,* 2013, 6, 1486.

3. A. H. Lu and F. Schuth, *Adv. Mater.*, 2006, 18, 1793.

4. S. R. Hall, V. M. Swinerd, F. N. Newby, A. M. Collins and S. Mann, *Chem. Mater.,* 2006, 18, 598.

5. L. Y. Huang, H. Xu, Y. P. Li, H. M. Li, X. N. Cheng, J. X. Xia, Y. G. Xu and G. B. Cai. *Dalton Trans.,*2013, 42, 8606.

6. S. W. Cao, Y. P. Yuan, J. Fang, M. M. Shahjamali, F. Y. C. Boey, J. Barber, S. C. J. Loo and C. Xue. *Int. J. Hydrogen Energy*, 2013, 38, 1258.

7. W. Liu, M. L. Wang, C. X. Xu, S. F. Chen and X. L. Fu, *J. Mol.Catal. A, Chem.,*2013, 368, 9.

8. L. Huang, Y. Li, H. Xu, Y. Xu, J. Xia, K. Wang, H. Li, X. Cheng. *RSC. Adv.,*2013, 44, 22269

9. X. H. Lu, S. L. Xie, T. Zhai, Y. F. Zhao, P. Zhang, Y. L. Zhang and Y. X. Tong.*RSC. Adv.,*2011, 1, 1207

10. H. Li, G. Wang, F. Zhang, Y. Cai, Y. Wang and I. Djerdi, *RSC. Adv.,*2012, 2, 12413

11. Y. J. Wang, R. Shi, J. Lin and Y. F. Zhu, *Energy Environ. Sci.,* 2011, 4, 2922.

Attached pages

Attached document A: Soft and hard templating of graphitic carbon nitride

Attached document B: Triple templating of graphitic carbon nitride to enhance photocatalytic properties

Journal of Materials Chemistry A

REVIEW

View Article Online
View Journal | View Issue

Cite this: J. Mater. Chem. A, 2015, 3, 14081

Received 24th March 2015
Accepted 8th May 2015

DOI: 10.1039/c5ta02156a

www.rsc.org/MaterialsA

Soft and hard templating of graphitic carbon nitride

Zhao Yang,[a] Yuanjian Zhang*[b] and Zoe Schnepp*[a]

Graphitic carbon nitride (g-CN) is an exciting material – a semiconductor comprised only of carbon and nitrogen. It is very easy to synthesize and there are many papers on the development of this material in key energy applications such as photoelectrochemical (PEC) conversion of solar energy into chemical fuels. As a promising candidate for sustainable photocathodes, g-CN has advantages such as low cost, visible light sensitivity and high chemical stability. However, to date, the performance of g-CN has been limited, partly because standard synthesis methods produce relatively dense materials with low surface area. To combat this, there are now many examples of hard and soft templating to change the structure and morphology of g-CN and introduce porosity. This review will discuss the key advances and challenges in this interesting new field.

1. Introduction

Graphitic carbon nitride (g-CN) structures have been developed for many potential applications (Fig. 1). Most of these involve catalysis such as oxidation of organics,[1] electrocatalysis,[2] photodegradation[3] and solar water splitting.[4] There are also examples of g-CN being used in sensing *e.g.* of glucose or metal ions.[5] Graphitic carbon nitride is composed of only carbon and nitrogen and therefore is very promising as a sustainable material for its many applications. Given this advantage, one of the most important applications for g-CN is in photocatalysis and particularly in the photo-driven generation of fuels such as hydrogen from water, as shown in Fig. 1b. This review will first focus on the fundamental concepts of photochemical reactions, including some of the challenges that g-CN may be able to target. Following this, the review will discuss the different templating methods that have been used to create specialized structures of g-CN (Fig. 1c) to enhance the properties of this material.

1.1 Photocatalysis

The use of light to drive chemical reactions is the foundation of life on Earth. Due to the renewable and unlimited nature of sunlight as a resource, this field vastly enriches the scope of

[a]School of Chemistry, University of Birmingham, Birmingham, B152TT, UK. E-mail: z.schnepp@bham.ac.uk

[b]School of Chemistry and Chemical Engineering, Southeast University, Nanjing 211189, China. E-mail: Yuanjian.Zhang@seu.edu.cn

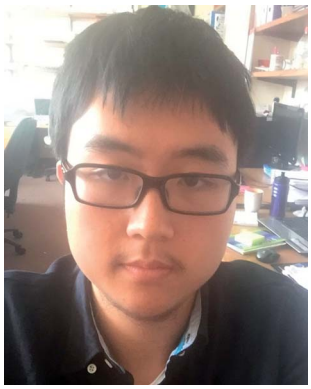

ZhaoYang received his BE from Beihang University (BUAA) in 2010. After that, he joined the Schnepp group at the University of Birmingham in the UK as an MRes student. His research interest is synthesis of graphitic carbon nitride by biotemplating methods.

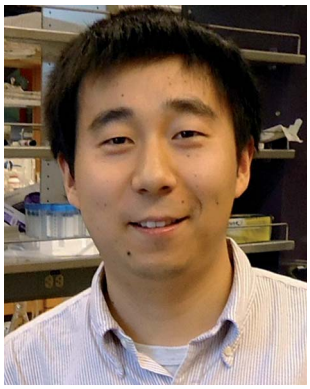

Yuanjian Zhang received his BSc from Nanjing University in 1998 and his PhD in Changchun Institute of Applied Chemistry, Chinese Academy of Sciences under Prof. Li Niu in 2007. After that, he joined Prof. Markus Antonietti's group at MPI of Colloids and Interfaces (Germany) as a postdoctoral researcher. From October 2009, he moved to National Institute for Materials Science as an ICYS researcher. In 2012, he was promoted as a Professor in School of Chemistry and Chemical Engineering, Southeast University, China. His research interests include but not limit to chemistry of carbon-rich materials and their applications for analytical chemistry and sustainable energy.

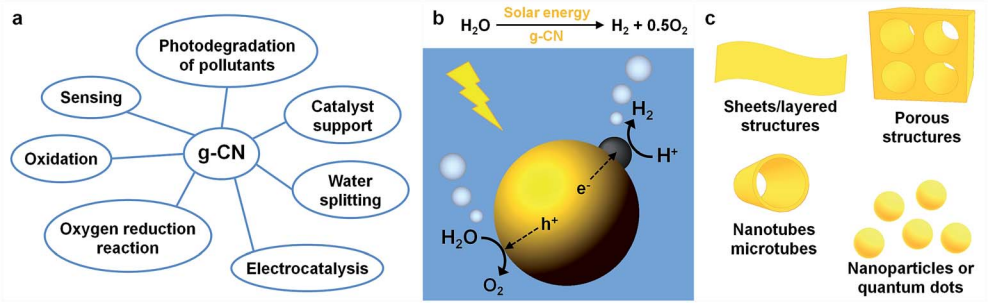

Fig. 1 (a) Different applications that have been demonstrated for g-CN, (b) schematic of photocatalytic water splitting over g-CN and (c) some of the different structures of g-CN targeted by templating methods.

green chemistry.[6,7] This is particularly important with the increasing drive towards 'solar fuels' such as hydrogen from water splitting.[8] Photochemical reactions can also have the advantage that they occur without additional reagents, thus reducing the formation of by products.

Many photochemical reactions are performed with the assistance of a semiconductor photocatalyst. These materials are characterized by a highest occupied energy band, called the valence band (VB), and a lowest occupied energy band, called the conduction band (CB); these are separated by the band gap. The mechanism of semiconductor photocatalysis can be summarized as follows. When the light energy incident on the surface of semiconductor photocatalyst is higher or equal to the band gap energy, an electron is promoted from the VB to the CB, forming a hole (h^+) in the VB. These may separate to different positions on the photocatalyst to react with donor (D) or acceptor (A) species adsorbed on or close to the surfaces. In a photocatalytic reaction, the reaction rate in the electronic ground state is determined by the activation barrier, the height of which can be controlled by catalysts and cocatalysts. If appropriate photocatalysts are chosen, the use of a photoactive center can provide high chemo- and regioselectivity. The possibility of using water as a solvent and photons as an energy source makes photocatalytic reactions very attractive for green chemistry and interest in the scientific and engineering application of semiconductor photocatalysts has grown exponentially.[9–12]

Since Fujishima and Honda discovered the photocatalytic splitting of water on TiO_2 electrodes in 1972,[13] there have been numerous studies of semiconductor photocatalysts for solar energy conversion and environmental purification. Generally however, the relatively low value of overall quantum efficiency still challenges and limits the use of semiconductor photocatalysts, which can be attributed to the high recombination rate of photo-induced electron–hole pairs at or near its surface.[12] There are many methods to enhance photocatalytic activity, such as doping materials with *e.g.* metal ions or heteroatoms or controlling crystallinity, particle size and porosity.[14,15] These methods can enhance photocatalytic performance by improving the rate of transfer of photo-induced charge carriers as well as optimizing the transport of reagents to the photocatalyst surface.[16,17] To date, a lot of focus has been on ceramic semiconductors such as TiO_2 or ZnO and the control of structure and morphology in these systems is well understood.[18,19] Other inorganic systems that have been shown to be very effective in photocatalysis are haematite (Fe_2O_3),[20] metal sulfides[21] and ternary or quaternary oxynitrides.[22]

In this review, we will focus on the polymeric photocatalyst graphitic carbon nitride (g-CN). This material has some interesting properties that may give it advantages over ceramic semiconductors. Most importantly, g-CN is composed only of carbon and nitrogen, which are both highly earth-abundant elements. The band gap of g-CN (a yellow solid) is also favourably placed in the visible region – with the positions of the valence and conduction bands centred around the water oxidation and reduction potentials (Fig. 2). The generation of photocatalysts that have a narrow enough band gap to absorb visible photons is a big challenge.[23]

Zoe Schnepp is passionate about green chemistry, both in her research and the potential for changing negative public perceptions of chemistry. With diverse interests in nanotechnology, catalysis and materials from biomass, Zoe leads a growing group in the School of Chemistry at the University of Birmingham, UK. Prior to her Birmingham Fellowship, she held Postdoctoral Fellowships in the International Center for Young Scientists at the National Institute for Materials Science in Japan and the Max Planck Institute for Colloids and Interfaces in Germany. She received her PhD from the University of Bristol.

1.2 Graphitic carbon nitride

Polymeric graphitic carbon nitride (g-CN) is a layered material consisting of C and N atoms with a structure similar to graphene. It is regarded as the most stable allotrope at ambient conditions. Liu *et al.* demonstrated that the hardness and low compressibility of diamond-like β-C_3N is close to that of

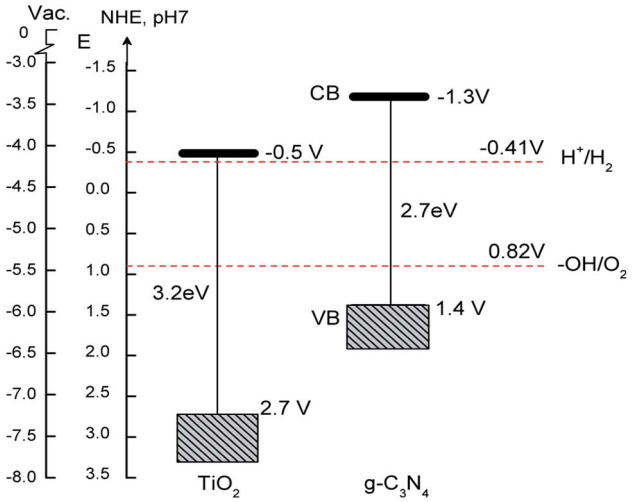

Fig. 2 Electronic band structure of g-CN, compared with TiO_2. Reprinted with permission from ref. 10, Copyright (2012) American Chemical Society.

diamond.[24] Thomas *et al.* illustrate the history of chemical approaches towards g-C_3N_4 and its derivatives specifically in one of their literature reviews.[25] In that paper, they mentioned g-CN synthesis can be based on polyaddition and polycondensation of cyanamide and dicyandiamide, which is an easy approach to synthesize g-CN. This simple approach is certainly one of the main advantages of g-CN. Briefly, the synthesis of g-CN from cyanamide can be summarized as a 4-step process. The first step of the reaction starts with condensation of the precursors towards melamine. The second step is a condensation reaction that eliminates ammonia and forms a dimer called melam which then converts into a tri-*s*-triazine called melem at approximately 390 °C. The tri-*s*-triazine is believed to be the tecton for the final graphitic carbon nitride product (Fig. 3a), which is formed *via* polymerization at approximately 520 °C.[26] It should be noted that there is another model for carbon nitride distinguished by different nitrogen-linked aromatic moieties – triazine (C_3N_3) units – in the individual sheets (Fig. 3b). Various precursors can be used to prepare g-CN, including cyanamide, dicyandiamide and melamine. In reality, ideal g-C_3N_4 is not formed due to the difficulty of fully condensing the precursors through release of NH_3. The material obtained is perhaps better described as a graphite-phase polymeric carbon nitride with the formula g-$C_xN_yH_z$ rather than g-C_3N_4. For simplicity in this paper, however, we will continue to refer to these as a class of materials called graphitic carbon nitrides (g-CN).

The tri-*s*-triazine tecton strongly influences the properties of graphitic carbon nitride since the aromatic structure tends to form a π-conjugated plane similar to graphite, as shown by wide angle X-ray diffraction (XRD).[27] Stacking in this way makes full use of van der Waals forces between the individual layers. This also makes it insoluble in most solvents.[26] The graphitic structure possesses high thermal stability up to 600 °C in air as well as high chemical stability when facing chemical attacks from acid, base and organic solvent. High stability is certainly desirable in a photocatalyst, but it is by no means the only requirement. Generally speaking, a photocatalyst with good performance would have all of the following abilities:

1. An appropriate band gap to absorb light in visible range
2. Stability
3. Non-toxic
4. Comprised of earth-abundant elements
5. Easy to manufacture in a controlled shape *e.g.* tailored porosity.

Given these stringent requirements, g-CN materials are attractive choices for photocatalysis. In addition to the positions of the valence and conduction bands, the band gap is readily tuned. As an example, Zhang *et al.* synthesized P-doped carbon nitride which dramatically changes the electronic features of g-CN as described in detail later in this review. Periodic density functional theory (DFT) calculations by Deifallah *et al.* showed that polymeric carbon nitride could possess a theoretical band gap of up to 5 eV, depending on structural variations or adatoms.[28] Despite these remarkable theoretical properties, there are many challenges to the implementation of g-CN as a widely-used photocatalyst. The low conversion efficiency of bulk g-CN is one challenge, which can be attributed to limited visible light absorption, low surface area and grain boundary effects. Indeed, despite the simple composition (carbon and nitrogen) and straightforward preparation, the estimated quantum efficiencies of most polymeric carbon nitrides synthesized to date have been rather low.[29]

These challenges point the direction for future research in graphic polymeric carbon nitrides. It is clear that one major focus must be on controlling grain size and surface area. Structural control of catalyst materials can result in more surface active sites, enhanced performance and in some cases, improved size and shape selectivity. A common method to

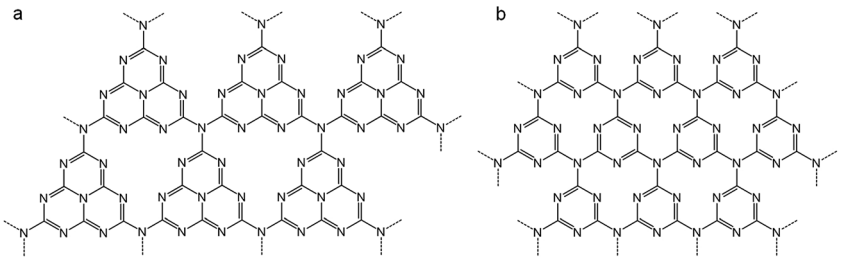

Fig. 3 (a) Tri-*s*-triazine and (b) triazine based idealized g-CN structures.

introduce porosity into solid materials such as ceramics, carbon and polymers is templating. Templating is often discussed in terms of 'soft' or 'hard'. Generally, 'soft' templating refers to the use of solution-phase molecules such as surfactants to direct assembly or precipitation of a material and frequently exploits the 'self-assembly' characteristics of amphiphilic molecules. Hard templating refers to the use of a solid material such as silica nanospheres or anodized alumina to 'cast' a second material. Given that graphitic carbon nitride has attributes of both 'soft' and 'hard' materials such as polymers and ceramics, it offers some challenges for templating. However it is also very promising, for example porous g-CN has been synthesized *via* templating with a surface area up to 830 $m^2 g^{-1}$.[30] As templating is increasingly applied to carbon nitrides, now is an ideal time to review the advances in this field.

2. Soft templating methods

2.1 Introduction of soft templating methods

Soft templating methods have witnessed great success in synthesizing porous inorganic micro- and nanostructures, For example, Collins *et al.* prepared hollow titania microsphere by using sodium dodecyl sulfate (SDS) as a surfactant in non-aqueous emulsions.[31] Yuan *et al.* used a non-ionic poly(alkylene oxide) amphiphile as a template to prepare mesoporous titania materials.[32] The molecular organic 'templates' are often called 'structure directing agents' due to their ability to assemble at interfacial regions and thus influence the growth of inorganic phases around them. In the formation of porous structures, the composition and properties of the organic template play a critical role although it is often challenging to determine the exact mechanism of the templating effect.[33]

A remarkable feature we cannot ignore during soft templating is "self-assembly". Amphiphilic molecules are well known to self-assemble in solution to form a range of different structures and in the case of templating these can combine with reaction precursors to form composite structures such as silica nanoparticles with mesopores filled with surfactant assemblies.[33] Solvent is an important factor in these systems. While it is not explicitly 'assembled', it's presence and properties can strongly affect the size and shape of assembled structures. In the process of "self-assembly", the most important part is normally (although not always) to ensure micelles or liquid crystalline phases develop. To form micelles in solution, two conditions need to be met, one is reaching the Krafft temperature and the other is reaching critical micelle concentration (cmc), which means at this concentration, any added surfactant can be incorporated into micelles and micelles can spontaneously form.[34] A concept, the packing parameter (g) is often used to describe the formation of micelles and considers the volume of the hydrophobic tail, the equilibrium area of the head group on the micelle surface and the chain length.[35] While useful as a guide for expected micelle shape, the packing parameter is not always appropriate and it would certainly be unwise to use it to predict templating effects. In the following section of this review, we will discuss three common soft templates, amphiphilic surfactants and block copolymers, ionic liquids (ILs), and gas bubbles.

2.2 Surfactants and block copolymers

Surfactants and block copolymers are common organic templates to synthesize mesoporous materials *via* soft templating. The use of different surfactants to obtain different morphologies in crystal growth is remarkable.[36] Perhaps the first example of this soft templating method is the work of Kresge *et al.*, who reported the synthesis of mesostructured molecular sieves from the calcination of aluminosilicate gels with surfactants. In this example, the proposed mechanism involved the aggregation of silicate species around cylindrical micelles. Combustion of the organic template then results in hollow inorganic cylinders.[37] One challenge for these molecular soft templates in the synthesis of carbon nitrides is their low stability. Graphitic carbon–nitride is not formed until >500 °C, which is a long way above the decomposition point of most surfactants. An interesting strategy is to introduce a hold sequence into the heating program according to the decomposition temperature of the surfactants, in order to maximize the influence of the template on the material structure.[38]

In the synthesis of carbon nitrides, several surfactants and block copolymers have been employed as templates. Wang *et al.* reported Triton X-100 can be combined with dicyandiamide (DCDA) as a precursor to produce g-CN with accessible pores (Fig. 4a).[39] Nitrogen adsorption isotherms of the g-CN sample revealed a BET surface area of 76 $m^2 g^{-1}$. A wide range of

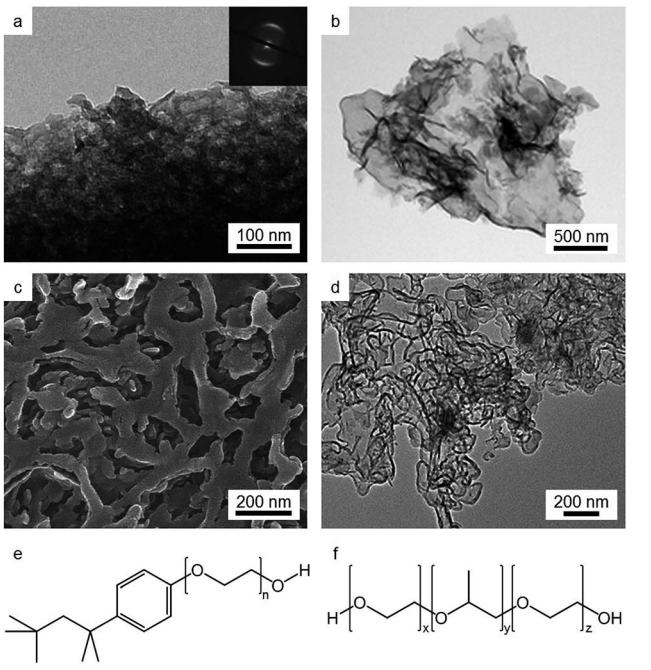

Fig. 4 TEM images of g-CN synthesized from (a) DCDA and Triton X-100 and (b) melamine and Pluronic P123. Also (c) SEM and (d) TEM images of g-CN synthesized by precipitating melamine sulfate around Triton X-100. Reproduced with permission from ref. 39–41. The structures of (e) Triton X-100 and (f) Pluronic P123 are also shown.

surfactants were tested in this paper and Triton X-100 found to be best due to its relatively high decomposition point. It was though that this factor avoided the formation of inaccessible closed pores that were a feature of other surfactant templates. A possible problem with the surfactant route as shown by this work was the high carbon–nitrogen molar ratio (0.8–2) observed in the products, indicating residual carbon from the decomposed surfactant. Using melamine as a precursor, Yan *et al.* reported the synthesis of porous g-CN photocatalysts with Pluronic 123 (P123) as a block copolymer template.[40] Fig. 4b shows a typical TEM image of a mesoporous g-CN sample in which the mass ratio of melamine : P123 is 5 : 1.The experiment result showed the as prepared g-CN had a low level of carbon dopants, high Brunauer–Emmett–Teller (BET) surface area and effective light absorption towards the peak intensity of the solar spectrum, reaching 800 nm. The data represent significant progress in the use of polymeric g-CN for catalyzing H_2 production from water. Melamine is a less reactive precursor, which can avoid direct chemical reaction of the precursor with the surfactant during heat treatment and makes melamine preferable over dicyandiamide (DCDA) and cyanamide in these synthesis techniques.[27] This method, however, does not remove the problem of residual carbon build-up.

An interesting advance that has been made recently is the use of surfactants to template the precursor rather than the g-CN product. Triton X-100 was combined with melamine followed by the addition of sulfuric acid to form solid melamine sulfate. The surfactant is then removed by washing before heating the porous melamine sulfate to form a porous g-CN with low C/N ratio of 0.66 and BET surface area up to 135 $m^2\ g^{-1}$.[41] Fig. 4c and d show the morphology and textural structure of a typical porous g-CN, the mass ratio of Triton X-100 to melamine is 0.5, and the final heating temperature is 580 °C. It will certainly be interesting to see how this method applies to other soft templates in the future.

In summary, surfactants provide useful soft templates for g-CN and have been used to produce a range of porous structures. The mechanisms have not been studied in detail and at the moment we can only point to the inherent self-assembly characteristics of the amphiphiles to produce structures that impart porosity into the developing g-CN material. This will be a valuable future area of research, particularly the use of small-angle scattering techniques to examine the interaction of melamine and DCDA precursors with various amphiphiles. However surfactants have shortages that most soft templates have in common: they are prone to hydrolysis, may cause some redox reactions and can have relatively weak interactions with the precursors. Finally, thermal breakdown of the template to carbon may occur during synthesis.[30] The possibility of removing the surfactant before calcination as in the work by Fan *et al.* offers a useful solution to this latter problem.

2.3 Ionic liquids (ILs)

In addition to surfactants and block copolymers, ionic liquids (ILs) are another choice of soft template for synthesizing graphitic carbon nitride. Ionic liquids are liquid state salts at a relatively low temperature (less than 100 °C), and have no measurable vapor pressure, thus can be heated without evaporation.[42] Most ILs contain an organic, nitrogen-containing cation, such as alkylammonium, *N*,*N*′-dialkylimidazolium, 1-ethyl-3-methylimidazolium (EMIM) or 3-methyl-1-butylpyridine (3-MPB) and an inorganic anion. Welton summarized two basic methods for the preparation of ionic liquids: one is metathesis of a halide salt with alkali metal or ammonium salt of the desired anion, the other is acid-base neutralization.[43]

Paraknowitsch *et al.* used 1-ethyl-3-methylimidazolium (EMIM) and 3-methy-1-butylpyridine (3-MPB) as organic cations and dicyandiamide (DCDA) as the anion to form ILs that consist only of C, N and H atoms.[44] The sample showed high nitrogen content when heating the IL precursor to 900–1000 °C, and a high conductivity similar to that of graphite. Besides working as precursors and templates to synthesize mesoporous g-CN, ILs can also be used as chemical doping strategy to modify the electronic structures of g-CN and enhance its ionic conductivity. Zhang *et al.* used one of the most common ionic liquids, 1-butyl-3-methylimidazolium hexafluorophosphate (BMIM-PF_6) as a mild phosphorus template with dicyandiamide (DCDA) as precursor. On heating, PF_6^- reacted with amine groups to integrate into the C–N framework and finally give P-doped carbon nitride solids. Since P-concentration was low, the P-doped carbon nitride maintained most of structural features of g-CN, but electronic features of g-CN changed dramatically, showing a significant increase in electric conductivity by 4 orders of magnitude as shown in Fig. 5.[45] The electrical conductivity of pristine g-CN was less than 1×10^{-10} S m^{-1}. Meanwhile, that of P-doped g-CN showed a value of *ca.* 5×10^{-7} S m^{-1}. A higher value of electric conductivity for g-CN indicates that it possesses a higher charge-carrier density, which would further increase the photocatalytic activity of g-CN. This method of simultaneous texturing and doping of g-CN was also employed by Lin *et al.* who polymerized urea with 1-butyl-3-methylimidazolium tetrafluoroborate ([BMIM][BF_4]) and heated to form B/F-doped carbon nitride nanosheets.[46]

These interesting examples provide a platform for future work with ionic liquids for synthesis of carbon nitrides. One

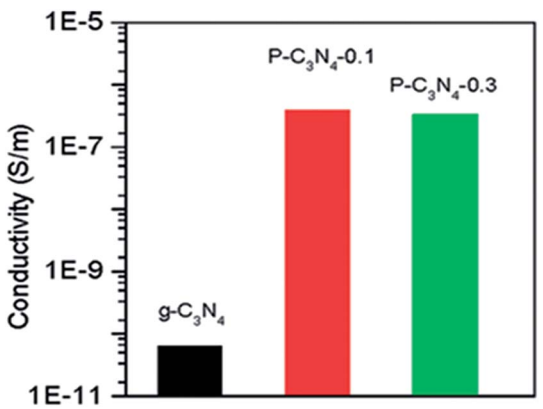

Fig. 5 Electrical conductivity of P-doped and pristine g-CN. Reprinted with permission from ref. 45, copyright 2010, American Chemical Society.

advantage of ionic liquids is their state – they can readily be incorporated with either liquid precursors or infiltrated into a porous template. The wide range of heteroatom chemistry available in ionic liquids (*e.g.* boron, phosphorus) means they are good precursors for introducing dopants during the templating process. The high thermal stability and negligible vapour pressure of ionic liquids also provides a valuable alternative to most solvents and enables a solid-state synthesis that is hybrid between sol–gel type chemistry and molten salt synthesis. Reactants are held in the solution state for much longer during the synthesis, which can completely change crystallization kinetics and even the crystallization pathway.[47] The solution state of these systems also enables the formation of a variety of structures such as thin films, wires and coatings. Obviously, there are some drawbacks to ionic liquids, not least the high cost relative to many other solvents and the incompatibility of some ionic liquids with water. However, there are certainly some interesting advances to be made in this field.

2.4 Gas bubbles

Some investigations also show that gas bubbles could be a choice for soft templating methods to synthesize g-CN. Han *et al.* introduced a heterogeneous nucleation to study the mechanism of hollow particles of $CaCO_3$ *via* the bubble templating method,[48] In this case, the bubble surface can significantly reduce the nucleation activation barrier and improve nucleation. The nuclei first formed at bubble surface, then aggregation started to form the inner layer of the shell and the crystals growing on the surface of the inner layer expanded the shell and formed its outer layer.

While the above example is based on the reaction of CO_2 in gas bubbles with Ca^{2+} in solution, it provides an interesting idea that can be more generally applied – the use of gas bubbles as templates for any material. In the case of g-CN, the application of gas bubbles has come from 'templating' of g-CN by *in situ* generated gas bubbles that are produced during synthesis. Zhang *et al.* heated urea directly to produce graphitic carbon nitride with a BET surface area of 70 m^2 g^{-1}.[49] During the synthesis, the urea decomposes and the polymerizes to form g-CN. As with other precursors, a considerable amount of ammonia is evolved but due to the oxygen atom on the urea, water is also given off. It is these bubbles of water vapour that are believed to be the template in this system. Compared to other templating methods for synthesis of g-CN, gas bubbles are simple and convenient and can synthesize hollow structures in a one-step approach, avoiding the introduction of impurities and post treatments. It will be fascinating to see how gas bubble templating can be advanced in g-CN synthesis, perhaps by precipitating solid g-CN precursors such as melamine sulfate around gas bubbles, followed by calcination.

2.5 Summary of soft templating methods

Soft templating is a relatively straightforward approach to the introduction of porosity into g-CN and is flexible through the choice of template and pyrolysis route. However, the use of organic templates can result in high levels of residual carbon, even on calcination in air. This is generally detrimental to the photocatalytic properties. A further drawback of soft templating is the lack of predictability due to the dynamic nature of many soft-templating systems. Soft templates are more challenging to characterize and understand than a solid-state 'hard' template. They also tend to decompose at relatively low temperatures and so may have limited influence on the porosity. This may hinder the application of soft templating to the formation of g-CN with highly-ordered mesoporous or microporous structure. Some of these drawbacks may be addressed by the use of hard templates.[50]

3. Hard templating methods

3.1 Introduction of hard templating methods

Hard templating methods have been widely applied to a range of 'soft' and 'hard' materials, including g-CN. Hard templating, also known as 'nanocasting', involves filling or coating of a rigid template with a precursor material, treatment of the precursor to form the desired material and finally removal of the template to create a replica. Templated materials can take a range of forms including hollow materials from coating a template, or inverse materials from infilling of voids within a template (Fig. 6). The essential difference between hard and soft templating methods is that soft methods rely on the cooperative assembly between the surfactant and inorganic phase, not replicating a certain surfactant structure. Compared with soft templating methods, the product of using hard template are relatively easy to control, since templates have fixed structures.[51,52] In this review, we will concentrate on silica, alumina oxide and carbon as templates to obtain g-CN.

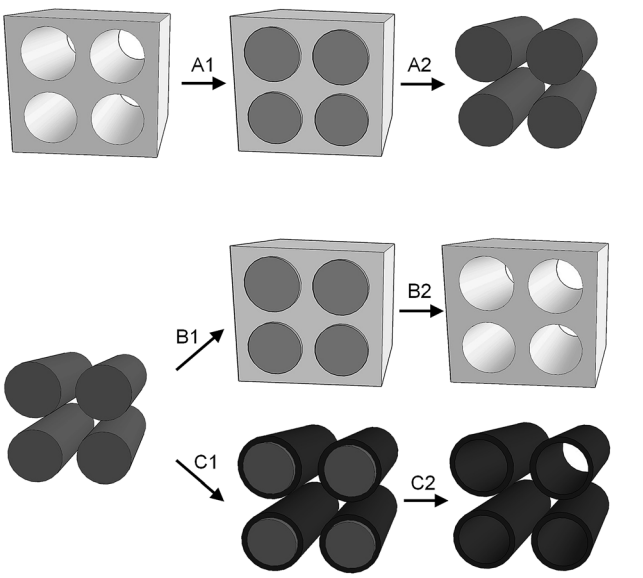

Fig. 6 A schematic of nanocasting steps including infilling of a hollow (A1) or particulate (B1) template or coating (C1) of a template followed by removal of the template to leave inverse (A2) or hollow (B2, C2) replicas.

3.2 Silica

Silica is a common material for hard templating methods due to its advantageous properties such as robustness under reaction environment, tunable pore size, easily controlled morphologies and stability under heat treatment. A common example is SBA15, an ordered mesoporous silica, which itself is formed *via* a templating method using a block copolymer. Hartmann *et al.* demonstrated a method to synthesize SBA-15 by using P123 ($EO_{20}PO_{70}EO_{20}$, average molecular weight 5800) an amphiphilic triblock copolymer. This is mixed with HCl solution, followed by the introduction of tetraethyl orthosilicate (TEOS) to the system under stirring and heat treatment. The final obtained solids are calcined in air at 540 °C.[53] Vinu *et al.* used SBA-15 as a hard template and added it to mixture of ethylenediamine and carbon tetrachloride. After stirring at 90 °C, the sample was heated-treated in N_2 flow to achieve carbonization. Carbon nitride material was obtained by dissolution of SBA-15 in 5% (by mass) hydrofluoric acid. XRD and Fourier-transform infrared (FTIR) spectrum confirmed the formation of g-CN and nitrogen porosimetry showed a BET surface area of 505 $m^2\ g^{-1}$, nitrogen adsorption isotherms reflected the characters of the uniform mesopores. High-resolution transmission electron microscopy (HRTEM) and energy filtered transmission electron microscopy EF-TEM images of the sample are shown in Fig. 7.[54] Vinu's study indeed firstly synthesized hexagonally ordered mesoporous carbon nitride material with uniform mesopore distribution, high specific surface area and high mesopore volume. But Chen *et al.* pointed out a drawback in Vinu's method,[55] that is the high ratio of carbon to nitrogen (C/N) makes the material more like a nitrogen doped carbon, rather than carbon nitride. They improved this by impregnating SBA-15 in cyanamide and heated the composite at 550 °C for 4 h to ensure condensation of the cyanamide into dicyandiamide. Removal of silica template finally resulted in carbon nitride as a yellow powder. The C/N ratio in this sample reduced to 0.72 and the sample also showed high surface area and pore volume.[56]

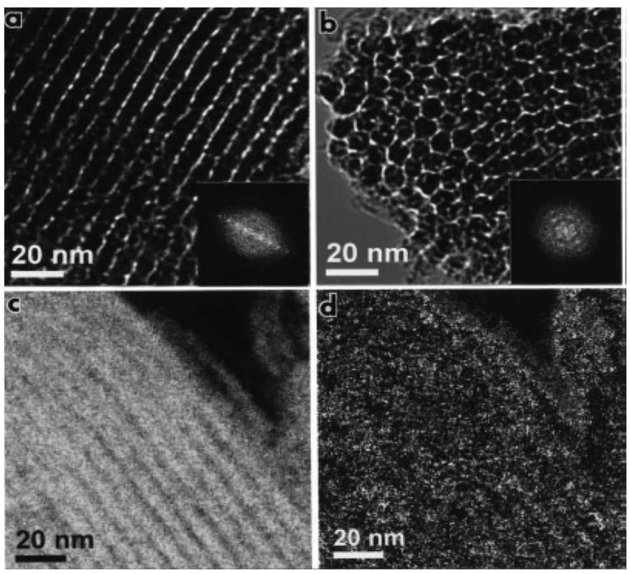

Fig. 7 (a and b) HRTEM and (c and d) EF-TEM images of mesoporous carbon nitride: (a) along the mesopores, (b) across the mesopores. Elemental maps of C (c) and N (d) correlate well. Reprinted with permission from ref. 54.

Meanwhile, we are pleased to see researchers have used different forms of silica template to synthesize carbon nitride. For instance, Li *et al.* used spherical mesostructured cellular silica foams (MCFs) as a hard template to synthesize porous carbon nitride. Compared with synthesizing SBA-15, the difference is that before and after adding TEOS, 1,3,5-trimethylbenzene (TMB) and ammonium fluoride were introduced to the solution, respectively. Then ethylenediamine (EDA) and carbon tetrachloride (CTC) were mixed with MCFs to form carbon nitride. Finally high nitrogen content (17.8 wt%) hierarchical mesoporous CN spheres were obtained. The Fourier transform infrared spectroscopy FT-IR spectrum suggested that the porous spheres mainly consist of pyridine and benzene rings interconnected by nitrogen atoms. The 3D hierarchical mesostructure has a specific surface area of 550 $m^2\ g^{-1}$ and a pore volume of 0.90 $cm^3\ g^{-1}$ and demonstrates good cycling stability as a CO_2 adsorbent.[57] Using silica as hard template shows a result of ordered mesoporous carbon nitride with large surface area, uniform pore size and 2D or 3D accessible framework. Inverting the structure, *i.e.* using silica spheres as a template instead of a silica foam, results in g-CN with an inverse opal structure.[58] The high accuracy of replication in this work was attributed to strong interactions between the cyanamide precursor and the silica surface. These ordered mesoporous carbon nitrides have potential in a number of applications, such as photocatalysis, gas storage and lubricants.

3.3 Anodic alumina oxide (AAO)

Besides silica, porous anodic alumina oxide (AAO) is another metal oxide hard template that can be used to synthesize g-CN. AAO is formed by potentiostatic anodization of aluminium. A hexagonal lattice with optical quality formed by cylindrical pores can be observed through further insight into the structure of AAO. Selective etching of the aluminum oxide facilitates the adjustment of pore sizes, ranging from 15 nm to 100 nm, which widely expands the scope of hexagonal porous silica to a larger size range. Even though the pore structure cannot be expected to confine the conformation of a single polymer chain, it can strongly influence polymer assembly.[59,60]

Bian *et al.* synthesized an ordered array of the g-CN nanotubes with uniform diameter and length by using porous AAO as the template with ethylenediamine and carbon tetrachloride as precursors (Fig. 8).[61] By using borohydride as reducing agent, they also deposited Pt nanoparticles on the surface of the g-CN nanotubes. Through TEM characterization, it was shown that g-CN nanotubes can promote high dispersion of Pt nanoparticles. This is not difficult to understand, due to the fact that g-CN nanotubes have a rough surface and the nitrogen atoms have two unbonded electron pairs, which can attract Pt ions to start the nucleation and growth of Pt nanocrystals.[62] This kind of g-CN nanotubes are a good support for noble metal nanoparticles and show a high catalytic activity in terms of cyclohexene

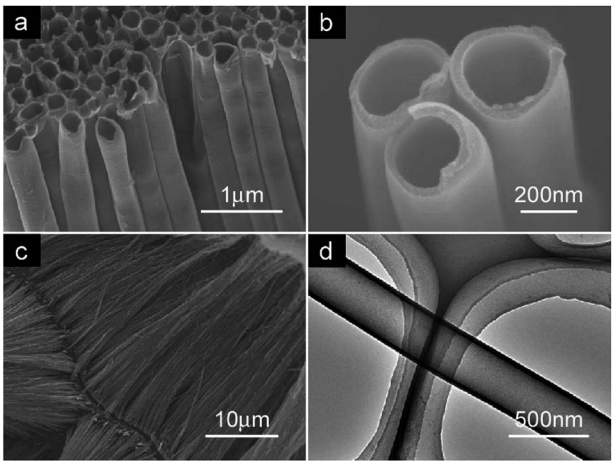

Fig. 8 (a) SEM image of g-CN nanotube; (b) higher magnification SEM image of g-CN nanotube; (c) SEM image of g-CN nanotube array from side view; (d) TEM image of g-CN nanotube. Reprinted with permission from ref. 61. Copyright (2009) American Chemical Society.

hydrogenation. However, two disadvantages still exist in this nanotube, one is the surface area is smaller than mesoporous g-CN, the other is that C/N ratio is 4.9, which is much higher than the theoretical value of 0.75, making it more like a nitrogen-doped carbon material than carbon nitride.

Li *et al.* synthesized rod-like g-CN by using AAO as template with cyanamide as precursor, and illustrated the improvement of orientation and the crystallization of g-CN due to confinement effect of the AAO template.[63] After acid etching the AAO template, rod like g-CN was obtained with a distribution of diameters near 260 nm. A slightly higher C/N ratio (0.72) than that of bulk g-CN(0.68) was observed by elemental analysis. The confinement effect of alumina channels was observed by transmission electron microscopy (TEM), carbon nitride firstly formed a close-packed layer on pore wall of the AAO. Then the as-formed layer became a nucleation center, leading to the condensed secondary crystals adsorbed on the pore wall, with approximately 76°orientation to the wall. The result of UV/vis spectrum shifted blue indicated rod-like g-CN has a lower HOMO position than bulk g-CN, and due to the lower HOMO position, the rod-like g-CN possesses improved photocatalytic performance in H_2 evolution from water splitting. By adjusting material nanostructures, AAO membranes with different dimensions and pore sizes improve the condensation and orientation of g-CN, which will effectively increase the crystallinity and lower the HOMO position, resulting in highly photoactive carbon nitride.

3.4 Carbon

Moving on from metal oxides, graphene, a single layer sheet of sp^2 carbon atoms with a honeycomb structure, which is from the family of carbon materials, can also work as a hard template to assist formation of g-CN. This is in part due to the interesting thermal and electrical properties of graphene. For example, graphene has a high thermal conductivity up to 5000 W m^{-1} K^{-1}, a high specific surface area approximately 2600 m^2 g^{-1}. Graphene can be obtained through a relatively simple approach, the first step is oxidation of natural graphite into graphene oxide (GO), the second step is reduction of GO, which gives graphene, an good starting point to synthesize graphene-based composites.[64,65]

Xiang *et al.* fabricated graphene/g-CN by means of polymerization of melamine in the presence of GO and hydrazine hydrate under a heat treatment at 550 °C with nitrogen flow, and studied its photocatalytic activity. This was the first report on photocatalytic activity of graphene/g-CN composite that generated hydrogen under irradiation of visible light.[66] The composite has a more compact structure than pristine g-CN since g-CN is believed to infiltrate between the graphene sheets *via* polymerization of melamine molecules, thus g-CN is fixed on graphene sheets surface to form a layered composite. Graphene sheets are thought to enhance the photocatalytic activity of g-CN by acting as conductive channels and as good electron acceptor materials. The proposed mechanism is that the graphene sheets in the composite can separate the photogenerated electrons and holes *via* the 2D π-conjugated structure and thus hinder charge recombination. The influence of the graphene weight percentage in the sample was also studied by photoluminescence (PL) emission and transient photocurrent. A lower value of PL emission and a higher value of photocurrent occur when the graphene percentage is 1.0% (as shown in Fig. 9), which shows a significant separation of photogenerated electron–hole pairs at the interface between g-CN and graphene. This work indicates that graphene is a promising choice for enhancing photocatalytic activity of g-CN and developing high photocatalysts.[67]

Another candidate from the carbon family that can work as a hard template is mesoporous carbon. Zheng *et al.* impregnated the hard template CMK-3, a highly ordered mesoporous carbon, with the liquid precursor cyanamide and heated to form g-CN in the voids of CMK-3.[68] The electrocatalytic activities were investigated and compared with a physical mixture of CMK-3 and g-CN as well as pristine mesoporous g-CN prepared by sacrificing SBA-15 template method. The test result of g-CN/CMK-3 shows a larger cathodic current than the other two, which indicates g-CN/CMK-3 composites possess excellent oxygen reduction reaction (ORR) catalytic efficiency. However, the photocatalytic properties of carbon-templated g-CN may be compromised by the high ratio of carbon. Carbon templates for synthesis of g-CN have already opened up new avenues to enhance its photocatalytic activities and make it possible for g-CN to become widely used in the fields such as photonic catalysis, hydrogen production and sensors.

As well as templating, the addition of carbon to g-CN materials can enhance photocatalytic properties by aiding electron transfer. As mentioned above, this has to be done in a way that does not impair light absorption. A possible approach is to use carbon quantum dots (CQDs), that can be synthesized relatively simply for example from sucrose.[69] Liu *et al.* synthesized CQDs electrochemically and treated them with ammonia before mixing with urea and heating to 550 °C to obtain CQD–gCN composites.[70] The CQDs were distributed in the g-CN matrix, which leads to an increase in the ultraviolet-visible (UV-Vis)

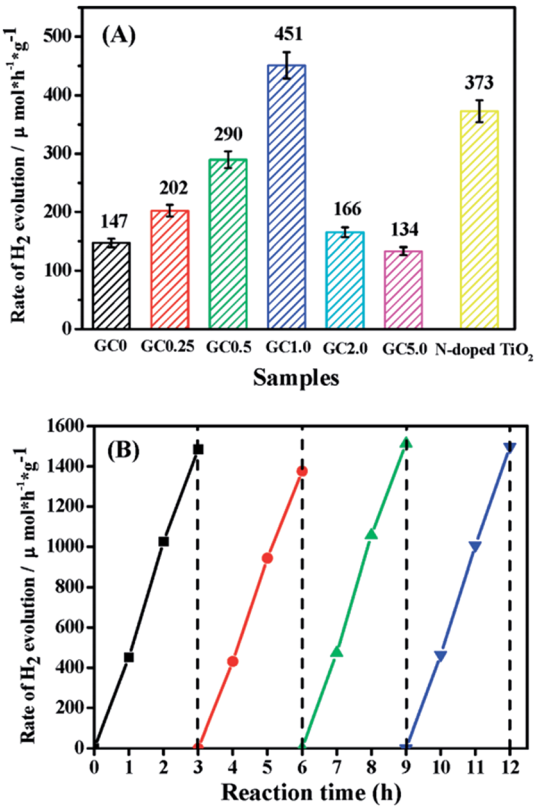

Fig. 9 (A) Comparison of the photocatalytic activity between GCx and N-doped TiO_2, for the generation of H_2 from methanol aqueous solution. (*x* is the weight percentage of graphene, $x = 0$, 0.25, 0.5, 1.0, 2.0, 5.0). (B) Cyclic H_2-evolution curve for GC1.0 sample. Reprinted with permission from ref. 66. Copyright (2011) American Chemical Society.

absorption and high water splitting efficiency, at least one order of magnitude larger than that of many stable water splitting photocatalysts reported before. Besides its high quantum efficiency, the CQD–gCN composites can be synthesized by low-cost, environmental friendly materials and it can also maintain a high rate of H_2 and O_2 generation in 200 runs of recycling stably. All advantages mentioned above show great potentials of using carbon quantum dots in templating g-CN.

Silica, AAO and carbon are common hard templates for g-CN synthesis but may have some problems associated with removal of the template. Recently, research on sustainable ways to synthesize porous g-CN has been reported by Wang *et al.* They used calcium carbonate particles as template,[71] which is potentially more sustainable, since $CaCO_3$ can be readily removed with dilute hydrochloric acid. Calcium carbonate particles are readily synthesized from abundant ingredients and so may also offer an economical advantage. To prepare porous g-CN, DCDA was mixed with $CaCO_3$ in different ratios, and to avoid side reactions, the samples were heated first to 400 °C, then to 550 °C before using dilute HCl to remove template. The as-prepared porous g-CN has been proven to possess not only enlarged surface areas but also high photocurrents, showing ~4.2 and 7.5 times under bias potential of −0.2 V and 0 V respectively when compared with that of bulk g-CN. The study shows that $CaCO_3$ templated g-CN has potential application in solar energy conversion and environmental purification as well. When taking economic factors into consideration, it also has potential in industrial applications.

3.5 Summary of hard templating methods

Hard templates have already witnessed great success in templating methods of synthesizing g-CN, the range of the templates applied in nanocasting of highly-ordered and porous g-CN have already extended from silica to alumina oxide and carbon. However, this kind of method still faces challenges. In many occasions, such as using silica template, aqueous ammonium bifluoride (NH_4HF_2) or hydrogen fluoride (HF) are needed to remove the template, which is hazardous to environment and also has many safety concerns. Furthermore the acid environment during removal of the template may damage the properties of target materials. This may not affect the g-CN itself but could damage other materials in a composite. Increasing the loading of the templates with high concentration precursor is another challenge, as much precursor is necessary to avoid collapse of the porous structure after removal of the templates.[72]

4. Biotemplating

4.1 Introduction of biopolymers and biotemplates

In previous sections of this review, we introduced soft and hard templating methods and showed that both of them have advantages and disadvantages. The relatively simple pyrolysis methods using soft templates makes them convenient but they often suffer from poor control and residual carbon. Hard templates have a more fixed and stable structure making the products easy to control. However, the removal of the template can be problematic and involve hazardous reagents such as HF or NH_4HF_2. While there are many future directions in the above methods, it seems difficult to achieve 'high order', 'sustainable' and 'convenient' all in the same method. With the increasing drive towards sustainability, the inspiration for new routes to graphitic carbon nitrides may come from nature. Just as the stripes of a zebra can inspire camouflage patterns, biological materials may provide ideal templates for g-CN.

The term biopolymer is used both for polymers that are synthesized from bio-derived monomers as well as macromolecules that are produced directly by living organisms. In this review, we will focus on the second one: that is macromolecules from living organisms. The reasoning for including biopolymers as a separate section is that they are not easy to classify as 'soft' or 'hard'' templates – it depends what feature of the biopolymer is being used. Some biopolymers display 'self-assembly' properties to form hierarchical aqueous gels of double or triple helices. The same biopolymers can be used to produce fibres or sponge-like structures that can be used as hard templates. In this way, biopolymers have been used as 'structure-directing agents' to organize crystalline particles or to control crystal growth in the solution phase. They are also widely used in 'sol–gel' chemistry to synthesize nanostructures

of metal oxides, nitrides and carbides. In the case of hard templating, as well as biopolymer fibres (*e.g.* cellulose nanofibers) and foams, whole biological structures can also be used such as bacteria, viruses and butterfly wings.[73]

4.2 Biotemplates

Both polysaccharides and polypeptides have been used to introduce porosity into graphitic carbon nitride. Alginate and gelatin were mixed with aqueous dicyandiamide (DCDA) and heated to prepare g-CN samples with a sponge-like nanostructure (Fig. 10).[74] Compared with pristine and bulk g-CN, the sponge structure g-CN can reduce the diffusion path, enhance mass transfer and improve optical adsorption during reactions such as photocatalysis. During PEC measurements, the photocurrent of sponge-like g-CN strongly indicated the positive impact of the biopolymer templates. The results showed that alginate and gelatin are two promising activating agents for synthesis of graphitic carbon nitride. Alginate and gelatin both form helical structures when cooled from a hot solution as in this research. The resulting gel gives a framework for the DCDA to polymerize around to form g-CN with the porous structure.

A very different example of a biological material being used to template g-CN is diatoms. These are unicellular photosynthetic organisms, which possesses unique frustule architectures with hierarchical structures. Diatoms were combined with cyanamide and heated to synthesize a carbon nitride material with a diatom frustule structure.[75] The SEM and confocal fluorescence both confirmed that carbon nitride wrapped on the frustule well. Mesoporous g-CN synthesized with commercial silica nanoparticles and bulk g-CN fabricated from the thermal condensation of cyanamide were used as control samples to make a comparison with diatom frustule g-CN. Their photocatalytic abilities were estimated by regeneration of NADPH from nicotinamide adenine dinucleotide phosphate (NADP). The result is diatom frustule g-CN gives the best regeneration yield, although the surface area of diatom frustule g-CN is lower than silica template g-CN, and diatom frustule didn't show ideal regeneration efficiency at the beginning of the reaction. This phenomenon could be ascribed to the diatom structure, since it has evolved enhanced light trapping and scattering abilities.

4.3 Summary of biotemplates

Biopolymers are new choices for templating methods to synthesize graphitic carbon nitride. Due to their unique properties and structures, they can endow g-CN with new structures and performances that synthetic templates may not give. Therefore, biopolymers widen the avenue of templating methods and many pioneering works on bio-templates are still continuing. Besides, when working as hard templates, biopolymers usually don't need to be removed by acid treatment, which gives a promising future for templating g-CN.

5. Summary of templating methods

In this article, we have reviewed research on templating methods to synthesize graphitic carbon nitride, including soft, hard and biological templates. Self-assembly characteristics of soft templates means g-CN can form different morphologies *via* a facile route. They are also flexible and if they are used to template the melamine sulfate precursor, there may also be a chance to remove and reuse the soft template. However, the thermal instability of most small molecule templates means that a carbon residue often remains in the sample, which decreases the nitrogen content, blocks light absorption and can compromise catalytic activity.

Hard templating methods, also known as nanocasting methods, offer the advantage that the template is generally very stable. Because of this and the rigidity of the template, it is often easier to control the morphology of g-CN in the final product and generate materials with more uniform structural characteristics. However, many of the common hard templates require removal with caustic or highly acidic media such as HF, which brings serious problems for safety and sustainability. Another issue is that the template may be relatively small scale or difficult to synthesize. It may also be problematic to load adequate amounts of the g-CN precursors such as melamine or DCDA into a meso or microporous template.

Biotemplating is well established as a general technique but is only recently being applied to g-CN materials. The unique properties of biopolymers and biomass, such as rich surface chemistry and strong gels, offer many advantages to the materials chemist. This enriches the field of g-CN templating and also offers the potential for improving sustainability, if an

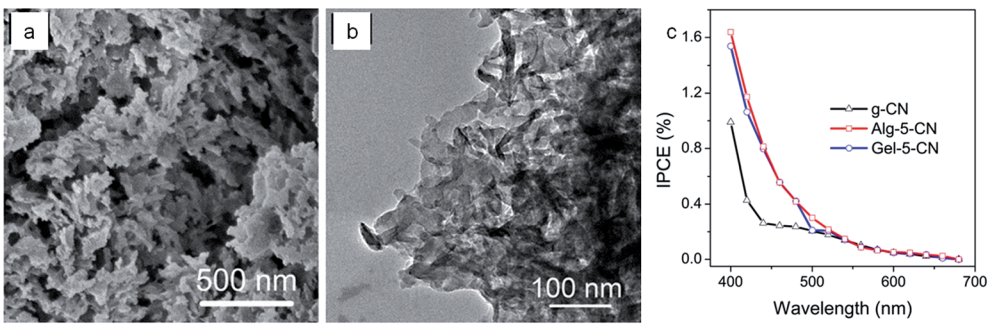

Fig. 10 (a) SEM and (b) TEM images of alginate-templated g-CN showing porous structure and (c) photo action spectra of control g-CN (black), alginate-templated g-CN (red), and gelatin-templated g-CN (blue) biased at −0.2 V *vs.* Ag/AgCl (sat. KCl). Modified with permission from ref. 74.

abundant and readily-extracted biomaterial is employed. Biotemplates may not overcome the limitations of residual carbon that traditional soft templates may have, or the problem of removing the template. However, given the shortage of reports on biotemplating of g-CN materials, there is considerable potential in this direction.

6. Conclusions

While reviewing the literature in this field, we have found three important factors that are common to many templating methods for g-CN. It may be useful to share these thoughts with readers. The first observation is the importance of the nitrogen content. The theoretical C/N ratio in pristine graphitic carbon nitride is 0.75. If the experimental value is higher and the sample appears dark, there is likely to be residual carbon which may significantly hinder photocatalytic properties,[50] or the material may be better classed as a nitrogen-doped carbon rather than a g-CN material. For very high values, the material may be better classed as a nitrogen-doped carbon rather than a g-CN material. The second observation is that the highest surface area does not necessarily mean the best performance. This is clear, for example, from the work with diatom frustules.[75] Photocatalytic activity of g-CN is determined by multiple chemical and physical factors for example pore size, pore accessibility and also doping with metal ions, heteroatoms or conductive carbon.

The last observation is the lack of study on the interaction between g-CN precursors and hard template surfaces. Most preparations simply 'mix' or 'impregnate' templates with precursors without considering whether the template–precursor interactions are favourable. This is in contrast with some of the extensive investigations of the mechanisms of soft templating (although not so much in the g-CN field). This may impact the loading ability of a template, which may impair the structural integrity of g-CN if it is too delicate to withstand chemical or physical removal of the template.[52] Of course, the template could be left with the material and if the g-CN is to be used in electrocatalysis this may not be a problem. However, it is likely to impact photocatalytic activity and certainly the material should no longer be referred to as g-CN, but a template-g-CN composite. Perhaps in the future, more studies on the interactions between hard templates and precursors are necessary. Certainly, there have been efforts to enhance precursor–template interactions in the templating of metal oxide materials, for example hydrolyzing the surface of biomass,[76] or careful layer-by-layer hydrolysis of a precursor.[77] Undoubtedly, many of the advances that have been made in the general field of templating can be applied to g-CN synthesis.

Acknowledgements

The authors thank M. J. Hollamby for valuable discussion.

References

1 X. Chen, J. Zhang, X. Fu, M. Antonietti and X. Wang, *J. Am. Chem. Soc.*, 2009, **131**, 11658–11659.
2 Y. Zheng, Y. Jiao, J. Chen, J. Liu, J. Liang, A. Du, W. Zhang, Z. Zhu, S. C. smith, M. Jaroniec, G. Q. Lu and S. Z. Qiao, *J. Am. Chem. Soc.*, 2011, **133**, 20116–20119.
3 N. Cheng, J. Tian, Q. Liu, C. Ge, A. H. Qosti, A. M. Asiri, A. O. Al-Youbi and X. Sun, *ACS Appl. Mater. Interfaces*, 2013, **5**, 6815–6819.
4 X. Wang, K. Maeda, X. Chen, K. Takanabe, K. Domen, Y. Hou, X. Fu and M. Antonietti, *J. Am. Chem. Soc.*, 2009, **131**, 1680–1681.
5 J. Tian, Q. Lium, C. Ge, Z. Xing, A. M. Asiri, A. O. Al-Youbi and X. Sun, *Nanoscale*, 2013, **5**, 8921–8924.
6 H. D. Roth, *Angew. Chem., Int. Ed.*, 1989, **28**, 1193–1207.
7 N. Hoffmann, *Chem. Rev.*, 2008, **108**, 1052–1103.
8 K. Maeda, K. Teramura, D. Lu, T. Takata, N. Saito, Y. Inoue and K. Domen, *Nature*, 2006, **440**, 295.
9 P. Wessig, *Angew. Chem., Int. Ed.*, 2006, **45**, 2168–2171.
10 X. Wang, S. Blechert and M. Antonietti, *ACS Catal.*, 2012, **2**, 1596–1606.
11 M. R. Hoffmann, S. T. Martin, W. Choi and D. W. Bahnemann, *Chem. Rev.*, 1995, **95**, 69–96.
12 J. Liqiang, Q. Yichun, W. Baiqi, L. Shudan, J. Baojiang, Y. Libin, F. Wei, F. Honggang and S. Jiazhong, *Sol. Energy Mater. Sol. Cells*, 2006, **90**, 1773–1787.
13 A. Fujishima and K. Honda, *Nature*, 1972, **238**, 37–38.
14 A. Kudo, R. Niishiro, A. Iwase and H. Kato, *Chem. Phys.*, 2007, **339**, 104–110.
15 J. Tian, Z. Zhao, A. Kumar, R. I. Boughton and H. Lou, *Chem. Soc. Rev.*, 2014, **43**, 6920–6937.
16 A. J. Maira, K. L. Yeung, C. Y. Lee, P. L. Yue and C. K. Chan, *J. Catal.*, 2000, **192**, 185–196.
17 S. Guo, X. Li, H. Wang, F. Dong and Z. Wu, *J. Colloid Interface Sci.*, 2012, **369**, 373–380.
18 J. H. Jung, H. Kobayashi, K. J. C. van Bommel, S. Shinkai and T. Shimizu, *Chem. Mater.*, 2002, **14**, 1445–1447.
19 Y. Sun, G. M. Fuge, N. A. Fox, D. J. Riley and M. N. R. Ashfold, *Adv. Mater.*, 2005, **17**, 2477–2481.
20 K. Sivula, F. Le Formal and M. Grätzel, *ChemSusChem*, 2011, **4**, 432–449.
21 K. Zhang and L. Guo, *Catal. Sci. Technol.*, 2013, **3**, 1672–1690.
22 K. Maeda and K. Domen, *J. Phys. Chem. C*, 2007, **111**, 7851–7861.
23 K. Maeda and K. Domen, *J. Phys. Chem. Lett.*, 2010, **1**, 2655–2661.
24 A. Y. Liu and M. L. Cohen, *Science*, 1989, **245**, 841–842.
25 A. Thomas, A. Fischer, F. Goettmann, M. Antonietti, J. Müller, R. Schlögl and J. M. Carlsson, *J. Mater. Chem.*, 2008, **18**, 4893–4908.
26 Z. Zhou, J. Wang, J. Yu, Y. Shen, Y. Li, A. Liu, S. Liu and Y. Zhang, *J. Am. Chem. Soc.*, 2015, **137**, 2179–2182.
27 M. Groenewolt and M. Antonietti, *Adv. Mater.*, 2005, **17**, 1789–1792.
28 M. Deifallah, P. F. McMillan and F. Corà, *J. Phys. Chem. C*, 2008, **112**, 5447–5453.
29 X. Wang, K. Maeda, A. Thomas, K. Takanabe, G. Xin, J. M. Carlsson, K. Domen and M. Antonietti, *Nat. Mater.*, 2008, **8**, 76–80.

30 Y. Zheng, J. Liu, J. Liang, M. Jaroniec and S. Z. Qiao, *Energy Environ. Sci.*, 2012, **5**, 6717–6731.
31 A. M. Collins, C. Spickermann and S. Mann, *J. Mater. Chem.*, 2003, **13**, 1112–1114.
32 Z. Y. Yuan, T. Z. Ren and B. L. Su, *Adv. Mater.*, 2003, **15**, 1462–1465.
33 M. J. Hollamby, D. Borisova, P. Brown, J. Eastoe, I. Grillo and D. Shchukin, *Langmuir*, 2011, **28**, 4425–4433.
34 N. D. Petkovich and A. Stein, *Chem. Soc. Rev.*, 2013, **42**, 3721–3739.
35 J. N. Israelachvili, *Intermolecular and Surface Forces*, Academic Press, Waltham, MA, 3rd edn, 2011.
36 K. Holmberg, *J. Colloid Interface Sci.*, 2004, **274**, 355–364.
37 C. T. Kresge, M. E. Leonowicz, W. J. Roth, J. C. Vartuli and J. S. Beck, *Nature*, 1992, **359**, 710–712.
38 Y. Wang, X. Wang and M. Antonietti, *Angew. Chem., Int. Ed.*, 2012, **51**, 68–89.
39 Y. Wang, X. Wang, M. Antonietti and Y. Zhang, *ChemSusChem*, 2010, **3**, 435–439.
40 H. Yan, *Chem. Commun.*, 2012, **48**, 3430–3432.
41 Q. Fan, J. Liu, Y. Yu and S. Zuo, *RSC Adv.*, 2014, **4**, 61877–61883.
42 P. Wasserscheid and W. Keim, *Angew. Chem.*, 2000, **39**, 3772–3789.
43 T. Welton, *Chem. Rev.*, 1999, **99**, 2071–2084.
44 J. P. Paraknowitsch, J. Zhang, D. Su, A. Thomas and M. Antonietti, *Adv. Mater.*, 2010, **22**, 87–92.
45 Y. Zhang, T. Mori, J. Ye and M. Antonietti, *J. Am. Chem. Soc.*, 2010, **132**, 6294–6295.
46 Z. Lin and X. Wang, *ChemSusChem*, 2014, **7**, 1547–1550.
47 D. C. Green, S. Glatzel, A. M. Collins, A. J. Patil and S. R. Hall, *Adv. Mater.*, 2012, **24**, 5767–5772.
48 Y. Han, M. Fuji, D. Shchukin, H. Möhwald and M. Takahashi, *Cryst. Growth Des.*, 2009, **9**, 3771–3775.
49 Y. Zhang, J. Liu, G. Wu and W. Chen, *Nanoscale*, 2012, **4**, 5300–5303.
50 W. Li and D. Zhao, *Chem. Commun.*, 2013, **49**, 943–946.
51 J. Xu, Y. Wang and Y. Zhu, *Langmuir*, 2013, **29**, 10566–10572.
52 A. H. Lu and F. Schüth, *Adv. Mater.*, 2006, **18**, 1793–1805.
53 M. Hartmann and A. Vinu, *Langmuir*, 2002, **18**, 8010–8016.
54 A. Vinu, K. Ariga, T. Mori, T. Nakanishi, S. Hishita, D. Golberg and Y. Bando, *Adv. Mater.*, 2005, **17**, 1648–1652.
55 X. Chen, Y. S. Jun, K. Takanabe, K. Maeda, K. Domen, X. Fu, M. Antonietti and X. Wang, *Chem. Mater.*, 2009, **21**, 4093–4095.
56 Y. S. Jun, W. H. Hong, M. Antonietti and A. Thomas, *Adv. Mater.*, 2009, **21**, 4270–4274.
57 Q. Li, J. Yang, D. Feng, Z. Wu, Q. Wu, S. S. Park, C.-S. Ha and D. Zhao, *Nano Res.*, 2010, **3**, 632–642.
58 F. Goettmann, A. Fischer, M. Antonietti and A. Thomas, *Angew. Chem., Int. Ed.*, 2006, **45**, 4467–4471.
59 H. Masuda and K. Fukuda, *Science*, 1995, **268**, 1466–1468.
60 A. Thomas, F. Goettmann and M. Antonietti, *Chem. Mater.*, 2008, **20**, 738–755.
61 S. W. Bian, Z. Ma and W. G. Song, *J. Phys. Chem. C*, 2009, **113**, 8668–8672.
62 H. Yoon, S. Ko and J. Jang, *Chem. Commun.*, 2007, 1468–1470.
63 X.-H. Li, J. Zhang, X. Chen, A. Fischer, A. Thomas, M. Antonietti and X. Wang, *Chem. Mater.*, 2011, **23**, 4344–4348.
64 M. J. Allen, V. C. Tung and R. B. Kaner, *Chem. Rev.*, 2010, **110**, 132.
65 D. R. Dreyer, S. Park, C. W. Bielawski and R. S. Ruoff, *Chem. Soc. Rev.*, 2010, **39**, 228–240.
66 Q. Xiang, J. Yu and M. Jaroniec, *J. Phys. Chem. C*, 2011, **115**, 7355–7363.
67 A. Du, S. Sanvito, Z. Li, D. Wang, Y. Jiao, T. Liao, Q. Sun, Y. H. Ng, Z. Zhu, R. Amal and S. C. Smith, *J. Am. Chem. Soc.*, 2012, **134**, 4393–4397.
68 Y. Zheng, Y. Jiao, J. Chen, J. Liu, J. Liang, A. Du, W. Zhang, Z. Zhu, S. C. Smith, M. Jaroniec, G. Q. Lu and S. Z. Qiao, *J. Am. Chem. Soc.*, 2011, **133**, 20116–20119.
69 H. T. Li, Z. H. Kang, Y. Liu and S. T. Lee, *J. Mater. Chem.*, 2012, **22**, 24230–24253.
70 J. Liu, Y. Liu, N. Liu, Y. Han, X. Zhang, H. Huang, Y. Lifshitz, S.-T. Lee, J. Zhong and Z. Kang, *Science*, 2015, **347**, 970–974.
71 J. Wang, C. Zhang, Y. Shen, Z. Zhou, J. Yu, Y. Li, W. Wei, S. Liu and Y. Zhang, *J. Mater. Chem. A*, 2015, **3**, 5126–5131.
72 J. Xu, Y. Wang and Y. Zhu, *Langmuir*, 2013, **29**, 10566–10572.
73 Z. Schnepp, *Angew. Chem., Int. Ed.*, 2013, **52**, 1096–1108.
74 Y. Zhang, Z. Schnepp, J. Cao, S. Ouyang, Y. Li, J. Ye and S. Liu, *Sci. Rep.*, 2013, **3**, 2163.
75 J. Liu and M. Antonietti, *Energy Environ. Sci.*, 2013, **6**, 1486–1493.
76 S. R. Hall, V. M. Swinerd, F. N. Newby, A. M. Collins and S. Mann, *Chem. Mater.*, 2006, **18**, 598–600.
77 J. Huang and T. Kunitake, *J. Am. Chem. Soc.*, 2003, **125**, 11834–11835.

AIP | APL Materials

Triple templating of graphitic carbon nitride to enhance photocatalytic properties

Z. Yang, A. E. Danks, J. Wang, Y. Zhang, and Z. Schnepp

Citation: APL Mater. **4**, 015706 (2016); doi: 10.1063/1.4936218
View online: http://dx.doi.org/10.1063/1.4936218
View Table of Contents: http://scitation.aip.org/content/aip/journal/aplmater/4/1?ver=pdfcov
Published by the AIP Publishing

Triple templating of graphitic carbon nitride to enhance photocatalytic properties

Z. Yang,[1] A. E. Danks,[1] J. Wang,[2] Y. Zhang,[2] and Z. Schnepp[1,a]
[1]*School of Chemistry, University of Birmingham, Birmingham B152TT, United Kingdom*
[2]*School of Chemistry and Chemical Engineering, Southeast University, Nanjing 211189, China*

(Received 28 August 2015; accepted 6 November 2015; published online 8 December 2015)

Graphitic carbon nitride materials show some promising properties for applications such as photocatalytic water splitting. However, the conversion efficiency is still low due to factors such as a low surface area and limited light absorption. In this paper, we describe a "triple templating" approach to generating porous graphitic carbon nitride. The introduction of pores on several length-scales results in enhanced photocatalytic properties. [http://dx.doi.org/10.1063/1.4936218]

Polymeric graphitic carbon nitride (g-CN) is a metal-free semiconductor that has been developed for a variety of applications, including solar water splitting, photodegradation, and metal-free catalysis.[1–3] Consisting of carbon and nitrogen atoms with a layered structure similar to graphite, g-CN shows high thermal stability up to 600 °C in air as well as high chemical stability.[4] g-CN has a band gap of approximately 2.7 eV, depending on structural variability or the presence of dopants, and so absorbs light in the visible region. Furthermore, the positions of the valence and conduction bands are centered around the oxidation and reduction potentials of water, making g-CN an attractive material for photo-driven water splitting.

Despite these advantages, the low conversion efficiency of bulk g-CN solids in sunlight is still a challenge. This can be due to several factors, including limited visible light absorption, low surface area, or grain boundary effects.[5] One of the main approaches to addressing this low conversion efficiency in g-CN and related materials has been to control grain size and porosity. The methods can be broadly characterized in terms of "soft" or "hard" templating. Soft templating typically employs self-assembling amphiphiles such as Triton X-100 to direct the growth of the g-CN phase from an aqueous precursor such as dicyandiamide (DCDA).[6] In this case, the formation of pores in the g-CN material may be partly due to a simple "casting" effect but can also be influenced by interactions between the amphiphile and the molecular precursor. In contrast, hard templating typically involves simple casting of the g-CN by filling a solid material such as silica,[7] anodized alumina,[8] or $CaCO_3$[9] with a precursor such as DCDA and heating to produce g-CN. Hard templating is very effective, giving surface areas up to 830 $m^2\ g^{-1}$.[10] However, harsh etchants such as hydrogen fluoride (HF) are often required to remove the original template.

Recently, biopolymers have been shown to be a promising option for controlling morphology in organic and inorganic materials.[11] The term "biopolymer" is sometimes used to describe polymers that are synthesized from bio-derived monomers, but we will consider only macromolecules produced by living organisms. Biopolymers encompass a wide range of structures and compositions, including polysaccharides and polypeptides. The chemical functionality of a biopolymer depends on the source and can include amine, amide, sulfate, carboxyl, or hydroxyl groups. In bioinspired materials chemistry, this means a biopolymer can be selected based on optimized physical properties or chemical interactions with the material of interest. One particular advantage of

[a]Electronic mail: z.schnepp@bham.ac.uk

many biopolymers is their ability to form strong gels in water that can organize molecular or ionic precursors. In the synthesis of a material, this can lead to high levels of morphological control or the controlled introduction of porosity. For example, biopolymers such as alginate (seaweed) and gelatin (animal skin) have been used to disperse and bind aqueous DCDA in a gel. Heating the gel produces a sponge-like g-CN nanostructure with active carbon-doped sites, which has shown good activity as a photocathode material.[5]

While biopolymer templating of g-CN is effective, there are still limitations to this method, mainly because the control of porosity is only on one length-scale. Indeed, this is a feature of most templating methods. One of the most attractive features of living organisms is their ability to control the structure of a material on multiple length-scales, giving hierarchical materials. For example, crustacean shells feature chitin nanofibres that bundle together into fibrils that in turn stack in a helical arrangement of fibre mats analogous to plywood.[12] Biopolymers have already been used to generate trimodal porosity in carbon materials, resulting in enhanced performance in electrocatalytic applications.[13] In g-CN and other photocatalytic materials, the ability to create hierarchical porosity would be particularly beneficial as this could help to enhance light absorption, reduce electron-hole recombination, and improve mass transport of fluids to and from the active photocatalyst surface.

In this paper, we demonstrate a triple-templating method to create a hierarchical g-CN material (Fig. 1). Rather than producing agar/DCDA gel and allowing it to dry and shrink in an oven before calcination, we freeze dry to maintain the open, porous structure of the gel. In this way, the air bubbles act as one template on the macroscale, whereas the biopolymer controls morphology on the meso-scale. To introduce a further level of porosity, $Mg(NO_3)_2$ is introduced in the initial agar gel. This decomposes during the heating process to produce very small particles of MgO. These can be removed with acid to leave pores in the carbon nitride structure, thus acting as a third template. The combined biopolymer, MgO, and air templates produce a material with enhanced photocatalytic activity compared to any single/dual template. Furthermore, the triple-templating procedure is based on a single homogeneous gel precursor, making this method very simple and easy to tune. The biopolymer selected for this work was agar as it forms very strong gels in water without the need for metal cations for crosslinking. In addition, agar is a relatively simple polysaccharide sourced from seaweed and contains only C, O, and H atoms and hydroxyl side groups (Fig. S1 of supplementary material).[14] This eliminates any contribution from N or S doping into the carbon nitride structure.

All reagents were purchased from Sigma Aldrich. Aqueous DCDA (99%, 5 g) was heated in water (50 ml) with different amounts of agar and $Mg(NO_3)_2.6H_2O$ (10% aqueous solution) to form a homogeneous solution that gelled on cooling to room temperature. The gels were frozen with liquid N_2 followed by freeze drying to give white solids with a porous sponge-like structure and negligible shrinkage from the original gel. Samples were heated to 550 °C in air for 4 h with a 2.3 °C/min ramp rate. MgO was removed from the samples by soaking in HNO_3 (50 ml, 1 M) for 24 h followed by repeated washing with water then drying in air. The removal of MgO was indicated by some fizzing on contact of the solid with the acid. Samples were denoted by a code depending on the preparation method: **D5-agar-x-F-Mg-y**, where D5 denotes 5 g DCDA solid, agar-x indicates the mass of agar (g), F indicates freeze drying, and Mg-y is the mass (g) of 10% (by mass) of $Mg(NO_3)_2$ solution used in the experiment. A series of control samples were prepared, including drying the gels in an oven at 80 °C rather than freeze drying. Further control samples were also prepared without agar,

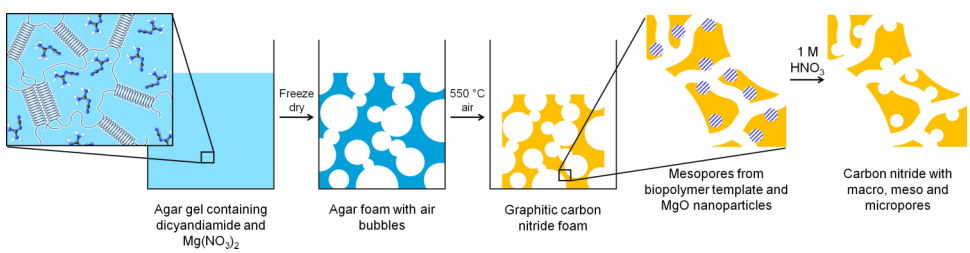

FIG. 1. Schematic showing the process for making porous g-CN templated by air, biopolymer, and MgO.

without $Mg(NO_3)_2$, and without either agar or $Mg(NO_3)_2$. These samples follow the same code, for example, a freeze dried sample of only aqueous DCDA would be denoted as D5-F.

The photocatalytic activities of the samples were evaluated by the degradation of rhodamine B (RhB), under visible light ($\lambda > 420$ nm). A 300 W xenon lamp with a 420 nm cutoff filter and a cooling water jacket outside was used as the light source. In a typical RhB degradation experiment, the sample for testing (0.02 g) was ground to a powder and dispersed in 200 ml of RhB aqueous solution (5 mg l^{-1}) in a container. The solution with g-CN was stirred in the dark for 1 h to ensure an adsorption-desorption equilibrium between the RhB and the photocatalyst. Samples were removed before and after addition of the powder to identify any reduction in RhB concentration in solution. After switching on the light, samples were collected with a syringe every 5 min and then filtered into cuvettes for analysis.

Agar was selected as the biopolymer for this study as it forms strong gels in cold water and was found to produce strong, homogeneous foams after the freeze drying process. As agar has never been used previously for g-CN templating, we firstly identified the optimum agar:DCDA ratio for the experiments with magnesium. The effect of freeze drying compared to oven drying was also investigated. After heating freeze dried agar/DCDA precursors to 550 °C, yellow, orange, brown, or black samples were obtained. Pure g-CN is yellow and the darker colour of some samples in this work was a result of amorphous carbon residue from the decomposed agar biopolymer. This can be seen in Figs. 2(a)-2(e), which shows samples with increasing agar content moving from yellow (control) to black (highest agar concentration). The presence of agar does not hinder the formation of the polymeric carbon nitride material, as confirmed by XRD patterns in Fig. 2(f). The peak at ~27.4°, a characteristic inter-layer stacking peak of the g-CN layers, was indexed as the (002), corresponding to an interlayer distance of 0.336 nm for g-CN. The other peak at 13.1°, was indexed as (100) and is related to an in-plane structural packing motif. The similar XRD patterns of all g-CN samples are a proof that the graphitic structure of the samples prepared with agar stay unchanged with respect to that of a control g-CN sample.

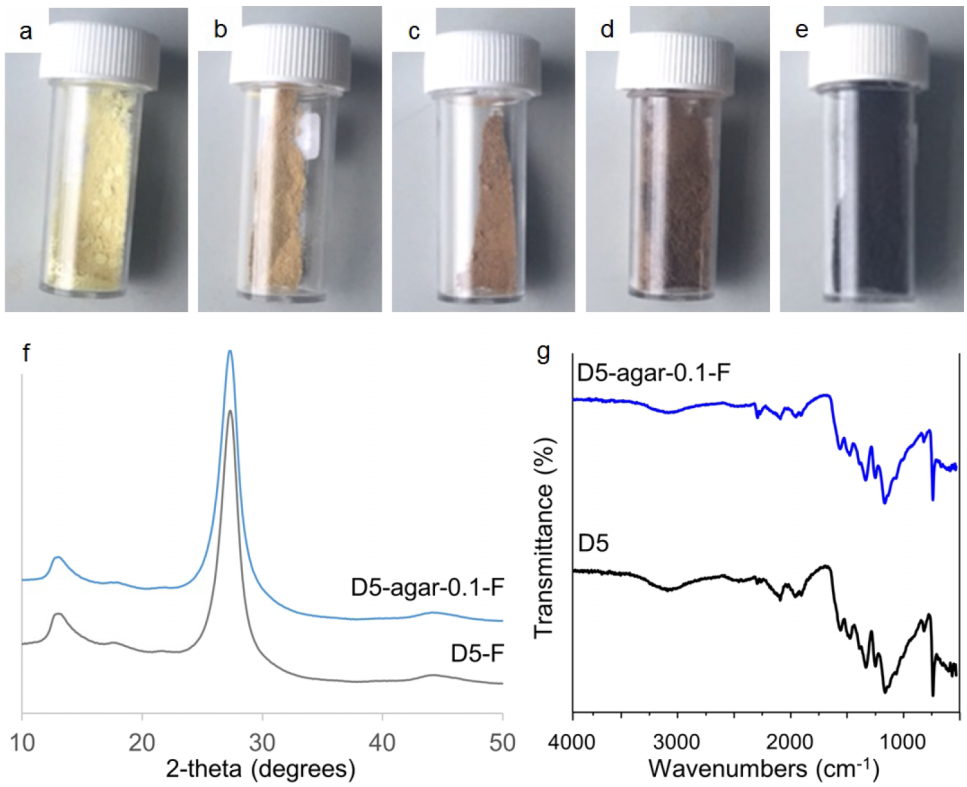

FIG. 2. Images of samples (a) D5-F, (b) D5-agar-0.01-F, (c) D5-agar-0.05-F, (d) D5-agar-0.1-F, (e) D5-agar-0.5-F, (f) XRD patterns, and (g) FTIR spectra for control vs agar samples.

The unchanged structure of the carbon nitride is also reflected in Fourier transform infrared (FTIR) spectra for samples vs a g-CN control (Fig. 2(g)), which show typical stretches of the C—N extended network ranging from 800 to 1700 cm^{-1}, indicating the successful preparation of g-CN. To be specific, the typical breathing mode of the tri-s-triazine units at 809 cm^{-1} and the aromatic C—N heterocycle stretches at 1200-1700 cm^{-1} can be detected from samples prepared with agar. It can be concluded that the —C═N— conjugated framework of bulk g-CN stayed mostly unchanged after the agar/air templating.

The effect of freeze drying and agar templating was evaluated by testing the materials as catalysts in photodegradation of an organic dye. Degradation of Rhodamine B (RhB) under visible light is a common method to evaluate the photocatalytic activities of g-CN[15,16] and metal containing carbon nitride materials.[17,18] Fig. 3 shows a plot of the peak intensity at the maximum of 554 nm in the UV-Vis absorbance spectrum against time for a range of oven-dried and freeze-dried samples. The result from decoloration of RhB shows that templating of g-CN with only agar did not change

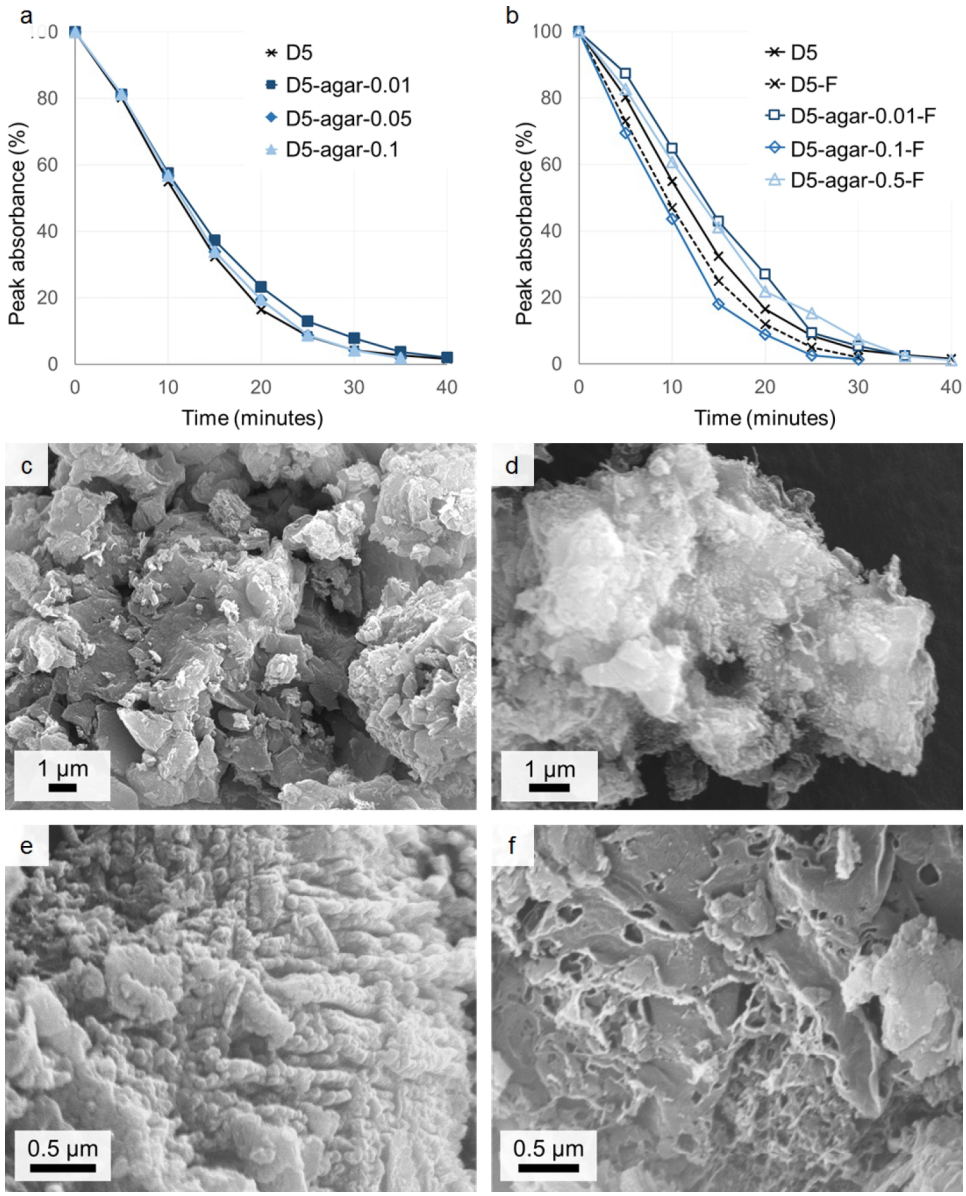

FIG. 3. Degradation of Rhodamine B over time plotted from the intensity of the UV-Vis peak absorbance at 554 nm for (a) oven dried and (b) freeze dried samples. SEM images of (c) D5, (d) D5-F, (e) D5-agar-0.1, and (f) D5-agar-0.1-F.

the photocatalytic activity of the carbon nitride compared to the control sample (D5). This may be due to shrinkage of the precursors during the oven drying process, as capillary forces in the agar gel lead to collapse of the network. The resulting material would have very low porosity which would decrease photocatalytic activity. The introduction of freeze drying to the process resulted in a small increase in activity. Interestingly, even freeze drying a solution of DCDA (D5-F) showed improvement over the oven-dried control. Freeze drying removes water through sublimation rather than evaporation and so eliminates the effect of capillary forces and reduces or eliminates shrinkage of the sample during drying. The combination of agar and freeze drying does not offer a significant improvement and in fact, a very small (0.01 g) or large (0.5 g) amount of agar was detrimental to the sample. In the case of the low agar concentration, it could be that the amount of biopolymer is too small to influence crystallization of the DCDA precursor and so may have little or no effect on templating the sample. In the case of 0.5 g agar, the low activity of the sample is probably due to the high carbon content. A small amount of carbon in a carbon nitride can be beneficial and can enhance absorption of visible light. However, if too much carbon residue is produced, the material moves towards being a nitrogen-doped carbon rather than a graphitic carbon nitride, which would significantly hinder photocatalytic properties.[19]

Elemental analysis was used to further characterize this excess carbon (Table I). On increasing the amount of agar, the molar ratio of C/N changes from 0.67 to 0.74, which is consistent with an increase in carbon content and with the visual observations of the samples. The relatively small increase in carbon overall is reasonable given that the theoretical yield of g-CN in this synthesis is 3.7 g and that even a "perfect" decomposition of 0.5 g agar (i.e., only releasing H_2O) would give a maximum yield of 0.2 g. Thermogravimetric analysis of a sample of pure agar shows ~20% mass retention (a black residue) at 600 °C, which also supports the formation of carbon in these samples (Fig. S2).[14] When compared to the theoretical C/N ratio of g-CN (0.75), all of these samples would appear to have a small (~5%) excess of nitrogen. This could be attributed to the fact that amine condensation is still not complete in the obtained material and the excess amine is from the formation of highly condensed polymeric melon not from the idealized single crystalline g-C_3N_4. The observation of ~2% hydrogen in all samples is consistent with uncondensed amino functional groups.

The observation of enhanced activity from freeze dried samples is consistent with results from electron microscopy. Scanning electron microscopy (SEM) images in Fig. 3 show that the oven dried g-CN (D5) consisted of large, irregularly shaped crystals, whereas freeze drying DCDA produced a material (D5-F) with a more "fluffy" appearance. The oven-dried agar sample (D5-agar-0.1) showed a very rough surface with features <100 nm in dimensions, suggesting that the agar has played a role in structuring the g-CN. However, the overall sample still appeared relatively dense. The most open and "sponge-like" sample is the one produced by freeze drying the agar/DCDA gel (Fig. 3(f)). Bubbles of the order of 100-500 nm can be clearly seen throughout the sample, suggesting that the open network structure of the agar gel was maintained during the freeze-drying process.

The open structure of the freeze dried agar sample is more clearly shown in TEM images. Fig. 4 shows TEM images for oven and freeze dried control and agar samples and, while all samples are porous, the sample prepared by freeze-drying the agar gel shows open "bubbles" in the structure. Nitrogen porosimetry for control (Fig. 4(e)) and agar (Fig. 4(f)) samples show type IV adsorption/desorption isotherms with type H3 hysteresis loops. The presence of a hysteresis loop, which

TABLE I. Elemental analysis of samples prepared with increasing agar content.

Composition (wt. %)	C	N	H
D5	34.4	59.8	1.91
D5-agar-0.01-F	34.3	59.7	1.90
D5-agar-0.1-F	34.1	58.3	1.91
D5-agar-0.5-F	35.3	55.2	2.00

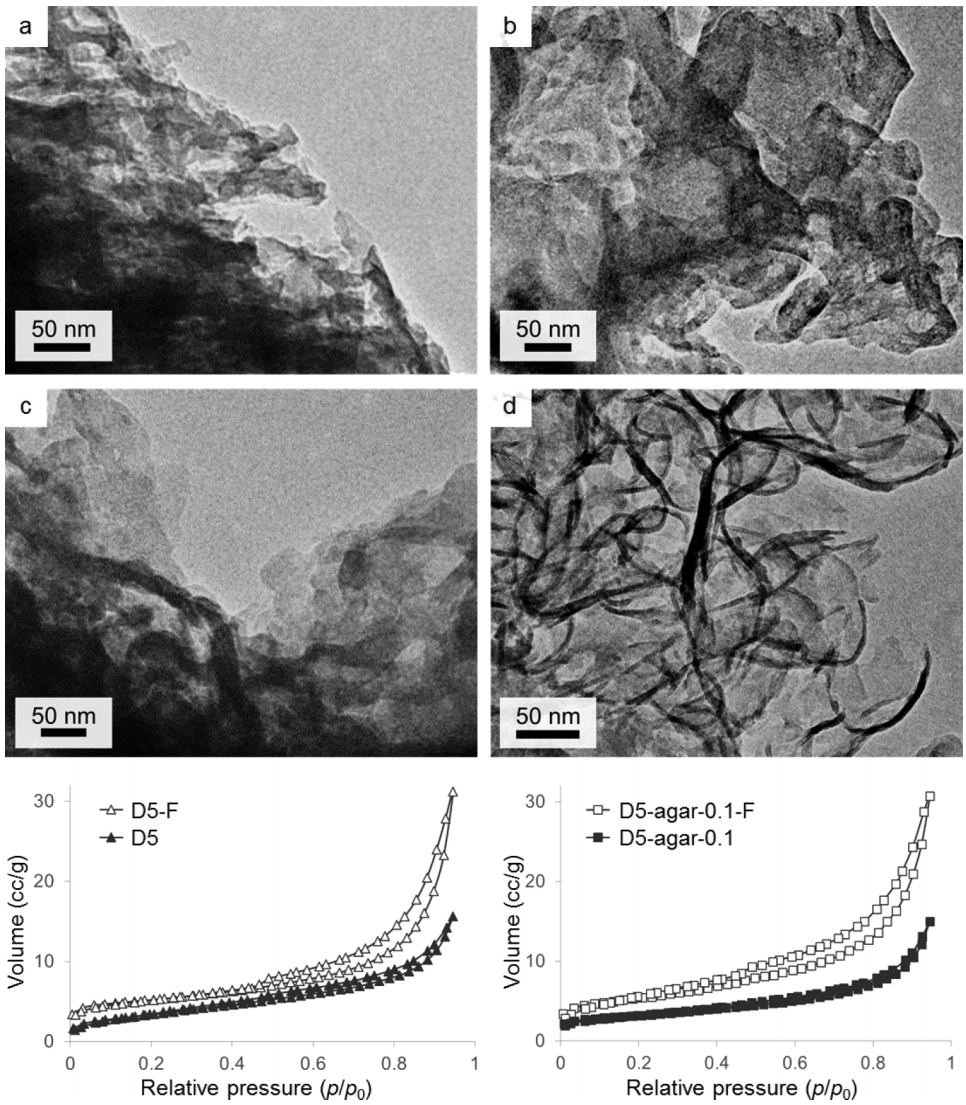

FIG. 4. TEM images of (a) D5, (b) D5-F, (c) D5-agar-0.1, and (d) D5-agar-0.1-F.

is particularly clear in the agar-templated sample, indicates mesoporosity (i.e., pores in the region of 2-50 nm). The lack of a plateau at high p/p_0 indicates that porosity in these samples extends into the macropore range (>50 nm), which is consistent with electron microscopy images. What is clear from both graphs is that freeze drying increases adsorbed volume significantly, whether agar is present or not. Given that most of this increase seems to come from meso and macroporosity, this does not substantially affect the BET (Brunauer-Emmett-Teller) surface areas which are 12 $m^2\ g^{-1}$, 17 $m^2\ g^{-1}$, 11 $m^2\ g^{-1}$, and 19 $m^2\ g^{-1}$ for D5, D5-F, D5-agar-0.1, and D5-agar-0.1-F, respectively. The slightly higher BET surface area in the freeze dried samples may be a factor in the slightly improved catalytic activity of these samples. Although the improvement is not significant, the effect of air/biopolymer combined templating on morphology is very clear. To achieve enhanced catalytic activity as well, a third template is needed.

The use of MgO as a third template was investigated, using the optimized mass ratio of DCDA:agar of 5:0.1. Different amounts of magnesium nitrate (1, 5, and 10 g of 10% w/w solution) were added to the aqueous DCDA/agar precursors before the freeze drying process. The samples were then heated to 550 °C to form g-CN and the magnesium salts were removed by washing with acid. This resulted in a slight fizzing, indicating a reaction of the acid with a basic magnesium oxide

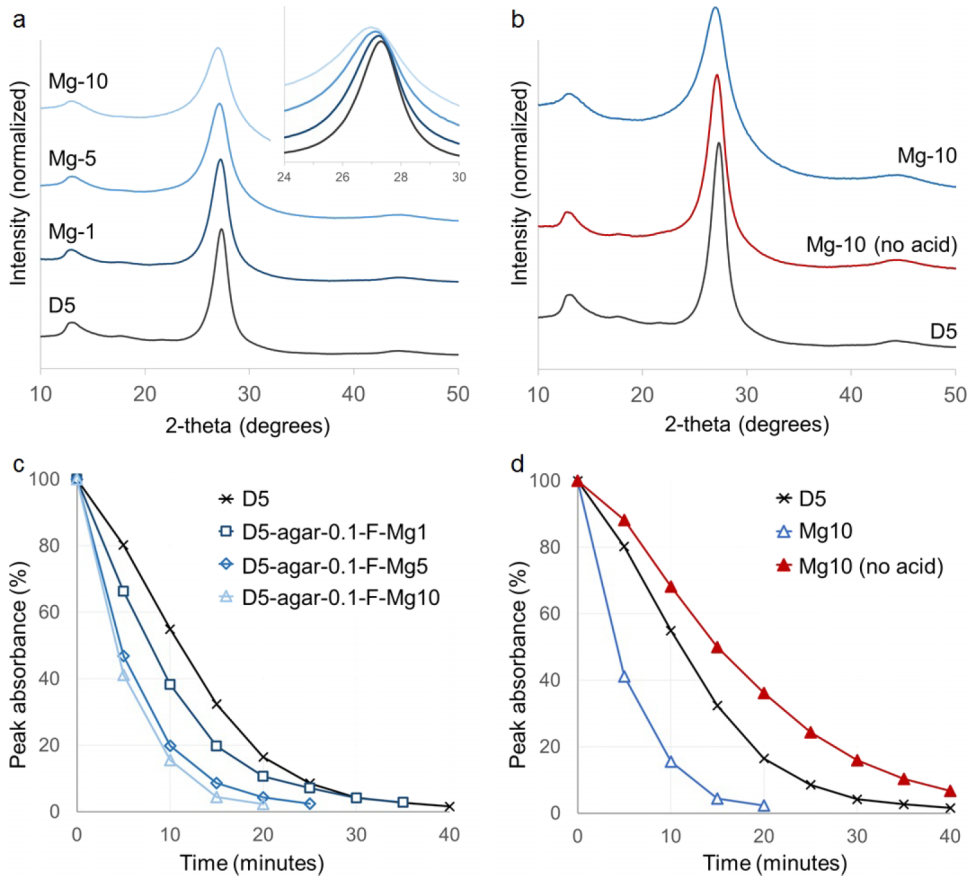

FIG. 5. (a) XRD patterns (offset along y axis) for a control (D5) sample compared to samples prepared with different amounts of magnesium, after acid washing. (b) XRD patterns showing the similarity between the sample D5-agar-0.1-F-Mg-10 before and after acid washing. (c) Photodegradation data for control vs Mg samples and (d) D5-agar-0.1-F-Mg-10 before and after acid washing.

salt. XRD patterns of the resulting samples are shown in Fig. 5(a). These show the characteristic peaks for g-CN, but the (002) peak is shifted to a slightly lower angle with increasing Mg concentration (inset), indicating a greater interlayer distance. The (002) peak is also broadened, indicating a smaller grain size in the sample prepared with high Mg and suggesting that the presence of Mg not only influences the textural features of agar-templated g-CN but also interacts with the condensation of DCDA. In a comparison of sample D5-agar-0.1-F-Mg-10 before and after acid washing, it can be seen that there are no peaks for MgO in either of the XRD patterns (Fig. 5(b)). This is not entirely surprising, since the theoretical yield of MgO in this synthesis is 0.16 g compared to the 3.7 g theoretical mass of g-CN, which would mean extremely small MgO peaks. Given that the aqueous $Mg(NO_3)_2$ precursor will be very highly dispersed in the agar/DCDA matrix, we would also expect the resulting MgO particles to be very small, meaning that any small XRD peaks would be broadened and even more likely to be lost in the background noise. When Mg levels were increased to a much higher level (e.g., D5-agar-0.1-F-Mg-60) it was possible to identify peaks for MgO in the product. After acid washing, these disappeared to leave the characteristic g-CN peak (Fig. S3).[14]

The most important result from this work is that a sample of agar/air/Mg-templated g-CN shows significantly improved activity in photodegradation of Rhodamine B. Fig. 5(c) shows the change in peak UV absorbance over time for a control g-CN compared to samples prepared with three levels of Mg. This is thought to be due to the removal of MgO with acid leaving additional pores in the g-CN matrix, providing more active sites for photocatalysis. To further illustrate that the enhanced activity comes from the porous structure and not simply the addition of MgO, a sample before and after acid washing is also shown (Fig. 5(d)). The result is very clear as it took more than

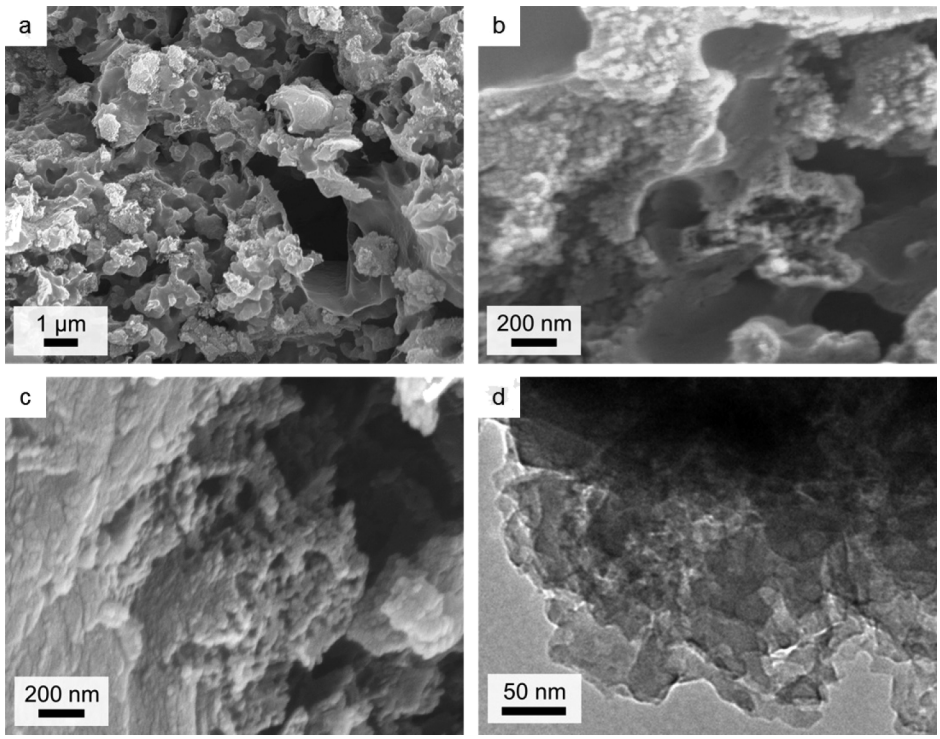

FIG. 6. SEM images of sample D5-agar-0.1-F-Mg-10 ((a) and (b)) before and (c) after acid washing, showing a particulate, honeycomb structure. (d) TEM image of sample D5-agar-0.1-F-Mg-10.

40 min for 100% RhB degradation with the sample that had not been acid-washed, indicating that MgO must be removed to produce the high-activity material. This is also emphasized by the photodegradation rate constants (k) for the various materials (Fig. S4),[14] giving a value of 0.18 min^{-1} for D5-agar-0.1-F-Mg-10 compared to 0.11 min^{-1} for the control sample.

Given the low levels of MgO in these samples, it was unsurprisingly difficult to identify this phase using microscopy techniques. Fig. 6 (and Fig. S5 or S6[14]) shows SEM samples of the D5-agar-0.1-F-Mg-10 sample before ((a) and (b)) and after (c) acid washing. Interestingly, the structure of the sample prepared with magnesium shows some significant differences to a sample prepared only with agar and freeze drying. The appearance is much more of a "honeycomb" structure with interconnected pores through the material. The solid itself has a grainy appearance when viewed at high resolution. After acid washing, the structure is very similar and the samples are indistinguishable by TEM imaging. The small amounts of MgO meant that MgO particles could not be identified in TEM images. This honeycomb-like structure in these samples is typical of metal oxides prepared by sol-gel combustion synthesis, where a metal nitrate is combined with a fuel (e.g., glycine or citrate) and ignited in a furnace.[20] The reaction between the nitrate and the organic material produces a lot of gas, which in turn generates pores in the material. We have also observed the formation of carbon foams by mixing metal nitrates with biopolymers such as gelatin.[13] It is possible that the nitrate from $Mg(NO_3)_2$ in this synthesis is reacting with the agar polymer to produce gases that enhance the porosity in this system. In this case, it might be thought that this additional introduction of porosity is in fact what is causing the enhancement in photocatalytic activity. However, this theory is precluded by the low activity of the sample before acid washing. Nitrogen porosimetry of these samples results in adsorption isotherms similar to those obtained without MgO and a low surface area of 5 $m^2\ g^{-1}$ for sample D5-agar-0.1-F-Mg-10. This is surprising given the high catalytic activity. However, N_2 is not the best gas for characterizing microporosity and so alternative porosimetry techniques may show a substantially different result.

Having established the effectiveness of the triple templating method, it is useful to discuss the mechanism of activity of the materials produced in this work. The use of g-CN as a photocatalyst

was first reported by Wang *et al.*[21] Under visible light irradiation, photoexcitation on the surface of the g-CN leads to a charge separation between the electron in the conduction band and the hole in the valence band. In this case, it has been suggested/calculated that nitrogen atoms act as the oxidation sites while the carbon atoms provide the reduction sites. For photodegradation of rhodamine B, there are two possible routes to decomposition, which have been illustrated in work by Shalom *et al.*[22] The first is cleavage of the aromatic conjugated structure and the second is N-deethylation. The main observable difference between the routes is that cleavage of the conjugated structure would retain the main absorption peak at 554 nm while the N-deethylation pathway would be blue-shifted up to 498 nm for the main absorption peak. The UV-Vis absorption in our system (Fig. S7)[14] suggests that there was a dramatic decrease at $\lambda = 553$ nm, accompanied by a blue shift of the absorption band, which indicated that the deethylation process was the dominant process for RhB degradation.[23]

As mentioned in the introduction, the improvement of photocatalytic activity of graphitic carbon nitride requires three factors. First, a high surface area can provide more active sites for reaction and adsorption sites for the target pollutant.[24] Second, a small grain size can shorten the migration distance between the photogenerated charge in the excitation sites and the active site for photodegradation.[25] Finally, intrinsic electronic properties,[23] including the bandgap, the band-edge potential, and charge-carrier mobility can improve the visible-light absorption efficiency of g-CN. In this work, we believe that the most significant effect of the triple template is on pore structure as well as g-CN grain size. Certainly, samples with increasing Mg-content display a broader g-CN peak, suggesting that the crystallite size of g-CN is constrained in the presence of the magnesium compounds. This could simply be a result of two separate crystalline phases forming simultaneously, or a result of the nitrate/agar reaction generating a more open structure. In any case, it is clear that the multiple levels of templating from the single precursor all combine to produce the optimized material. Freeze drying is advantageous as it avoids shrinkage of the soft, gel-like precursors of DCDA/agar, thus introducing macroporosity in the sample. This general method of freeze drying DCDA-containing precursors could have wider applications in g-CN templating; first, as it provides a way to ensure homogeneity is maintained during drying and could avoid phase separation or "settling out" of a hard template. Second, the biopolymer is a good choice for g-CN templating, not only for the range of physical properties and functional groups but also for the wide availability of these materials and the potential for industrial scale-up. Finally, the use of magnesium essentially adds a hard template (MgO) to soft templates (agar, air) to generate multiple types of pores in the sample.

In summary, we have demonstrated templating methods to synthesize g-CN materials with a range of porous structures. By combining three templates (air, biopolymer, and MgO), all generated from a single gel precursor, we have optimized the g-CN structure to enhance the photocatalytic activity. Freeze drying is to the best of our knowledge a new approach to structuring g-CN and makes it possible to enhance the templating effect of biopolymer gels. As a combination of soft and hard templating method, g-CN was obtained via self-assembly of agar and the casting of pores by MgO particles from a $Mg(NO_3)_2$ precursor. Compared with traditional hard-templating methods, MgO is particularly advantageous as it can be removed with dilute acids such as HCl or HNO_3 compared to the hazardous HF typically used in removing SiO_2 or anodic aluminium oxide templates. Furthermore, the "soft" biopolymer templates, being sourced on a large scale from nature, have some significant advantages over synthetic surfactant templates.

The authors acknowledge the University of Birmingham, EPSRC and the National Natural Science Foundation of China (No. 91333110) for funding. Lianne Hill is thanked for assistance with elemental analysis.

[1] N. Cheng, J. Tian, Q. Liu, C. Ge, A. H. Qusti, A. M. Asiri, A. O. Al-Youbi, and X. Sun, ACS Appl. Mater. Interfaces **5**, 6815 (2013).
[2] X. Wang, K. Maeda, X. Chen, K. Takanabe, K. Domen, Y. Hou, X. Fu, and M. Antonietti, J. Am. Chem. Soc. **131**, 1680 (2009).
[3] K. Maeda, X. Wang, Y. Nishihara, D. Lu, M. Antonietti, and K. Domen, J. Phys. Chem. C **113**, 4940 (2009).
[4] Z. Zhou, J. Wang, J. Yu, Y. Shen, Y. Li, A. Liu, S. Liu, and Y. Zhang, J. Am. Chem. Soc. **137**, 2179 (2015).
[5] Y. Zhang, Z. Schnepp, J. Cao, S. Ouyang, Y. Li, J. Ye, and S. Liu, Sci. Rep. **3**, 2163 (2013).

[6] Y. Wang, X. Wang, M. Antonietti, and Y. Zhang, ChemSusChem **3**, 435 (2010).
[7] Q. Li, J. Yang, D. Feng, Z. Wu, Q. Wu, S. S. Park, C.-S. Ha, and D. Zhao, Nano Res. **3**, 632 (2010).
[8] X. H. Li, J. Zhang, X. Chen, A. Fischer, A. Thomas, M. Antonietti, and X. Wang, Chem. Mater. **23**, 4344 (2011).
[9] J. Wang, C. Zhang, Y. Shen, Z. Zhou, J. Yu, Y. Li, W. Wei, S. Liu, and Y. Zhang, J. Mater. Chem. A **3**, 5126 (2015).
[10] Y. Zheng, J. Liu, J. Liang, M. Jaroniec, and S. Z. Qiao, Energy Environ. Sci. **5**, 6717 (2012).
[11] Z. Schnepp, Angew. Chem., Int. Ed. **52**, 1096 (2013).
[12] D. Raabe, C. Sachs, and P. Romano, Acta Mater. **53**, 4281 (2005).
[13] Z. Schnepp, Y. Zhang, M. J. Hollamby, B. R. Pauw, M. Tanaka, Y. Matsushita, and Y. Sakka, J. Mater. Chem. A **1**, 13576 (2013).
[14] See supplementary material at http://dx.doi.org/10.1063/1.4936218 for structure of agar polymer, XRD patterns for a sample with a much higher Mg content, photodegradation kinetics calculations, and temporal UV-Vis absorption spectra for a RhB aqueous solution during photodegradation by sample D5-F.
[15] Y. Cui, Z. Ding, P. Liu, M. Antonietti, X. Fu, and X. Wang, Phys. Chem. Chem. Phys. **14**, 1455 (2012).
[16] G. Dong and L. Zhang, J. Mater. Chem. **22**, 1160 (2012).
[17] S. Ye, L. G. Qiu, Y. P. Yuan, Y. J. Zhu, J. Xia, and J. F. Zhu, J. Mater. Chem. A **1**, 3008 (2013).
[18] X. Wang, X. Chen, A. Thomas, X. Fu, and M. Antonietti, Adv. Mater. **21**, 1609 (2009).
[19] W. Li and D. Zhao, Chem. Commun. **49**, 943 (2013).
[20] Y. Li, L. Xue, L. Fan, and Y. Yan, J. Alloys Compd. **478**, 493 (2009).
[21] X. Wang, K. Maeda, A. Thomas, K. Takanabe, G. Xin, J. M. Carlsson, K. Domen, and M. Antonietti, Nat. Mater. **8**, 76 (2009).
[22] M. Shalom, S. Inal, C. Fettkenhauer, D. Neher, and M. Antonietti, J. Am. Chem. Soc. **135**, 7118 (2013).
[23] L. W. Zhang, H. B. Fu, and Y. F. Zhu, Adv. Funct. Mater. **18**, 2180 (2008).
[24] W. Wei, C. Yu, Q. Zhao, G. Li, and Y. Wan, Chem.–Eur. J. **19**, 566 (2013).
[25] Y. F. Li, D. Xu, J. Oh, W. Shen, X. Li, and Y. Yu, ACS Catal. **2**, 391 (2012).